The Dissertation Committee for Matthew Cranston Cowperthwaite certifies that this is the approved version of the following dissertation:

Mutation: Lessons from RNA Models

Committee:

Lauren Ancel Meyers, Supervisor

James J. Bull

Andrew D. Ellington

Claus O. Wilke

Thomas E. Juenger

Mutation: Lessons from RNA Models

by

Matthew Cranston Cowperthwaite, B.S.

Dissertation

Presented to the Faculty of the Graduate School of

The University of Texas at Austin

in Partial Fulfillment

of the Requirements

for the Degree of

Doctor of Philosophy

The University of Texas at Austin

May 2008

Dedicated to my parents, Patricia and George,
and to my wife, Claudia.

Acknowledgments

I would like to take this opportunity to thank a lot of people who helped make graduate school a wonderful experience.

First, I would like to thank my supervisor, Dr. Lauren Ancel Meyers. Indeed, I could not conceive of a better supervisor than Lauren. Lauren gave me the opportunity to develop and pursue my interests, and invested significant time and energy helping me succeed. Lauren's enthusiasm, creativity, and brilliance were always a source of inspiration that kept me motivated. In addition to being a wonderful mentor, Lauren is also a good friend.

I would like to thank Dr. James J. Bull for his essential guidance over the years. Jim was absolutely instrumental in completing this research. Jim is also a fun person with which to collaborate, and an all-around great guy who could always make me laugh with a wise crack or two.

A huge thanks to Dr. Andrew Ellington. Perhaps most importantly, Andy introduced me to Lauren in the first place. But, Andy also has an infectious enthusiasm that made for fun collaborations. I would like to thank Dr. Claus O. Wilke for advice on this work, as well as enjoyable and fruitful collaborations. Dr. Thomas E. Juenger for input and advice that significantly improved this body of work.

I owe huge thanks to the members of the Meyer's lab – Eric, Robert, Sam, Shweta, Evan, Will (adjunct) – a great group of scientists that I will always consider good friends. Evan, Will, and Eric were instrumental in completing the study

discussed in chapter four. I am very grateful for their insights into this research

I would like to thank Dr. David Hillis for the IGERT fellowship that not only provided financial support, but also greatly expanded my math and computer science background. I also acknowledge the James S. McDonnell foundation for supporting me over the past two years. I am incredibly grateful to the Texas Advanced Computing Center (TACC) for maintaining the computers that made most of this work possible, and for providing much-needed technical assistance. I also would like to thank Chris Simmons and Craig Dupree for building and maintaining Phylocluster.

Finally, I would like to thank my family for their support: My wife, Claudia, for her understanding, endless patience and oft-needed encouragement; Mom and Dad to whom I am eternally indebted for a lifetime of love and support; Coke for both occasional math advice and fun times on the "golf" course; Scott, Betsy, Philip, Carolyn, and Charley for being great brothers and sisters; Sylvia for being a wonderful mother in law; Riley, Bonnie, and Reed for being fun nieces and nephews; my dogs, Morgan and Lulu, have been great companions.

Matthew Cranston Cowperthwaite

The University of Texas at Austin
May 2008

Mutation: Lessons from RNA Models

Publication No. _____

Matthew Cranston Cowperthwaite, Ph.D.
The University of Texas at Austin, 2008

Supervisor: Lauren Ancel Meyers

Mutation is a fundamental process in evolution because affects the amount of genetic variation in evolving populations. Molecular-structure models offer significant advantages over traditional population-genetics models for studying mutation, mainly because such models incorporate simple, tractable genotype-to-phenotype maps. Here, I use RNA secondary structure models to study four basic properties of mutation.

The first section of this thesis studies the statistical properties of beneficial mutations. According to population genetics theory, the fitness effects of new beneficial mutations will be exponentially distributed. I show that in RNA there is sufficient correlation between a genotype and its point mutant neighbors to produce non-exponential distributions of fitness effects of beneficial mutations. These results

suggest that more sophisticated statistical models may be necessary to adequately describe the distribution of fitness effects of new beneficial mutations.

The second section of this thesis addresses the dynamics of deleterious mutations in evolving populations. There is a vast body of theoretical work addressing deleterious mutations that almost universally assumes that the fitness effects of deleterious mutations are static. I use an RNA simulation model to show that, at moderately high mutation rates, initially deleterious mutations may ultimately confer beneficial effects to the individuals harboring them. This result suggests that deleterious mutations may play a more important role in evolution than previously thought.

The third section of this thesis studies the global patterns of mutations connecting phenotypes in fitness landscapes. I developed a network model to describe global characteristics of the relationship between sequence and structure in RNA fitness landscapes. I show that phenotype abundance varies in a predictable manner and critically influences evolutionary dynamics. A study of naturally occurring functional RNA molecules using a new structural statistic suggests that these molecules are biased towards abundant phenotypes. These results are consistent with an "ascent of the abundant" hypothesis, in which evolution yields abundant phenotypes even when they are not the most fit.

The final section of this thesis addresses the evolution of mutation rates in finite asexual populations. I developed an RNA-based simulation model in which each individual's mutation rate is controlled by a neutral modifier locus. Using this model, I show that smaller populations maintain higher mutation rates than larger populations. I also show that genome length and shape of the fitness function do not significantly determine the evolved mutation rate. Lastly, I show that intermediate rates of environmental change favor evolution of the largest mutation rates.

Contents

List of Figures

List of Tables

Chapter 1

Introduction

Evolutionary biologists have long sought to understand the evolutionary processes that transcend any particular biological system. Models have proved to be indispensable tools for gaining such insights. During the 20th century, evolutionary theoreticians built a powerful conceptual framework upon simple mathematical models. Recently, however, thanks to startling advances in molecular biology and computational power, a new generation of higher resolution quantitative models is changing our perspectives on the origins and processes that have led to the current diversity of life on earth.

DNA, RNA and proteins are the three essential biological macro-molecules. Although RNA lies at the heart of the "central dogma of molecular biology", mediating information transfer from DNA genes to functional proteins, it has historically been overshadowed by DNA and proteins. Several recent discoveries, however, have brought RNA to center stage. RNA turns out to play a vital regulatory role (for recent reviews see (Mattick and Makunin, 2006; Niwa and Slack, 2007; Winkler and Breaker, 2005)) in many cellular processes and is the primary genetic material for a large number of viruses, including influenza and HIV. Molecular biologists are thus working hard to characterize the molecular structures of RNA and the relationship between RNA structure and biological function.

Evolutionary biologists have harnessed the efforts of RNA molecular biologists. They have built evolutionary models that explicitly consider the relationship between RNA sequence and RNA structure. These models are vastly more biologically realistic than traditional mathematical models of the relationship between

genotype (sequence) and phenotype (structure). Through computational simulations of evolutionary dynamics, these models yield rapid results, yet incorporate significantly greater biological detail than traditional mathematical models. They have been used to study a wide range of evolutionary patterns and processes, such as the evolution of robustness (Ancel and Fontana, 2000), the distribution of fitness effects of mutations (Cowperthwaite et al., 2005, 2006), the causes and implications of neutral evolution (van Nimwegen et al., 1999), evolutionary transitions (Fontana and Schuster, 1998b; Huynen et al., 1996), and the structures of fitness landscapes (Schuster et al., 1994).

This modeling framework originates in the work of Manfred Eigen and, later, Peter Schuster (Eigen, 1971; Eigen and Schuster, 1979). They sought to address "origin of life" questions, and, in particular, develop a general theory for the emergence of biological information and self-replicating life from "molecular chaos". Based on the assumption that early life must have undergone highly error-prone replication, Eigen sought to understand the evolutionary consequences of high mutation rates (Eigen, 1971).

Two influential concepts emerged from this work. Eigen and Schuster used mathematical models to demonstrate that the balance between mutation and selection could result in a quasispecies – a population that stably includes not only the wildtype (best type) but also sub-optimal mutants of that wildtype (Eigen and Schuster, 1979). At very high mutation rates, a population may, in fact, include only very few wildtype genotypes and many poorer variants. The quasispecies concept has often been thought to describe an entirely novel set of evolutionary principles, however, recently it has been shown to be an extension of classic mutation-selection balance theory (Bull et al., 2005; Wilke, 2005). The concept has been embraced by virologists who regularly observe that rapidly mutating viral strains may achieve high levels of diversity, yet there is debate as to whether this is evidence that some viruses evolve as a quasispecies (Domingo, 2002; Eigen, 1996; Holmes and Moya, 2002).

Eigen's second influential concept is the error catastrophe, the genetic meltdown of a population experiencing excessively high mutation rates. He showed mathematically that, under fairly reasonable assumptions, there would be a critical mutation rate below which populations would stably persist as quasispecies and above which the wildtype and its close mutants would disappear entirely. Based

on these ideas, virologists have sought to cure viral infections by using chemical mutagens to induce error catastrophes.

To test these ideas, Eigen encouraged the development of mathematical and computer models of evolving molecular structures (Eigen, 1971). He recognized that such biologically-grounded and highly detailed models would elucidate evolutionary dynamics at a higher level of resolution that previously possible. Many researchers since have taken his charge and developed models of evolving RNA and protein molecules (see Chan and Bornberg-Bauer (2002) and references therein). Here, we describe the structure of RNA-based models and the resulting insights into evolutionary processes.

1.1 The RNA Folding Model

RNA molecules are composed of four nucleotides – adenine (A), guanine (G), cytosine (C) and uracil (U). Pairs of nucleotides in an RNA molecule can form stable electrostatic interactions, thus holding two parts of a molecule close together. The strength of an interaction varies with the specific combination of nucleotides, and stable interactions tend to form at the expense of less stable interactions. Through such pairing, RNA molecules "fold" into secondary structures (hereafter "shapes"). The shape of an RNA molecule is composed of combinations of familiar motifs, such as stems (helical base-paired regions) and loops or bulges (unpaired regions) (**Figure 1.1**).

The shape of an RNA molecule may be vital to its function, particularly for functional RNA molecules (as opposed to protein-coding RNA molecules) like ribosomal RNA, micro-RNA and ribozymes. In fact, the function of a molecule will depend on not only its (two-dimensional) shape, but on its (three-dimensional) tertiary configuration. This includes additional far-reaching pairings between nucleotides already participating in secondary motifs. The formation of tertiary interactions, however, is not particularly well understood. Fortunately, RNA secondary structures can be predicted with reasonable accuracy, and constitute most of the full structure of a typical molecule (Hofacker et al., 1994; Mathews et al., 1999, 2004; Zuker and Stiegler, 1981).

Theoreticians originally developed a set of rules for predicting RNA secondary structure, based on thermodynamic considerations (Waterman, 1978). These

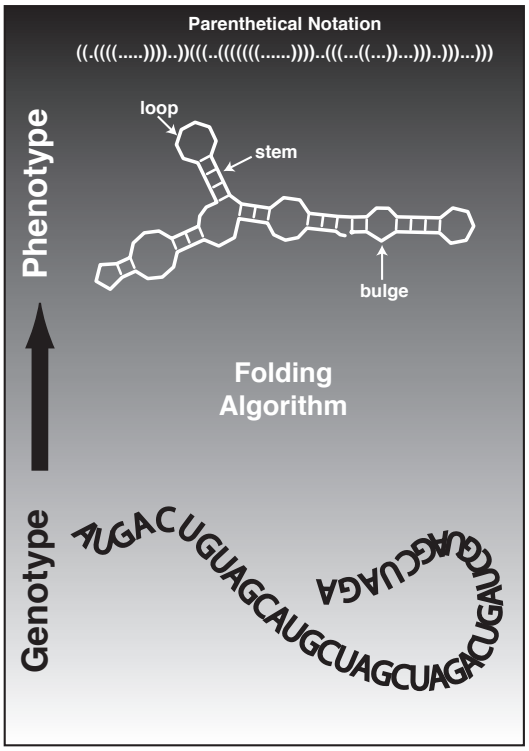

Figure 1.1: Diagram of genotype-to-phenotype map in the RNA model system. The genotype is the primary nucleotide sequence and the phenotype is the most probable secondary structure (shape). Shape is predicted from sequence using thermodynamic folding algorithms. We label the primary RNA secondary structure motifs. Stems are contiguous stretches of base pairs that include at least two base pairs, loops are unpaired bases that connect the two halves of a stem, and a bulge is an unpaired region in the middle of a stem. Parenthetical notation represents paired bases as matching parentheses and unpaired bases as dots. It contains all of the structural information present in the graphical representation.

rules assume that a molecule will fold into the shape that releases the most energy upon formation, and thus is the most stable configuration. This is called the minimum free energy shape of a molecule. The RNA folding rules are much simpler than the analogous set for proteins, largely because RNA has a smaller set of building blocks (four nucleotides versus twenty amino acids) and generally forms simpler secondary structural motifs. Michael Zuker and colleagues developed the first efficient computer algorithms to predict RNA secondary structure using this approach (Zuker

and Stiegler, 1981; Zuker, 1989). Their software, called mFold, is still actively developed and freely available at `http://www.bioinfo.rpi.edu/applications/mfold/`. More recently, Ivo Hofacker and colleagues have been developing and maintaining the ViennaRNA package, which includes many computational tools for folding and analyzing RNA structures and is freely available from `http://www.tbi.univie.ac.at/~ivo/RNA/` (Hofacker et al., 1994). Researchers are continually improving the accuracy and scope of these folding algorithms. For example, new versions can predict the shapes of RNA molecules during interactions with other molecules (Bernhart et al., 2006; Mathews, 2006; Mathews and Turner, 2006).

The thermodynamic folding algorithms are reasonably accurate for smaller RNA molecules. The thermodynamic approach makes several simplifying assumptions, however. Notably, they cannot predict pseudoknots (a common tertiary motif) or non-canonical base interactions (Hofacker et al., 1994). Researchers have developed comparative-genomics based approaches that generally yield more accurate predictions of RNA secondary structure, particularly for large RNA molecules (Gutell et al., 2002). The comparative approach, however, is much slower than the thermodynamic approach and requires large sets of homologous sequences to predict the shape of any given sequence. Thus it is not computationally tractable for evolutionary simulations.

The thermodynamic folding algorithms are sufficiently fast to incorporate into simulation models of evolving populations. Such models typically simulate a large population of RNA molecules evolving via mutation and natural selection. The fitness of any given molecule is determined by first predicting its shape(s) and then applying a pre-specified fitness function to these predictions (described in detail below). Molecules replicate in proportion to their fitnesses and, upon replication, bases mutate randomly. Generally, mutation is assumed to occur at a constant rate, however, we later explore the consequences of relaxing this assumption. Some RNA models assume discrete populations (Cowperthwaite et al., 2006) , whereas others assume a continuous individual-based, birth-death process (Ancel and Fontana, 2000; Fontana and Schuster, 1998b; Huynen et al., 1996; van Nimwegen et al., 1999).

1.1.1 Fitness in RNA Models

Phenotypes are produced by manifold interactions between genetic, cellular, organismal, and environmental factors. The term genotype-to-phenotype map refers to this complicated route from genotype to phenotype. The phenotypes of an organism (physiological and behavioral) collectively interact with the environment (including other organisms) to determine fitness. Ultimately, evolutionary biologists aspire to characterize these complex processes and their evolutionary consequences, but these studies have just begun.

The main advantage of the RNA models is that the folding algorithms serve as a biologically motivated, yet tractable, genotype-to-phenotype map (Schuster et al., 1994). Unlike many traditional population genetic models which completely ignore phenotype and assume simple one-to-one maps from genotype to fitness, the phenotypes in the RNA models result from detailed interactions among genes and their micro-environment (Eigen, 1971; Fontana and Schuster, 1987). In RNA models, each nucleotide is a genetic locus with four possible alleles (A, C, G, or U), interactions among these loci determine the phenotype, and mutations cause a locus to switch from one allele to another, which, depending on the rest of the molecule, may alter the phenotype. The genotypes are primary nucleotide sequences and the phenotypes are the shapes predicted from these sequences via thermodynamic folding algorithms.

Perhaps most importantly, RNA-based models do not make many of the assumptions often found in classic evolutionary models. For instance, fitness stems from a biologically-grounded model of molecular folding. Thus the fitness of a given mutant does not come from an assumed distribution but rather is determined organically. The likelihood that a mutation is beneficial or deleterious, and the nature of epistatic (non-additive) interactions among loci are similarly unconstrained.

The fitness of an RNA molecule is determined in two steps. First the shape(s) of a molecule are predicted using thermodynamic algorithms and then a fitness value is attained via a function from shapes to real numbers. We use the term fitness function to refer just to this second function from phenotype to fitness and the term fitness landscape to describe the projection of a large set of genotypes (a so-called "sequence space") to their ultimate fitness values.

The fitness functions used in RNA models are often based on the similarity

of a molecule's shape(s) to a predetermined ideal target shape. Fitness typically decreases monotonically as a function of the distance to the target shape. These models thereby use shape as a proxy for function and do not model function explicitly. This is justified (at least somewhat) by the dominant role typically played by secondary structure in functional tertiary structure and the extreme conservation of secondary structure throughout the evolutionary history of most functional RNA molecules (Doudna, 2000).

In this chapter, we describe the conceptual foundations of fitness in RNA-folding models, and we describe specific details where necessary in later chapters. We begin with the simplest fitness function used in RNA models; hereafter, we refer to this as the "simple" model. The simple model considers only the minimum free energy (mfe) shape of each molecule, which is the single most stable structure that an RNA molecule is predicted to assume (**Figure 1.2A**). Fitness is thus solely determined by the distance between the mfe shape and the target shape.

In reality, however, an RNA molecule may not necessarily fold into its minimum free energy shape, and may even spontaneously switch among several thermodynamically probable shapes. Thus the phenotype is actually an ensemble of possible shapes. Thus researchers introduced a more complex, but perhaps more biologically realistic, model in which sequences are mapped to the set lowest free energy shapes (**Figure 1.2B**) (Ancel and Fontana, 2000). We will refer to these as "plastic" models since they capture structural plasticity produced by Brownian motion.

Wuchty et al. (1999) extended the standard thermodynamic prediction algorithms to estimate the ensemble of lowest free energy structures of an RNA molecule. We refer to this ensemble of low free energy shapes as the *suboptimal repertoire*, which is estimated by suboptimal folding. Suboptimal folding ignores energy barriers among alternative states and assumes that a molecule equilibrates among all shapes with free energy within $5kT$ of the ground state, where k is the Boltzmann constant and T is the temperature. This is approximately equivalent to 3 kcal/mol at 37^o C, and corresponds to the breaking of 2 G-C/G-C stacking interactions (base pairs). We used the Boltzmann factor to estimate the probability of any particular shape in the suboptimal repertoire of an RNA molecule. For any specific shape σ, the Boltzmann probability of σ, $p_\sigma = e^{-\Delta G_\sigma / kT}/Z$, measures the relative stability of σ with respect to the entire repertoire. Z is the partition function of a molecule

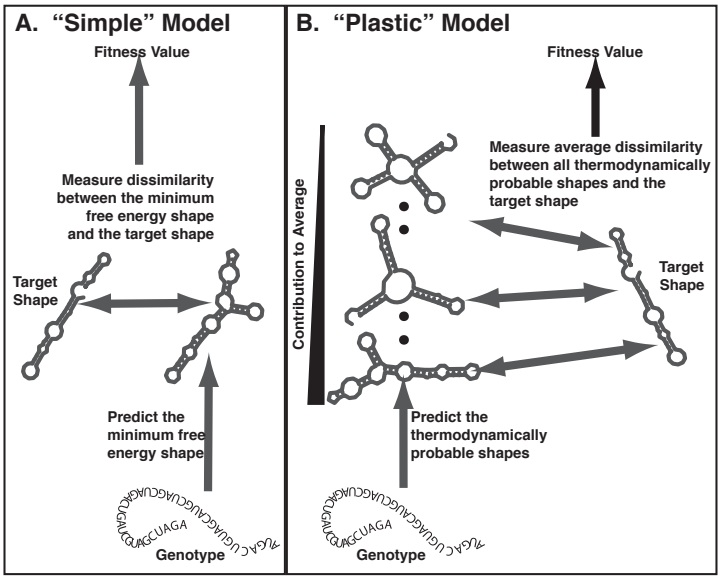

Figure 1.2: The two fitness models for RNA. **A**. Under the simple model, the fitness of an RNA genotype depends only on the similarity of its minimum free energy shape to the target shape. **B**. Under the plastic model, the fitness of a molecule is determined by the entire ensemble of probable (low free energy) shapes. The similarity of any given shape to the target contributes to the final fitness in proportion its Boltzmann factor, which is an estimate of the thermodynamic stability of a shape.

and is computed according to the method described in McCaskill (1990):

$$Z = \sum_{\sigma} e^{-\Delta G_{\sigma}/kT} \tag{1.1}$$

where ΔG_{σ} is the free energy of σ and the sum includes all shapes in the suboptimal repertoire. Assuming equilibration, p_{σ} estimates the probability of finding σ in a large sample of identical RNA molecules and approximates the amount of time any given molecule spends in σ. The mfe conformation is the most probable shape in any suboptimal repertoire.

There are several methods for quantifying the structural distance between two shapes (Ancel and Fontana, 2000; Stadler et al., 2001). For example, one can represent each shape in parenthetical notation, where dots stand for unpaired bases and matching parenthesis stand for paired bases (as in **Figure 1.2**), and then com-

pute a Hamming distance between two such representations of shapes. Alternatively, the tree-edit distance measures the differences between the binary-tree representations of two shapes. Although researchers have used a variety of shape distance metrics, several studies have suggested that most observations in RNA models are relatively robust to the specific choice of distance metric (Ancel and Fontana, 2000; Fontana and Schuster, 1998a).

The form of the fitness function, that is, how exactly fitness declines as distance to the target grows, can profoundly influence the outcome of evolution. One might naively assume that this is linear, such that any unit decrease in similarity to the target shape results in the same loss of fitness. Given that RNA structures are highly evolutionary conserved, however, it is more likely that fitness declines faster than similarity. That is, even slight deviations from the ideal shape result in substantial loss of function. Many studies have therefore assumed hyperbolic fitness functions (Ancel and Fontana, 2000; Cowperthwaite et al., 2005, 2006; Fontana and Schuster, 1998b).

1.2 Evolutionary Insights into Fitness Landscapes

Since Sewall Wright introduced fitness landscapes in 1932, the concept has profoundly influenced evolutionary thinking (Wright, 1932). Fitness landscapes are maps from large sets of genotypes to their fitnesses. Metaphorically, as populations evolve, they traverse the surfaces of fitness landscapes with mutation and recombination sampling new regions and natural selection pushing uphill. Though fitness landscapes are extremely high dimensional for most real biological systems, they are often illustrated as two-dimensional surfaces in three-dimensional Euclidean space. The structure of a fitness landscape is thought to constrain many micro- and macro-evolutionary processes, including the rates of adaptation and speciation (Gavrilets, 2004).

With the advent of high throughput laboratory methodologies and modern computation, researchers are starting to undertake large-scale characterizations of fitness landscapes (Cowperthwaite et al., 2005; Fontana and Schuster, 1998a; Gruner et al., 1996a,b; Li et al., 1996; Lunzer et al., 2005; Weinreich et al., 2006). The RNA model system offers the ideal balance of biological complexity and computational tractability for such studies. Some of the earliest and most exciting ideas about

fitness landscapes have come out of this body of work (Cowperthwaite et al., 2005; Fontana and Schuster, 1998a,b; Gruner et al., 1996a,b; Schuster et al., 1994).

Technically, an RNA fitness landscape is a projection from genotype space – the set of all possible sequences of a given length – to fitness space (often the real numbers). Recall, however, that these models use secondary structure as a proxy for fitness. Consequently, the landscapes that have been characterized are actually maps from sequence space to shape space, where the mapping functions are thermodynamic folding algorithms. All of the RNA landscape studies so far are based on the simple map from sequence to minimum free energy shape (which ignores alternative low free energy structures).

The total number of sequences of a specific length n is 4^n. There is extensive degeneracy in the map from sequences to shapes, with many sequences folding into the same minimum free energy structure, which means the size of the shape space will always be less than the size of the sequence space (Schuster et al., 1994). Waterman first proposed an upper bound for the number of shapes of length n – $S_n = 1.4848 \times n^{-\frac{3}{2}}(1.8488)^n$ based on several assumptions about the nature of the shapes, such as stem length and loop size (Waterman, 1978). In the first large scale computational surveys to estimate the extent of redundancy, Gruner and colleagues folded all 30-nucleotide binary RNA molecules (composed of only A/C or G/U). Approximately one billion unique sequences folded into approximately 220,000 and 1,000 unique shapes in the G/C and A/U landscapes, respectively (Gruner et al., 1996a,b). Evidence for similar degeneracy was found in partial surveys of four-nucleotide RNA landscapes (Fontana and Schuster, 1998a; Schuster et al., 1994).

A many-to-one relationship between genotypes and phenotypes is not unique to RNA. For instance, there is considerable sequence divergence in 16S rDNA sequences, yet extensive functional conservation. As a result, these are key molecules for phylogenetic analysis (Delsuc et al., 2005). Degeneracy has been observed in proteins based on lattice models of protein structure (Chan and Bornberg-Bauer, 2002), and is at the heart of the neutral theory of molecular evolution, which asserts that most mutations have negligible phenotypic consequences (Kimura, 1968), and the molecular clock hypothesis (Zuckerkandl and Pauling, 1962). We discuss later how this redundancy profoundly affects the evolutionary dynamics of RNA.

1.2.1 Mutational Networks

Evolutionary transitions from one phenotype to another are mediated by mutations to their underlying genotypes. Historically, evolutionary biologists have thought of mutations in terms of distributions of fitness effects and have sought to measure the fractions of mutations that are typically beneficial, neutral and deleterious. While these distributions are critical determinants of local evolutionary dynamics, they provide little information about larger-scale processes. To this end, it is useful to think in terms of mutational paths connecting distant genotypes and more generally, in terms of the large-scale patterns of mutational connectivity within genotype spaces.

Specifically, the space of all genotypes can be construed as a mutational network in which each genotype is a node and mutations between genotypes are edges. In other words, any two genotypes that differ by exactly a single point mutation are connected by an edge (**Figure 1.3**, bottom). One can then represent phenotypes (or fitness values) as colors. The coloration in **Figure 1.3** illustrates the degeneracy in the sequence-shape relationship discussed above. The colored edges represent neutral mutations that preserve the phenotype, while black edges represent non-neutral mutations that may be beneficial or deleterious. RNA mutational networks are regular graphs, that is, each genotype is mutationally connected to exactly $3L$ other genotypes, where L is the sequence length.

1.2.2 Neutral Networks

Each colored patch in **Figure 1.3** is a neutral network – a mutationally connected set of genotypes that produce the same phenotype (or fitness value). This concept originated and has been studied extensively in the RNA model system Fontana et al. (1993b); Gruner et al. (1996a,b); Huynen et al. (1996); Schuster et al. (1994); van Nimwegen et al. (1999). Following Eigen's quasispecies theory, it is perhaps the most influential idea to emerge from this body of work.

Consider a phenotype in a fitness landscape. The structure of its neutral network and its mutational connectivity to the neutral networks of other phenotypes determines the likelihood that it will evolve, and if so, whether it will give rise to other phenotypes. To understand constraints on phenotypic evolution, we must address questions like: Are neutral networks confined to small sections of sequence

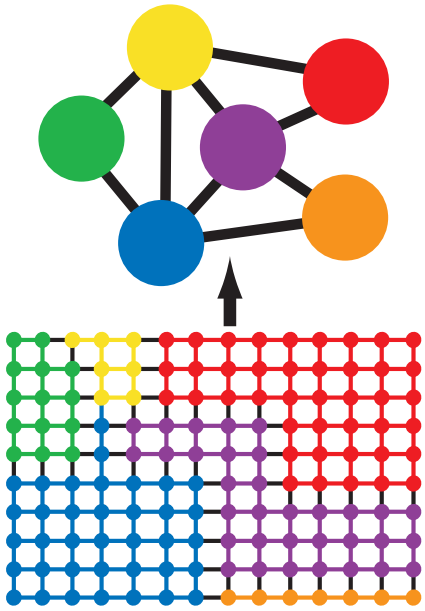

Figure 1.3: Mutational networks capture patterns of mutational connectivity among genotypes and phenotypes. In the bottom network, each node is a genotype and each edge is a point mutation. Colors represent phenotypes, and each group of genotypes that share the same color forms a neutral network. The top half shows a phenotype network in which each phenotype is condensed into a single node and two phenotypes are connected by an edge if there is at least one point mutation that converts one phenotype to the other.

space or do they span the entire space? Do phenotypes have single contiguous neutral networks or several disjoint components? What patterns of adjacency exist between neutral networks for different phenotypes?

The first generality to emerge from neutral network studies is that "not all phenotypes are equal" (Fontana and Schuster, 1998a; Schuster et al., 1994). Within an RNA fitness landscape, any given shape may be realized by many or only a few sequences. In other words, the sizes of the neutral networks vary considerably. The distributions of neutral network sizes within RNA fitness landscapes have been shown to follow a generalized Zipf's law, a type of semi-exponential distribution (Fontana et al., 1993a,b; Schuster et al., 1994). The critical implication is that most RNA shapes are relatively rare while a few are quite abundant.

The neutral network of a particular phenotype may be composed of a single

component or multiple disjoint components (Gruner et al., 1996a,b). A component is a set in which all genotypes are connected by paths of neutral mutations. If a neutral network is comprised of disjoint components, then it contains two or more components that are not connected to each other by neutral mutations. Surprisingly, the number of disjoint components in a phenotype's neutral network does not appear to correlate with its abundance (Cowperthwaite and Meyers, unpublished).

The neutral networks of highly abundant phenotypes have been shown to typically span entire fitness landscapes (Fontana et al., 1993b; Schuster et al., 1994). In other words, it is possible to mutate (in succession) every nucleotide in a sequence, all the while preserving its shape. Maynard Smith proposed a similar phenomena in protein fitness landscapes (Smith, 1970). This suggests that neutral networks may facilitate evolution by allowing populations to explore vast expanses of genotype space (via mutation) while maintaining constant fitness (Kirschner and Gerhart, 1998; Wagner, 2005).

Phenotype Networks

As illustrated in **Figure 1.3**, mutational networks connecting genotypes give rise to mutational networks connecting phenotypes, or phenotype networks. In particular, we aggregate all genotypes that produce a particular phenotype into a single node, and connect two phenotypes with an edge if there is at least one point mutation that converts one phenotype to the other. For RNA, we say that two shapes A and B are mutationally adjacent if there exists at least two sequences a and b that differ by exactly one mutation and produce A and B. Mutationally adjacent shapes are connected by edges in the corresponding phenotype network.

RNA phenotype networks appear to be highly irregular, with few nodes connected to many others and most nodes connected to few others (Schuster et al., 1994; Stadler et al., 2001). In contrast, classical population genetic models often assume that genotypes map one-to-one onto phenotypes, and that the mutational connectivity among phenotypes is fairly homogeneous. Thus the RNA model system can offer valuable insights into patterns of mutational connectivity and the evolutionary implications of such patterns (Fontana and Schuster, 1998b; Huynen et al., 1996).

One of the first studies to characterize the mutational adjacencies of RNA

shapes found that almost any genotype is surrounded by a specific set of highly abundant phenotypes (Schuster et al., 1994). In other words, almost any genotype is within one or a few point mutations of the most common shapes in the landscape; and vice versa, these common shapes are mutationally close to most other phenotypes in the landscape. This hypothesis is called shape-space covering. In phenotype network terms, abundant shapes are connected to almost every other shape.

Fontana and colleagues developed a formal theory to describe the genetic accessibility among mutationally adjacent phenotypes and the implications of different mutational structures on evolutionary dynamics (Stadler et al., 2001). Mutationally adjacent shapes are those shapes for which there exists at least one point mutation that can cause a change between those two shapes. These efforts and earlier simulation studies suggest that the degree of mutational connectivity is not simply a binary property (connected or unconnected by point mutations) (Fontana and Schuster, 1998a,b; Huynen et al., 1996). Rather some mutationally adjacent phenotypes are nearer to each other than other mutationally adjacent phenotypes, meaning that they are more likely to reach each other via mutation (Fontana and Schuster, 1998a). Furthermore, this connectivity is always asymmetrical, resulting from the non-uniform boundaries among adjacent neutral networks (Fontana and Schuster, 1998a; Stadler et al., 2001). For example, consider two phenotypes A & B: asymmetry means that mutating from A frequently produces B, while mutating from B does not frequently produce A. In phenotype network terms, this variation in connectivity can be represented as weighted, directed edges between nodes. The weight on an edge pointing from A to B indicates the probability that any given genotype in the neutral network for A will mutate to phenotype B, and, vice versa, the weight on the edge pointing in the opposite direction indicates the fraction of mutations to genotypes in the neutral network for B that produce phenotype A.

Rugged Neutral Networks: An Important Caveat

Most RNA neutral network studies have assumed the simple model in which the fitness of a molecule is determined entirely by its minimum free energy structure (mfe). The neutral networks in these studies are simply sets of RNA molecules that share the same mfe. In reality, however, the fitness of a molecule will be determined by other factors, notably the kinetics and energetics of folding. Two molecules

that share the same mfe may have very different thermodynamic properties and, consequently, different fitnesses. Thus, so-called neutral networks may not truly be neutral.

The plastic model, introduced by Ancel and Fontana, inserts ruggedness into neutral networks (Ancel and Fontana, 2000). Recall that, in this model, the fitness of an RNA molecule is determined by its entire ensemble of energetically favorable structures (the specific structures in the ensemble and their relative thermostabilities). Whereas the simple fitness function was discrete (only a finite set of possible values corresponding to a finite set of mfe's), the plastic fitness function is continuous (infinitely many possibilities). In general, any two molecules that share the same mfe will have different fitnesses under this model. Ancel and Fontana (2000) found that neutral networks have distinct patterns of heterogeneity, with the most thermodynamically stable molecules lying at the dense centers of neutral networks, where most mutations preserve the mfe. Thus, if fitness positively correlates with thermodynamic stability, then mfe neutral networks are no longer plateaus but rather mounds which may impede the neutral drift of a population towards alternative phenotypes.

Given that the plastic model is probably more realistic than the simple model, one might be tempted to reject the notion of a neutral network altogether. We argue, however, that the concept remains instructive. The mfe is the most likely structure and an important determinant of fitness. Although neutral networks may be more rugged than often assumed, they still contain expansive sets of mutationally connected molecules with roughly similar fitness.

1.3 Evolutionary Dynamics

Intuitively, the structure of fitness landscapes fundamentally constrain evolution. In this section we review a number of theories linking mutational connectivity to evolutionary dynamics that originated in and/or have been tested using the RNA model system. First we focus specifically on the evolutionary consequences of mutational networks and then turn to more general studies of mutations and their interactions.

1.3.1 Evolutionary Dynamics on Mutational Networks

There is a widely-believed claim that neutral networks increase the evolvability of populations (Kirschner and Gerhart, 1998; Stadler et al., 2001; Wagner, 2005). The rationale is that populations evolving on neutral networks may undergo significant genetic change with only negligible phenotypic change, and can thereby explore fitness landscapes. In other words, neutral mutations can accumulate until a genetic background arises that is poised for beneficial change. Under this scenario, neutral mutations will be transient, ultimately facilitating adaptation by subsequent beneficial mutations (Wagner, 2005).

Several RNA simulation studies have shown that populations evolving toward a target shape tend to experience long periods of phenotypic stasis, interspersed with short periods of rapid phenotypic change (Ancel and Fontana, 2000; Cowperthwaite et al., 2006; Fontana and Schuster, 1987, 1998a,b; Huynen et al., 1996). The first of these studies showed that the number of unique sequences in the population increased during periods of phenotypic stasis and used multi-dimensional scaling to illustrate the genetic dispersal of the population. The population typically subdivides into several genetically different yet phenotypically equivalent subpopulations, each exploring a different region of the fitness landscape via mutation and natural selection.

1.3.2 Punctuated Equilibria: Crossing from One Neutral Network to the Next

One striking feature of the fossil record is the extensive discontinuity in forms (Eldredge et al., 2005), that is, periods of rapid phenotypic change are often separated by longer periods of relative stability. While this may stem partly from observational biases (Eldredge et al., 2005), punctuated equilibria have also been observed in RNA models (Ancel and Fontana, 2000; Cowperthwaite et al., 2006; Fontana and Schuster, 1987, 1998a,b; Huynen et al., 1996), protein models (Chan and Bornberg-Bauer, 2002), digital organisms (Wilke et al., 2001) and microorganisms (Burch and Chao, 1999).

Figure 1.4 shows a typical simulation of RNA molecules evolving towards a target shape. As described earlier, populations disperse through neutral networks during the long periods of stasis. Fontana and colleagues set out to characterize the

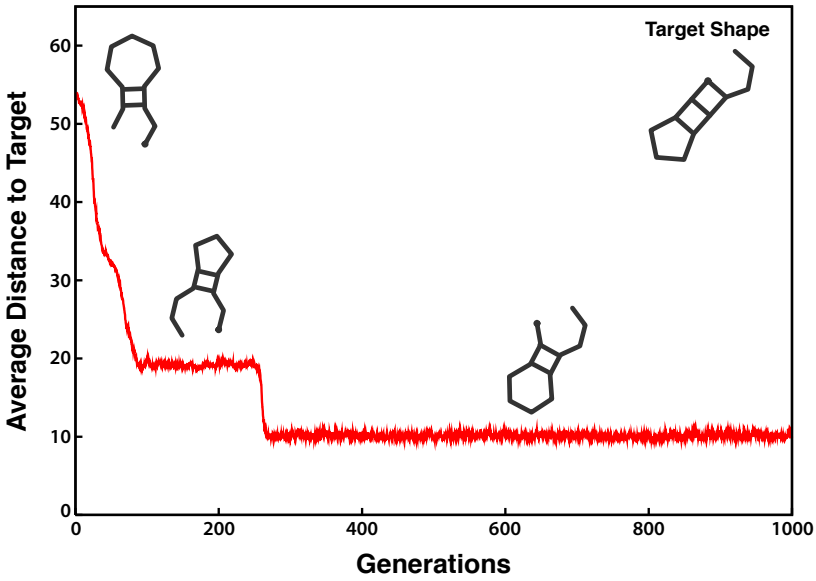

Figure 1.4: Typical evolutionary dynamics in the RNA model system. Evolving populations experience relatively long poques of phenotypic stasis interspersed with short periods of rapid phenotypic change. This figure is based on a simulation of a population containing 500 RNA molecules, in which selection favors molecules that resemble the target shape (upper right). The Y-axis gives the average phenotypic distance of the population to the target shape, and thus low values correspond to high fitness. Shapes that dominate the population are depicted above the curve.

evolutionary transitions between these epochs (Fontana and Schuster, 1998b). They claimed that there were two types of transitions –"continuous" and "discontinuous", and proposed a simple criterion to distinguish them (Fontana and Schuster, 1998a; Stadler et al., 2001). Recall that phenotypes differ greatly in their nearness and a phenotype is said to be near any other phenotype that is likely to be produced by mutation. Continuous transitions are those that involve nearby phenotypes and discontinuous transitions are those that involve phenotypes that are relatively distant (unlikely to be realized by a single mutation). This study reconstructed the steps leading to each major transition. The initial period of rapid adaptation in the simulations occurred primarily through continuous phenotypic transitions; while the transitions taking place during the subsequent punctuated dynamics were predominantly discontinuous. Thus, major adaptations are hypothesized to occur through fairly improbable jumps between barely adjacent neutral networks.

These jumps are thought to be mediated by extensive neutral drift (Fontana and Schuster, 1998b; Huynen et al., 1996). Genotypes that produce one phenotype but are converted to a very different (but better) phenotype by a single mutation must precede these jumps. Such genotypes are likely to be very rare, and may only appear after long periods of evolutionary wandering through neutral networks (Fontana and Schuster, 1998b; Schuster and Fontana, 1999).

In a related in vitro RNA study, researchers synthesized a single RNA sequence that assumes two entirely different phenotypes, each of which catalyzes a distinct ribozyme reaction (Joyce, 2000; Schultes and Bartel, 2000). By making relatively few mutational changes to this sequence, the authors could produce new ribozymes that were highly active for one or the other ribozyme reaction. Thus this single sequence lies at the intersection of the two neutral networks for each function. The authors suggest that intersection sequences (those that realize both phenotypes) may mediate discontinuous transitions (Schultes and Bartel, 2000).

Genetic Robustness: Evolving to the Heart of a Neutral Network

Organisms exist in an ever-changing world. They must evolve to withstand heterogeneous conditions, which include both environmental and genetic perturbations (Meyers and Bull, 2002). Evolutionary biologists seek to identify the mechanisms to achieve environmental and genetic robustness and the evolutionary origins of those mechanisms.

Genotypes are genetically robust when mutations (or recombination) leave the resulting phenotype unchanged. In mutational network terms, genetically robust genotypes lie in the "dense" regions of a neutral networks, where most mutations are likely to create genotypes within the same neutral network. In **Figure 1.3**, a genotype in the middle of a colored region would be completely robust as all of its mutations are neutral.

While it is easy to envision natural selection favoring organisms that can cope with environmental variation (Meyers and Bull, 2002), the origins of genetic robustness are less intuitive (de Visser et al., 2003). Since a deleterious germ-line mutation does not manifest itself until the next generation, there is no immediate natural selection to prevent it. Under certain circumstances, however, natural selection can act over several generations to reduce the burden of such mutations

(de Visser et al., 2003; van Nimwegen et al., 1999). There are several other theories for the origins of genetic robustness, some of which are non-evolutionary (de Visser et al., 2003; Gibson and Wagner, 2000).

This discussion goes back to the founders of the modern synthesis – Haldane, Fisher and Wright – who offered different theories for the evolution of dominance. Dominance is a simple mechanism for robustness by which potentially deleterious mutations at a diploid locus are silenced by the dominant allele. Evolutionary biologists have focused on three scenarios which could give rise to genetic robustness: (i) adaptive robustness – robustness evolves by natural selection, (ii) intrinsic robustness – robustness is a correlated byproduct of character selection, and (iii) congruent robustness – genetic robustness is a correlated byproduct of selection for environmental robustness (de Visser et al., 2003). These mechanisms are not necessarily mutually exclusive.

Natural RNA molecules and RNA viruses appear to be both environmentally (thermodynamically) and genetically robust (Meyers et al., 2004; Sanjuan et al., 2006a,b; Wagner and Stadler, 1999). Studies using the RNA model system have contributed significantly to our understanding of genetic robustness, particularly scenarios (i) and (iii) above. First scenario (i). Van Nimwegen and colleagues developed an elegant mathematical model to show that the trans-generational costs of deleterious mutations are enough to drive populations into the hearts of neutral networks, in other words, that adaptive robustness is possible (van Nimwegen et al., 1999). In particular, this model considers a population evolving on an arbitrary neutral network and assumes that all mutations off the network are lethal. They successfully tested the predictions of their model using RNA simulations. Genetic robustness only evolved in these models, however, under relatively high mutation rates.

Turning to scenario (iii), Wagner was the first to hypothesize that genetic robustness may evolve as a by-product of selection for environmental robustness (Wagner et al., 1997). The first semi-empirical support for this hypothesis came somewhat accidentally from an RNA study (Ancel and Fontana, 2000). Micro-environmental thermal fluctuations can cause an RNA molecule to wiggle between alternative low free energy shapes. An environmentally robust molecule is one that will fold rapidly and reliably into its optimal shape despite these fluctuations.

To study the evolution of environmental robustness, Ancel and Fontana in-

troduced the plastic model, which maps sequences to their ensemble of thermodynamically favorable shapes (described above). Selection for stable folding into a target shape indeed yielded populations of highly stable (environmentally robust) molecules. Surprisingly, the dominant shapes in the evolved populations looked nothing like the target shape. This was in dramatic contrast to natural selection under the simple (minimum free energy only) model which almost always led populations to the target shape.

Why did selection for environmental robustness drive populations into apparent evolutionary dead ends? The evolved populations were also highly genetically robust, to the extent that mutations almost never produce phenotypic novelty, thus precluding further adaptation. The researchers eventually connected the dots, when they discovered a correlation between the alternate shapes that a molecule produces under thermodynamic noise and the shapes it produced upon mutation. They called this general property of the map from genotype-to-phenotype "plastogenetic congruence" (Ancel and Fontana, 2000). As a consequence, molecules that are insensitive to thermal noise are also insensitive to the effects of mutation. A similar correlation has been observed for proteins (Bornberg-Bauer and Chan, 1999; Bussemaker et al., 1997; Vendruscolo et al., 1997). Extreme genetic robustness, to the point of an evolutionary standstill, thus evolved simply as a byproduct of environmental robustness.

This study has other evolutionary implications. First, plastogenetic congruence may extend beyond biopolymers and be a general feature of genotype-to-phenotype maps. Phenocopies – epigenetic mimics of genetically based phenotypes – provide anecdotal evidence for plastogenetic congruence in other complex phenotypes (Queitsch et al., 2002; Rutherford and Lindquist, 1998; True et al., 2004; Waddington, 1959, 1950). This may shed new light on Waddington's theory of developmental canalization from the 1950's (Waddington, 1959, 1950). He was among the first to argue that organisms have evolved developmental pathways that are robust to both environmental and genetic perturbations, and thus produce standard phenotypes in the face of variable environments and mutation. He does not, however, claim that these two forms of robustness share a common evolutionary origin. If plastogenetic congruence holds for organismal phenotypes, then this RNA study suggests that genetic canalization may arise as a byproduct of environmental canalization.

Second, the extremely robust molecules found at the end of the evolutionary simulations were also extremely modular (Ancel and Fontana, 2000). They can be easily partitioned into structural subunits that withstand thermodynamic perturbations or genetic changes elsewhere in the molecule. Modularity, as it shifts the syntax of genetic variation, opens new avenues for phenotypic innovation. Though this advantage is compelling, it does not explain the origins of modularity in the first place. We have a chicken-and-egg predicament: Until both the modules themselves and recombinational mechanisms are in place, it is not clear that natural selection would favor such organization. The RNA study suggests an origin of modularity that does not rely on the eventual evolutionary benefits modularity might provide. In particular it arises as a (second) byproduct of selection for environmental robustness. Consider a rough analogy between RNA folding and organismal development. Interactions between nucleotides influence the kinetic pathway of the molecule and its robustness to both the environment and mutations. Similarly, interactions between genes determine the outcome and stability of developmental pathways. Perhaps natural selection for environmental stability similarly sets the stage for modularity in genetic networks.

Survival of the Flattest: Quasispecies and error thresholds in complex mutational networks

Recall that populations evolving under moderate mutation rates can form quasispecies – mutational clouds around a wildtype (optimal) genotype (Eigen, 1971). Quasispecies have been observed in simulated populations of evolving RNA (Ancel and Fontana, 2000), proteins (Wilke et al., 2001), and digital organisms (Wilke et al., 2001). Many RNA viruses are believed to exist as quasispecies, though there has been considerable debate over the utility of the term (Holmes and Moya, 2002; Moya et al., 2000; Wilke, 2005).

Recall further that error catastrophes occur when mutation swamps selection and a population is unable to maintain the wildtype or its close relatives. Eigen originally discovered the error threshold (the critical mutation rate above which catastrophes occur) in a model that assumes there is a single wildtype genotype and all other genotypes have identical significantly lower fitnesses (Eigen and Schuster, 1979). What happens when the wildtype phenotype is produced by an entire neutral

network of genotypes and not just one? Roughly speaking, an error threshold still exists, but it increases with the breadth of the neutral network, that is, the number of and mutational connectivity among genotypes contained within it. The larger and more connected the neutral network, the more likely a mutation will preserve the wildtype.

Similar reasoning suggests that neutral network breadth may influence the likelihood that a population will evolve one phenotype versus another. Imagine a population evolving in a complex mutational network where the topologies of neutral networks vary considerably among phenotypes. Under high mutation rates, phenotypes that have high fitness but small neutral networks may be easily displaced by less fit but more robust phenotypes. The extent to which neutral networks influence such competition among phenotypes depends on the mutation rate. Under very low mutation rates, fitness considerations alone dictate dynamics, while under high mutation rates, the breadth of neutral networks can be as or more important than fitness. This hypothesis has been called "survival of the flattest" (Wilke et al., 2001) and is a natural extension of Eigen's theory.

"Survival of the flattest" has been developed and tested in a series of mathematical models and simulations of evolving RNA and digital organisms (Bull et al., 2005; Wilke et al., 2001). In first of these studies, populations of digital organisms were evolved under two distinct mutation rates (high and low). When subsequently place in competition under high mutation rates, populations that originally evolved under high mutation rates out-competed those that evolved under low mutation rates even though they had lower fitnesses (Wilke et al., 2001). More recently, a plant virus competition experiment has suggested that similar tradeoffs may hold for plant viral pathogens (Codõner et al., 2006).

While virologists have latched onto these ideas and harnessed them to develop effective antiviral strategies (Domingo, 2003), Bull and colleagues have suggested that the theory may be widely misinterpreted (Bull et al., 2005). In particular, they distinguish between error catastrophes, in which high mutation rates lead to the complete loss of the wildtype in favor of suboptimal genotypes, and extinction catastrophes, in which lethal mutations are so common that no viable genotype can persist. The use of mutation-inducing drugs may not drive viral populations toward error catastrophes as has been claimed (reviewed in (Anderson et al., 2004)) but rather toward extinction catastrophes.

1.3.3 The Mutational Spectra of RNA

The phenotypic effects of mutations determine the rate and outcome of evolution. Evolutionary biologists have thus sought to characterize the distributions of fitness effects based on theoretical considerations (Gillespie, 1984; Orr, 2002, 2003) as well as laboratory mutation accumulation, knockout, and mutagenesis experiments (Estes et al., 2004; Imhof and Schlotterer, 2001; Rozen et al., 2002; Sanjuan et al., 2004). The RNA model system offers a pseudo-experimental compromise approach to estimating these distributions. It is more biologically grounded than the theoretical models yet yields vastly more information than experimental approaches. Here we review a series of RNA studies that offer new perspectives on local mutational structures, as opposed to global properties of entire mutational networks.

Beneficial Fitness Effects: Many small mutations and few large ones

Beneficial mutations are those that increase the fitness of individuals carrying them, and are the fuel of adaptation. Somewhat counter-intuitively, recent theoretical work suggests that distributions of beneficial fitness effects are similar for many fitness landscapes (Gillespie, 1984; Orr, 2003). This theory is based on Gillespie's mutational landscape model which considers a high fitness wildtype that has just experienced a minor environmental change (Gillespie, 1984). The model assumes that the environmental perturbation was small, and thus the wild-type genotype remains reasonably fit, that fit genotypes are rare in the fitness landscape, and that the fitness of any given mutant is chosen at random from the distribution of all fitnesses. Gillespie claimed that the distribution of beneficial mutations could be predicted using extreme-value theory (EVT) and Orr subsequently derived the shape of this distribution (Orr, 2003). EVT states that, for a large class of common distributions, the differences between the top few values in a large random sample will be exponentially distributed. According to Gillespie's assumptions, the wild-type would be among the largest values in a random sample from the distribution of all fitnesses and thus the fitness effects of any beneficial mutations would fall within the purview of EVT (Gillespie, 1984). Orr concluded that the fitness effects of beneficial mutations should therefore be exponentially distributed regardless of biological system (Orr, 2003).

Several groups have attempted to test this hypothesis experimentally, with

most offering mixed support of the Orr-Gillespie theory (Imhof and Schlotterer, 2001; Rokyta et al., 2005; Sanjuan et al., 2004). The most comprehensive of these studies used the RNA virus ϕX174 and supported a modified version of the model that incorporated a mutation bias, which could account for the higher frequency of transitions than transversions (Rokyta et al., 2005). An other study, in vesicular stomatitis virus (VSV), however, measured beneficial fitness effects that did not appear to be exponentially distributed (Sanjuan et al., 2004).

Recently, the Orr-Gillespie theory was tested using the RNA model system (Cowperthwaite et al., 2005). First, the researchers randomly chose two large sets of sequences and measured the fitness effects of every possible point mutation to each sequence in the set. These sets of genotypes differed in their average fitness - one set had relatively low fitness and the other set had relatively high fitness. The distributions of beneficial fitness effects in both low and high fitness regions of the landscape were decidedly non-exponential. There was a significant overabundance of small-effect mutations; and the distribution appeared exponential only upon truncation of the lower 99% of it.

The discrepancy between the theory and the RNA study rests on an fairly un-biological assumption of the Orr-Gillespie model – that the fitness of any given mutant is essentially a random draw from the distribution of all fitnesses (Cowperthwaite et al., 2005). Intuitively, the fitnesses of mutants are often highly correlated to the fitnesses of their parents, as has been demonstrated in RNA and proteins (Atchley et al., 2000; Fontana et al., 1993b; Parsch et al., 2000). The RNA study suggests that a predictive theory of beneficial fitness effects must consider fitness correlations. Orr recently extended his mathematical analysis to consider fitness correlations, and found that EVT does indeed break down under extreme correlations (Orr, 2006).

Epistasis: Mutational effects vary with genetic background

The RNA model system determines fitness from first principles of molecular folding. The shapes of molecules arise out of complex thermodynamic interactions among the nucleotides in the primary sequence. The contribution of any particular nucleotide to the shape (and thus fitness) of the molecule often intricately depends on the nucleotides at several other sites. For example, see **Figure 1.5**. Epistasis – when the action of one gene is modified by one or more other genes – is thus a ubiquitous

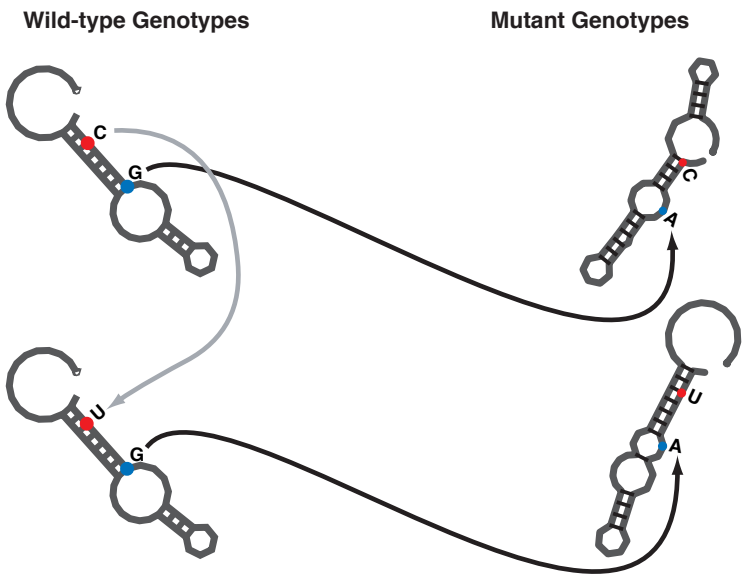

Figure 1.5: Epistasis in RNA results when the phenotypic effects of mutations depend on the surrounding nucleotides. The two molecules on the left differ at one position (red) but fold into the same shape. Mutations at the same site in each of these molecules (blue) produces very different shapes. Thus, through epistasis, a silent change in background (grey arrow) dramatically influences the fitness effect of the subsequent mutation (black arrows).

property of RNA fitness landscapes.

The presence, magnitude, and direction of epistasis are key inputs to many evolutionary theories, including those that seek to explain the evolution and maintenance of sexual reproduction and the rate of adaptation in asexual organisms (Peters and Otto, 2003; Whitlock et al., 1995). Epistatic interactions are often divided into two classes: (i) antagonistic epistasis occurs when simultaneous mutations at interacting sites yield a smaller fitness effect than the sum (or product) of their individual effects, and (ii) synergistic epistasis occurs when the combined effect of the mutations is greater than the sum (or product) of their individual effects. A third form of epistasis has recently appeared in the literature: sign epistasis occurs when the direction of a fitness effect (deleterious or beneficial) is reversed by interactions with other mutations (Weinreich and Chao, 2005). One study in the RNA system suggests that most interactions are antagonistic (Wilke et al., 2003). In particular, starting from a high fitness genotype, as deleterious mutations accumulate, the rate

of fitness decline decreases, regardless of the order of those mutations.

Compensatory Evolution

While beneficial mutations are essential for evolution, it is more likely that mutations entering a population will be neutral or deleterious. There is well-developed evolutionary theory that predicts the fates of deleterious mutations in evolving populations (Crow and Kimura, 1970; Gillespie, 2004). Deleterious mutations are likely to be eliminated by natural selection, but can occasionally reach fixation by chance (drift) alone, particularly in small populations, or by hitchhiking along with beneficial mutations elsewhere in the genome (Johnson and Barton, 2002; Kim and Stephan, 2000; Peck, 1994). A recent RNA study has shown that, under high mutation rates, a third process, compensatory evolution, may lead to the fixation of deleterious mutations much more frequently than either of these other well-studied processes (Cowperthwaite et al., 2006).

Consider a new deleterious mutation. It is possible that, when combined with a subsequent mutation, the original mutation becomes less deleterious, or even beneficial. For example, a mutation to a paired base may break that pairing, to the detriment of the molecule. A subsequent mutation at the matching site may recover that pairing, or perhaps even strengthen (or weaken) the interaction, to the benefit of the molecule. The latter scenario is an example of compensatory evolution through sign epistasis in RNA molecules.

Prior studies of compensatory evolution have focused primarily on compensatory mutations that occur after initial deleterious mutations have fixed in the population, and thus do not contribute the fixation events themselves (Burch and Chao, 1999; Escarmis et al., 1999; Poon and Chao, 2005). In one of these studies, researchers grew an RNA virus at small population sizes to increase the strength of genetic drift and likelihood of fixing deleterious mutations. They then allowed strains that had experienced a deleterious mutation to evolve at larger population sizes, and found that compensatory mutations generally afforded modest recoveries in viral fitness in comparison to the initial deleterious mutation (Burch and Chao, 1999). A later study found that compensatory evolution mediated fitness recoveries in roughly three-quarters of populations in which deleterious mutations fixed (Poon and Chao, 2005). There is further evidence for compensatory evolution across many

natural and model systems (Poon et al., 2005).

Compensatory evolution may occur prior to fixation of the initial deleterious mutation, and, consequently, make fixation of the mutation more likely. As recently illustrated in the RNA model system, this is common under relatively high mutation rates (like those found in RNA viruses) (Cowperthwaite et al., 2006). In evolutionary simulations, initially deleterious mutations fixed far more frequently than expected by drift alone. Initially harmful mutations interacted with subsequent mutations to increase fitness beyond that of the ancestor, and thus experience fitness reversals. Such compensatory events explained as many as 70% of the deleterious fixation events.

Comparative genomic studies have identified possible fixed deleterious mutations in insect and human genomes (Kondrashov et al., 2002; Kulathinal et al., 2004). These observations must be interpreted with caution, however, because the order in which the mutations entered the genome is unknown, and currently deleterious mutations may not have been so when they first appeared. Nonetheless, these studies highlight the complicated nature of mutational interactions and suggests that deleterious mutations may be more than just temporary nuisances. Metaphorically speaking, they may provide stepping stones to distant adaptive peaks.

1.4 Conclusion

In the last two decades, a new generation of computationally intensive and biologically grounded models have changed our perspectives on evolutionary dynamics. We now have a more global understanding of mutational relationships and how they constrain evolution. Here we have reviewed a class of such models that have been particularly fruitful. Detailed simulations of evolving RNA structures, have inspired general predictive theories about the nature of adaptation, the determinants of evolvability, the origins and mechanisms of robustness, and more. As volumes of biological data accumulate and computational power grows, these models will improve and continue to enrich comprehension of the natural world.

References

Lauren Ancel and Walter Fontana. Plasticity, Modularity and Evolvability in RNA. *Journal of Experimental Zoology*, 288(3):242–283, 2000.

Jon P. Anderson, Richard Daifuku, and Lawrence A. Loeb. Viral error catastrophe by mutagenic nucleosides. *Annual Review of Microbiology*, 58(1):183–205, 2004.

William R. Atchley, Kurt R. Wollenberg, Walter M. Fitch, Werner Terhalle, and Andreas W. Dress. Correlations Among Amino Acid Sites in bHLH Protein Domains: An Information Theoretic Analysis. *Mol Biol Evol*, 17(1):164–178, 2000.

Stephan Bernhart, Hakim Tafer, Ulrike Muckstein, Christoph Flamm, Peter Stadler, and Ivo Hofacker. Partition function and base pairing probabilities of rna heterodimers. *Algorithms for Molecular Biology*, 1(1):3, 2006.

Erich Bornberg-Bauer and Hue Sun Chan. Modeling evolutionary landscapes: Mutational stability, topology, and superfunnels in sequence space. *Proc Natl Acad Sci USA*, 96(19):10689–10694, 1999.

J. J. Bull, Lauren Ancel Meyers, and Michael Lachmann. Quasispecies Made Simple. *PLoS Computational Biology*, 1(6):0450–0460, 2005.

Christina L. Burch and Lin Chao. Evolution by Small Steps and Rugged Landscapes in the RNA Virus phi6. *Genetics*, 151(3):921–927, 1999.

H. J. Bussemaker, D. Thirumalai, and J. K. Bhattacharjee. Thermodynamic Stability of Folded Proteins against Mutations. *Phys. Rev. Lett.*, 79(18):3530–3533, 1997.

Hue Sun Chan and Erich. Bornberg-Bauer. Perspectives on protein evolution from simple exact models. *Applied Bioinformatics*, 1(3):121–144, 2002.

Francisco M. Codõner, José-Antonio Darós, Ricard V. Solé, and Santiago F. Elena. The Fittest versus the Flattest: Experimental Confirmation of the Quasispecies Effect with Subviral Pathogens. *PLoS Pathogens*, 2(12):1187–1193, 2006.

Matthew C. Cowperthwaite, J. J. Bull, and Lauren Ancel Meyers. Distributions of Beneficial Fitness Effects in RNA. *Genetics*, 170(4):1449–1457, 2005.

Matthew C. Cowperthwaite, J. J. Bull, and Lauren Ancel Meyers. From bad to good: Fitness reversals and the ascent of deleterious mutations. *PLoS Computational Biology*, 2(10):1292–1300, 2006.

James F. Crow and Motoo Kimura. *An Introduction to Population Genetics Theory*. Burgess Publishing Company, 1970.

J. Arjan G. M. de Visser, Joachim Hermisson, Gunter P. Wagner, Lauren Ancel Meyers, Homayoun Bagheri-Chaichian, Jeffrey L. Blanchard, Lin Chao, James M. Cheverud, Santiago F. Elena, Walter Fontana, Greg Gibson, Thomas F. Hansen, David Krakauer, Richard C. Lewontin, Charles Ofria, Sean H. Rice, George von Dassow, Andreas Wagner, and Michael C. Whitlock. Perspective: Evolution and Detection of Genetic Robustness. *Evolution*, 57(9):1959–1972, 2003.

Frederic Delsuc, Henner Brinkmann, and Herve Philippe. Phylogenomics and the Reconstruction of the Tree of Life. *Nature Reviews Genetics*, 6(5):361–375, 2005.

Esteban Domingo. Quasispecies Theory in Virology. *Journal of Virology*, 76(1): 463–465, 2002.

Esteban Domingo. Quasispecies and the development of new antiviral strategies. *Prog Drug Res*, 60:133–158, 2003.

Jennifer A. Doudna. Structural genomics of RNA. *Nature Structural Biology*, 7(11): 954–6, 2000.

M Eigen. Selforganization of matter and the evolution of biological macromolecules. *Naturwissenschaften*, 58(10):465–523, 1971.

Manfred Eigen. On the nature of virus quasispecies. *Trends in Microbiology*, 4(6): 216–218, 1996.

Manfred Eigen and Peter Schuster. *The Hypercycle: A Principle of Natural Self-Organization*. Springer-Verlag, 1979.

Niles Eldredge, John N. Thompson, Paul M. Brakefield, Sergey Gavrilets, David Jablonski, Jeremy B. C. Jackson, Richard E. Lenski, Bruce S. Lieberman, Mark A. McPeek, and III Miller, William. The dynamics of evolutionary stasis. *Paleobiology*, 31(2):133–145, 2005.

C Escarmis, M Davila, and E Domingo. Multiple molecular pathways for fitness recovery of an rna virus debilitated by operation of muller's ratchet. *J Mol Biol*, 285(2):495–505, 1999.

Suzanne Estes, Patrick C. Phillips, Dee R. Denver, W. Kelley Thomas, and Michael Lynch. Mutation Accumulation in Populations of Varying Size: The Distribution of Mutational Effects for Fitness Correlates in Caenorhabditis elegans. *Genetics*, 166(3):1269–1279, 2004.

Walter Fontana and Peter Schuster. A computer model of evolutionary optimization. *Biophysical Chemistry*, 26(2-3):123–147, 1987.

Walter Fontana and Peter Schuster. Shaping Space: the Possible and the Attainable in RNA Genotype-Phenotype Mapping. *Journal of Theoretical Biology*, 194(4): 491–515, 1998a.

Walter Fontana and Peter Schuster. Continuity in evolution: on the nature of transitions. *Science*, 280(5368):1451–1455, 1998b.

Walter Fontana, Danielle A.M. Konings, Peter F. Stadler, and Peter Schuster. Statistics of RNA secondary structures. *Biopolymers*, 33(9):1389–1404, 1993a.

Walter Fontana, Peter F. Stadler, Erich Bornberg-Bauer, Thomas Griesmacher, Ivo L. Hofacker, Manfred Tacker, Pedro Tarazona, Edward D. Weinberger, and Peter Schuster. RNA Folding and Combinatory Landscapes. *Physical Review E*, 47:2083–2099, 1993b.

Sergey Gavrilets. *Fitness Landscapes and the Origin of Species*, volume 41 of *Monographs in Population Biology*. Princeton University Press, 2004.

Greg Gibson and Gunter P. Wagner. Canalization in evolutionary genetics: a stabilizing theory? *Bioessays*, 22(4):372–380, 2000.

John H. Gillespie. Molecular Evolution Over the Mutational Landscape. *Evolution*, 38(5):1116–1129, 1984.

John H. Gillespie. *Population Genetics: A Concise Guide*. Johns Hopkins University Press, Baltimore, 2004.

W. Gruner, U. Giegerich, D. Strothmann, C. Reidys, J. Weber, I. Hofacker, P. Stadler, and P. Schuster. Analysis of RNA sequence structure maps by exhaustive enumeration. I. Neutral Networks. *Monatshefte fur Chemie*, 127:355–374, 1996a.

W. Gruner, U. Giegerich, D. Strothmann, C. Reidys, J. Weber, I. Hofacker, P. Stadler, and P. Schuster. Analysis of RNA sequence structure maps by exhaustive enumeration. II. Structure of neutral networks and shape space covering. *Monatshefte fur Chemie*, 127:375–389, 1996b.

Robin R Gutell, Jung C Lee, and Jamie J Cannone. The accuracy of ribosomal RNA comparative structure models. *Current Opinion in Structural Biology*, 12 (3):301–310, 2002.

Ivo L. Hofacker, Walter Fontana, Peter F. Stadler, L. Sebastian Bonhoeffer, Manfred Tacker, and Peter Schuster. Fast Folding and Comparison of RNA Secondary Structures. *Monatshefte fur Chemie*, 125:167–188, 1994.

Edward C. Holmes and Andres Moya. Is the Quasispecies Concept Relevant to RNA Viruses? *J. Virol.*, 76(1):460–462, 2002.

Martijn A. Huynen, Peter F. Stadler, and Walter Fontana. Smoothness within ruggedness: the role of neutrality in adaptation. *Proc Natl Acad Sci USA*, 93(1): 397–401, 1996.

Marianne Imhof and Christian Schlotterer. Fitness effects of advantageous mutations in evolving *Escherichia coli* populations. *Proc Natl Acad Sci USA*, 98(3):1113–1117, 2001.

Toby Johnson and Nick H. Barton. The Effect of Deleterious Alleles on Adaptation in Asexual Populations. *Genetics*, 162(1):395–411, 2002.

Gerald F. Joyce. RNA Structure: Ribozyme Evolution at the Crossroads. *Science*, 289(5478):401–402, 2000.

Yuseob Kim and Wolfgang Stephan. Joint Effects of Genetic Hitchhiking and Background Selection on Neutral Variation. *Genetics*, 155(3):1415–1427, 2000.

Motoo Kimura. Evolutionary Rate at the Molecular Level. *Nature*, 217(5129): 624–626, 1968.

Mark Kirschner and John Gerhart. Evolvability. *Proceedings of the National Academy of Sciences*, 95(15):8420–8427, 1998.

Alexey S. Kondrashov, Shamil Sunyaev, and Fyodor A. Kondrashov. Dobzhansky-Muller incompatibilities in protein evolution. *Proc Natl Acad Sci USA*, 99(23): 14878–14883, 2002.

Rob J. Kulathinal, Brian R. Bettencourt, and Daniel L. Hartl. Compensated Deleterious Mutations in Insect Genomes. *Science*, 306(5701):1553–1554, 2004.

Hao Li, Robert Helling, Chao Tang, and Ned Wingreen. Emergence of preferred structures in a simple model of protein folding. *Science*, 273(5275):666–669, 1996.

Mark Lunzer, Stephen P. Miller, Roderick Felsheim, and Antony M. Dean. The Biochemical Architecture of an Ancient Adaptive Landscape. *Science*, 310(5747): 499–501, 2005.

David H. Mathews. Revolutions in RNA Secondary Structure Prediction. *Journal of Molecular Biology*, 359(3):526–532, 2006.

David H Mathews and Douglas H Turner. Prediction of RNA secondary structure by free energy minimization. *Current Opinion in Structural Biology*, 16(3):270–278, 2006.

David H. Mathews, Jeffrey Sabina, Michael Zuker, and Douglas H. Turner. Expanded sequence dependence of thermodynamic parameters improves prediction of rna secondary structure. *Journal of Molecular Biology*, 288(5):911–940, 1999.

David H. Mathews, Matthew D. Disney, Jessica L. Childs, Susan J. Schroeder, Michael Zuker, and Douglas H. Turner. Incorporating chemical modification constraints into a dynamic programming algorithm for prediction of RNA secondary structure. *Proc Natl Acad Sci USA*, 101(19):7287–7292, 2004.

John S. Mattick and Igor V. Makunin. Non-coding RNA. *Human Molecular Genetics*, 15(R1):R17–R29, 2006.

JS McCaskill. The equilibrium partition function and base pair binding probabilities for RNA secondary structure. *Biopolymers*, 29(6-7):1105–1109, 1990.

Lauren Ancel Meyers and J. J. Bull. Fighting change with change: adaptive variation in an uncertain world. *Trends in Ecology and Evolution*, 17(12):551–557, 2002.

Lauren Ancel Meyers, Jennifer F. Lee, Matthew Cowperthwaite, and Andrew D. Ellington. The Robustness of Naturally and Artificially Selected Nucleic Acid Secondary Structures. *Journal of Molecular Evolution*, 58(6):618–625, 2004.

Andres Moya, Santiago F. Elena, Alma Bracho, Rosario Miralles, and Eladio Barrio. The evolution of RNA viruses: A population genetics view. *Proc Natl Acad Sci USA*, 97(13):6967–6973, 2000.

R. Niwa and F.J. Slack. The evolution of animal microRNA function. *Curr. Opin. Genet. Dev.*, in press., 2007.

H. Allen Orr. The Population Genetics of Adaptation: The Adaptation of DNA Sequences. *Evolution*, 56(7):1317–1330, 2002.

H. Allen Orr. The Population Genetics of Adaptation on Correlated Fitness Landscapes: The Block Model. *Evolution*, 60(6):1113–1124, 2006.

H. Allen Orr. The Distribution of Fitness Effects Among Beneficial Mutations. *Genetics*, 163(4):1519–1526, 2003.

John Parsch, John M. Braverman, and Wolfgang Stephan. Comparative Sequence Analysis and Patterns of Covariation in RNA Secondary Structures. *Genetics*, 154(2):909–921, 2000.

J. R. Peck. A Ruby in the Rubbish: Beneficial Mutations, Deleterious Mutations and the Evolution of Sex. *Genetics*, 137(2):597–606, 1994.

Andrew D Peters and Sarah P Otto. Liberating genetic variance through sex., 2003.

Art Poon and Lin Chao. The Rate of Compensatory Mutation in the DNA Bacteriophage ϕX174. *Genetics*, 170(3):989–999, 2005.

Art Poon, Bradley H. Davis, and Lin Chao. The Coupon Collector and the Suppressor Mutation: Estimating the Number of Compensatory Mutations by Maximum Likelihood. *Genetics*, 170(3):1323–1332, 2005.

Christine Queitsch, Todd A. Sangster, and Susan Lindquist. Hsp90 as a capacitor of phenotypic variation. *Nature*, 417(6889):618–624, 2002.

Darin R. Rokyta, Paul Joyce, Brian B. Caudle, and Holly A. Wichman. An empirical test of the mutational landscape model of adaptation using a single-stranded DNA virus. *Nature Genetics*, 37(4):441–444, 2005.

Daniel E. Rozen, J. Arjan G. M. de Visser, and Philip J. Gerrish. Fitness Effects of Fixed Beneficial Mutations in Microbial Populations. *Current Biology*, 12(12): 1040–1045, 2002.

S. L. Rutherford and S. Lindquist. Hsp90 as a capacitor for morphological evolution. *Nature*, 396(6709):336–342, 1998.

Rafael Sanjuan, Andres Moya, and Santiago F. Elena. The distribution of fitness effects caused by single-nucleotide substitutions in an RNA virus. *Proc Natl Acad Sci USA*, 101(22):8396–8401, 2004.

Rafael Sanjuan, Javier Forment, and Santiago F. Elena. In Silico Predicted Robustness of Viroids RNA Secondary Structures. I. The Effect of Single Mutations. *Mol Biol Evol*, 23(7):1427–1436, 2006a.

Rafael Sanjuan, Javier Forment, and Santiago F. Elena. In Silico Predicted Robustness of Viroid RNA Secondary Structures. II. Interaction between Mutation Pairs. *Mol Biol Evol*, 23(11):2123–2130, 2006b.

Erik A. Schultes and David P. Bartel. One Sequence, Two Ribozymes: Implications for the Emergence of New Ribozyme Folds. *Science*, 289:448–452, 2000.

Peter Schuster and Walter Fontana. Chance and necessity in evolution: lessons from RNA. *Physica D*, 133(1-4):427–452, 1999.

Peter Schuster, Walter Fontana, Peter F. Stadler, and Ivo L. Hofacker. From sequences to shapes and back: a case study in RNA secondary structures. *Proceedings of the Royal Society of London B*, 255(1344):279–284, 1994.

John Maynard Smith. Natural selection and the concept of a protein space. *Nature*, 225(5232):563–564, 1970.

Barbel M. R. Stadler, Peter Stadler, Gunter P. Wagner, and Walter Fontana. The topology of the possible: Formal spaces underlying patterns of evolutionary change. *Journal of Theoretical Biology*, 213(2):241–74, 2001.

Heather L. True, Ilana Berlin, and Susan L. Lindquist. Epigenetic regulation of translation reveals hidden genetic variation to produce complex traits. *Nature*, 431(7005):184–187, September 2004.

E van Nimwegen, JP Crutchfield, and M Huynen. Neutral evolution of mutational robustness. *Proc Natl Acad Sci USA*, 17(76):9716–9720, 1999.

Michele Vendruscolo, Amos Maritan, and Jayanth R. Banavar. Stability threshold as a selection principle for protein design. *Phys. Rev. Lett.*, 78(20):3967–3970, 1997.

C. H. Waddington. Canalization of Development and Genetic Assimilation of Acquired Characters. *Nature*, 183(4676):1654–1655, 1959.

C.H. Waddington. Genetic Assimilation of an Acquired Character. *Evolution*, 7(2): 118–126, 1950.

A. Wagner and Peter F. Stadler. Viral RNA and evolved mutational robustness. *Journal of Experimental Zoology*, 285(2):119–127, 1999.

Andreas Wagner. Robustness, evolvability, and neutrality. *FEBS Letters*, 579(8): 1772–1778, 2005.

Gunter P. Wagner, Ginger Booth, and Homayoun Bagheri-Chaichian. A population genetic theory of canalization. *Evolution*, 51(2):329–347, 1997.

M. Waterman. Secondary structure of single-stranded nucleic acids. In *Studies on foundations and combinatorics, Advances in mathematics supplementary studies*, volume 1, pages 167–212. Academic Press N.Y., 1978.

Daniel M Weinreich and Lin Chao. Rapid evolutionary escape by large populations from local fitness peaks is likely in nature. *Evolution*, 59(6):1175–82, 2005.

Daniel M. Weinreich, Nigel F. Delaney, Mark A. DePristo, and Daniel L. Hartl. Darwinian Evolution Can Follow Only Very Few Mutational Paths to Fitter Proteins. *Science*, 312(5770):111–114, 2006.

Michael C Whitlock, Patrick C Phillips, Francisco B.-G. Moore, and Stephen J Tonsor. Multiple Fitness Peaks and Epistasis. *Annual Review of Ecology and Systematics*, 26:601–629, 1995.

Claus Wilke. Quasispecies theory in the context of population genetics. *BMC Evolutionary Biology*, 5(1):44, 2005.

Claus Wilke, Richard Lenski, and Christoph Adami. Compensatory mutations cause excess of antagonistic epistasis in rna secondary structure folding. *BMC Evolutionary Biology*, 3(1):3, 2003.

Claus O. Wilke, Jia Lan Wang, Charles Ofria, Richard E. Lenski, and Christoph Adami. Evolution of digital organisms at high mutation rates leads to survival of the flattest. *Nature*, 412(6844):331–333, 2001.

Wade C. Winkler and Ronald R. Breaker. Regulation of Bacterial Gene Expression by Riboswitches. *Annual Review of Microbiology*, 59(1):487–517, 2005.

S. Wright. The roles of mutation, inbreeding, crossbreeding and selection in evolution. *Proceedings of the VI International Congress of Genetrics*, 1:356–366, 1932.

Stephan Wuchty, Walter Fontana, Ivo L. Hofacker, and Peter Schuster. Complete suboptimal folding of RNA and the stability of secondary structures. *Biopolymers*, 49(2):145–165, 1999.

Emile Zuckerkandl and Linus Pauling. Molecular disease, evolution, and genetic heterogeneity. In M. Kasha and B. Pullman, editors, *Horizons in Biochemistry*, pages 189–225. Academic Press N.Y., 1962.

M Zuker and P Stiegler. Optimal computer folding of large RNA sequences using thermodynamics and auxiliary information. *Nucl. Acids. Res.*, 9(1):133–148, 1981.

Michael Zuker. On Finding All Suboptimal Foldings of an RNA Molecule. *Science*, 244(4900):48–52, 1989.

Chapter 2

Distributions of Beneficial Fitness Effects in RNA

The distribution of the fitness effects of beneficial mutations is of special interest in evolutionary biology, as it profoundly influences the rate and course of adaptation. In turn, adaptive dynamics influence competition, the propensity toward extinction and maintenance in communities, speciation and a plethora of other macroevolutionary processes. It seems almost a truism that the array of beneficial fitness effects must depend idiosyncratically on the biological details of an organism and its environment. Nonetheless, population geneticists have begun to derive generalities describing these distributions that may be at least partly independent of biology.

Gillespie (1983) offered the beginnings of a general theory for the distribution of beneficial fitness effects with the following argument: if the wild-type allele is sufficiently fit, then it resides far in the right-hand tail of the distribution of mutational effects. Any beneficial mutations lie further in the tail, hence their distribution falls in the domain of extreme-value theory (EVT) from statistics. Extreme-value theory tells us that if the underlying distribution of allelic fitnesses is "well-behaved"(See Leadbetter et al. (1983) for a detailed treatment) in several respects, then the spacings between the highest fitnesses in an appropriately large random sample are independent, exponentially-distributed random variables (Gumbel, 1958; Weissman, 1978). Therefore, if one assumes that the few beneficial mutants of a high-fitness wildtype allele are a random sample from an underlying distribution of allelic fitnesses, then, when the mutant alleles are rank ordered by size, the spacings between

the consecutive beneficial alleles should be approximately exponential.

Orr (2002; 2003) expanded upon Gillespie's work and derived two potentially important corollaries: (1) the distribution of beneficial fitness effects (that is, the difference between the mutant fitness and the wildtype fitness) is exponential and (2) wildtype genotypes differing in the number of beneficial mutations accessible by a single mutation (henceforth, "one-step beneficial mutations") have nearly identical distributions of beneficial fitness effects. These properties were proposed to be general for all evolving systems, provided that the fitness function falls under the purview of EVT and the fitness of the wildtype genotype is greater than almost all mutant alleles. Gillespie and Orr proposed that these are reasonable assumptions for populations that have recently experienced an environmental shift, which has caused the previously optimized wildtype to become slightly suboptimal.

A fundamental assumption of recent adaptation theory is that the fitnesses of a wild-type genotype and its mutant genotypes are not correlated. This assumption conflicts with known properties of at least some biological systems (Atchley et al., 2000; Parsch et al., 2000) and, in particular, with the RNA fitness function used in this study (Fontana et al., 1993). However, the results of EVT are known to be robust to certain types of non-independence among the values in the distribution (Leadbetter et al., 1983). By extension, adaptation theory should be able to tolerate at least modest amounts of correlation among fitness values. Indeed, the predictions of the Gillespie-Orr theory regarding "one-step" beneficial mutations are robust to modest correlation, although they break down with strong correlation (H.A. Orr, pers. comm.).

Experimental tests of these theories are extremely difficult to conduct, because one must measure the fitness of all beneficial mutations for a large number of genotypes. Nonetheless, several groups have recently put forth significant efforts to characterize the distributions of beneficial fitness effects in experimental populations of bacteria and viruses (Imhof and Schlotterer, 2001; Rozen et al., 2002). However, as pointed out by Orr (2003), these experiments are not able to test the theory in a comprehensive manner. The approach used by Sanjuan et al. (2004) is perhaps the most promising method to directly test the Orr-Gillespie theory because known point mutations of a viral clone were constructed *in vitro*. Yet, despite an incredible empirical effort by the respective groups, all of these studies utilize a relatively small number of genotypes, which limits their statistical power.

Given the potential generality of the Gillespie-Orr theory, it seemed important to conduct a rigorous test of its predictions. Here we describe a quasi-empirical approach in which we computationally estimate the fitness of RNA molecules based on the similarity of predicted secondary structures to target structures. This system is a computationally tractable and biologically grounded model that has previously provided insights into evolutionary dynamics and fitness landscapes (Ancel and Fontana, 2000; Fontana and Schuster, 1998; Huynen et al., 1996; Meyers et al., 2004; van Nimwegen et al., 1999; Wilke and Adami, 2001). In this study, we measured the fitnesses of millions of genotypes and found that the fitnesses of random genotypes follow a Gumbel-type distribution. We found that the distributions of beneficial fitness effects had a single characteristic shape throughout genotype space. The characteristic shape, however, significantly deviates from exponential and the means of the distributions vary with the fitness of the parental genotype.

2.1 Model

2.1.1 RNA folding

In many systems, molecular shape is the most important component of function, and hence fitness. Single-stranded RNA molecules carry electrostatic charges that cause them to fold into functional, three-dimensional shapes (tertiary structure). RNA three-dimensional folding is still poorly understood. Yet, the secondary structure of an RNA molecule, which provides the primary scaffold for tertiary structure, is relatively well understood and can be rapidly predicted. Secondary structure results from the formation of complementary base pairs and can be reliably predicted for arbitrary short molecules based on free-energy minimization (Nussinov and Jacboson, 1980; Waterman, 1978; Zuker and Stiegler, 1981). Two limitations of this approach must be noted: (1) free-energy minimization may not be the only force driving secondary structure formation, and (2) pseudo-knots, a common secondary structural motif, are disallowed because their formation is poorly understood. For this study, we used the dynamic programming implementation in the Vienna RNA package for these calculations (Hofacker et al., 1994).

In particular, we estimated the set of lowest free energy structures of an RNA molecule using an extension (Wuchty et al., 1999) of standard thermodynamic

prediction algorithms (Nussinov and Jacboson, 1980; Waterman, 1978; Zuker and Stiegler, 1981; Zuker, 1989). We refer to this ensemble of low free energy shapes as the *suboptimal repertoire* of a molecule, which is estimated by suboptimal folding. Suboptimal folding ignores energy barriers among alternative states and assumes that a molecule equilibrates among all shapes with free energy within $5kT$ of the ground state, where k is the Boltzmann constant and T is the temperature. This is approximately equivalent to 3 kcal/mol at 37^o C, and corresponds to the breaking of 2 G-C/G-C stacking interactions (base pairs). We used the Boltzmann factor to estimate the probability of any particular shape in the suboptimal repertoire of an RNA molecule. For any specific shape σ, the Boltzmann probability of σ, $p_\sigma = e^{-\Delta G_\sigma/kT}/Z$, measures the relative stability of σ with respect to the entire repertoire. Z is the partition function (McCaskill, 1990) of a molecule and is computed thus:

$$Z = \sum_{\sigma} e^{-\Delta G_\sigma/kT} \tag{2.1}$$

where ΔG_σ is the free energy of σ and the sum includes all shapes in the suboptimal repertoire. Assuming equilibration, p_σ estimates the probability of finding σ in a large sample of identical RNA molecules and approximates the amount of time any given molecule spends in σ. The minimum free energy conformation is the most probable shape in any suboptimal repertoire.

For any sequence, we can thereby rapidly compute its suboptimal repertoire and the approximate probability of each shape in the repertoire. This constitutes a biologically-grounded map from genotype (sequence) to phenotype (shape ensemble).

2.1.2 Measuring fitness

Our computational RNA genotype-to-phenotype model is able to accommodate a variety of biologically realistic fitness functions. For example, RNA molecules have been selected experimentally to bind a ligand with high affinity (Ellington, 1994). We cannot yet explicitly model such binding interactions, but we can approximate such systems by assuming there exists an ideal secondary structure and the nearer the shape ensemble of a molecule is to that ideal the better it will bind (Ancel and Fontana, 2000; Schuster et al., 1994). In our model, at equilibrium, a fraction p_σ of

a large number of identical sequences assumes shape σ and binds to a ligand with a corresponding constant.

For each shape in the suboptimal repertoire, we used a hyperbolic decaying function $f(\sigma)$ to calculate a selective value based on how well σ matched a target shape:

$$f(\sigma) = \frac{1}{\alpha + (d(\sigma, t)/L)^{\beta}} \tag{2.2}$$

where α and β are scaling constants, $d(\sigma, t)$ is the Hamming distance between the current shape and the target shape, and $L = 76$ is the length of the sequence. The value $\alpha = 1$ was chosen to scale the fitness values between ≈ 1 and 100; $\beta = 1$ was chosen to produce the hyperbolic decaying shape of the selective-value function and maintain consistency with prior work (Ancel and Fontana, 2000; Fontana and Schuster, 1998). By scaling the distance with a hyperbolic decaying function, we modeled strong selection for target structure.

We chose a nucleotide sequence of length 76 for several reasons. This length has 228 one-step mutants, which should be sufficiently large for EVT to apply (Gillespie, 1983). The free-energy minimization algorithms are most accurate for short sequences, thus our results will not be confounded by folding errors. This length also gives us computational tractability – we can measure the fitness of every one-step mutant sequence in a reasonable time. Finally, most tRNA molecules in natural organisms are approximately 76 nucleotides in length.

The overall fitness, W, of a molecule is the average of the selective values of the shapes in its suboptimal repertoire, each weighted by its probability, $W = \sum_{\sigma} f(\sigma) p_{\sigma}$. The range of fitness values (W) possible given our choice of parameters is 0.99 - 100. This function simultaneously considers secondary structure and thermodynamic stability such that the highest fitness molecules will be those that fold stably into minimum free energy shapes that look much like the target shape. This fitness function is essentially continuous because no two sequences have identical suboptimal repertoires.

2.1.3 Obtaining low-rank genotypes

The rank of a wildtype allele (i) is simply its position in a set of fitnesses that are rank ordered from 1 (most fit) to $m+1$ (least fit), where m is the number of single-mutant sequences (Orr, 2003). The Gillespie-Orr theory depends on the fitness of

the wildtype allele being higher than nearly all of its 1-step mutants, that is, it is based on genotypes with very few 1-step mutations of higher fitness ($i << m + 1$). Our results are based on large samples of low-rank genotypes, which are relatively rare and therefore difficult to find by random sampling. Thus, we generated samples of low-rank genotypes using adaptive walks. We emphasize that these walks were not intended to simulate biological evolution, but simply served as a heuristic for locating appropriate sequences for our study.

Adaptive walks were initiated with random RNA sequences with no base-composition bias. We refer to the sequence at the current step of an adaptive walk as the wildtype sequence. At each step of the walk, the fitness of every one-step mutant of the current wildtype sequence was measured as described above. We randomly selected a single one-step *beneficial* mutant sequence to be the next wildtype sequence. The process was repeated until the wildtype sequence arrived at a local optimum (i.e. no mutations were beneficial). A single wildtype allele of each rank class was selected at random from each adaptive walk to obtain a set of suitable low-rank genotypes. The shape of the distributions of beneficial fitness effects we obtained was robust to two different types of adaptive walks (randomly selected beneficial mutant vs selecting the best mutant at each step, data not shown), thus our results appear robust to the choice of an adaptive walk model.

2.1.4 Generating high-fitness sequences

We generated sets of high-fitness molecules using an algorithm that produces sequences which specifically fold into a particular secondary structure. The program, 'RNAinverse' in the ViennaRNA package, initially divides the target shape into several smaller regions and the starting sequence into segments, which each correspond to a small region of the target structure (Hofacker et al., 1994). Each segment of the starting sequence is individually optimized through single base changes or compatible base-pair changes. Once all of the separate regions of the starting sequence have been individually optimized the full sequence is created and further optimized. This results in molecules that fold into the specified minimum free energy structure, but may or may not have a high degree of thermodynamic stability.

2.1.5 Estimation of exponential parameters

Gillespie (1983) and Orr (2003) proposed that the distribution of absolute fitness differences among the few fittest alleles will follow an exponential distribution (density $\lambda e^{-\lambda x}$, where λ is the exponential parameter characterizing the distribution). The mean μ of the distribution is $1/\lambda$ and can be estimated by maximum likelihood as

$$\hat{\mu} = \frac{\sum_n (W_j - W_i)}{n} \tag{2.3}$$

where W_j is the fitness of the j-th beneficial mutation, W_i is the fitness of the wildtype allele and n is the number of alleles, such that $W_j > W_i$. Since the estimate of the exponential parameter as $1/\hat{\mu}$ is biased, we work with the estimate of the mean, which has the advantage of being more interesting biologically than its reciprocal. Another useful property of an exponential distribution is that a log-linear plot of the total observations greater than x yields a straight line, and deviations from exponential are thus easily observed in such a plot [CDF: $P\{X > x\} = e^{-\lambda x}; ln(e^{-\lambda x}) = -\lambda x$].

Orr (2002) claimed that distributions of *fixed* beneficial fitness effects in actual biological systems may deviate from exponentiality at the left end (small benefit mutations) but obey exponentiality in the right end (large benefit mutations). Left truncation of the distributions of *new* beneficial fitness effects may therefore yield the exponential property even though the full distribution may not. To estimate μ of the full distribution from a truncated distribution, we first compute the mean μ_T of the truncated distribution

$$\mu_T = E(x) = \frac{\int_T^\infty x\lambda e^{-\lambda x} dx}{\int_T^\infty \lambda e^{-\lambda x} dx} = \mu + T \tag{2.4}$$

where T is the truncation threshold. Thus, an unbiased estimate of the mean $\hat{\mu}$ of the full distribution is

$$\hat{\mu} = \mu_T - T \tag{2.5}$$

If the full distribution is exponential, then $\hat{\mu}$ is unaffected by truncation when corrected in this fashion.

2.2 Results

Gillespie and Orr proposed that EVT could be applied to describe the distribution of fitness effects of beneficial mutations to high-fitness genotypes. The use of EVT rests on several assumptions: (1) allelic fitnesses are drawn from an underlying well-behaved distribution of allelic fitnesses, (2) the one-step mutants of a genotype are an i.i.d. random sample from this distribution, and (3) the wildtype allele lies well into the right-hand tail of the underlying distribution, thus the fitness effects of beneficial one-step mutations of the wildtype allele will be further in the tail. We therefore set out to rigorously test the fundamental predictions of the theory.

2.2.1 The RNA fitness distribution obeys EVT

In order to determine whether the fitness distribution for random RNA molecules belongs to one of the three classes of extreme-value distributions, we measured the fitnesses of approximately 3.6 million random sequences. The distribution of fitnesses in this set of genotypes shows a strong peak at $W \approx 1.2$ and the fraction of sequences with $W > 3.0$ is less than 10^{-4} (**Figure 2.1**). Any sequences with $W > 3.0$ would be expected to be sufficiently far into the tail to be in the domain of EVT.

A fitness difference Δ_i is the absolute fitness difference between the alleles of rank i and $i + 1$ in a set of allelic fitnesses ranked from 1 (most fit) to N (least fit) (Orr, 2003). For the top few i, EVT predicts Δ_i to be asymptotically exponentially distributed and $\mathrm{E}(\Delta_i) = \mathrm{E}(\Delta_1)/i$. The set of 3.6 million sequences was randomly divided into 15,880 subsets of 229 sequences. The number 229 was chosen because it is the number of one-step mutants plus the wildtype allele of a 76-nucleotide sequence, which we consider in the adaptive walks discussed below. We measured Δ_1, Δ_2 and Δ_3 for each set of 229 random sequences. The inset to **Figure 2.1** confirms the exponential distribution of Δ_1, Δ_2 and Δ_3. Δ_1 was found to be 1.99 and 2.87 times the size of Δ_2 and Δ_3, respectively, which are close to the expected values 2 and 3, respectively.

We find the fitnesses follow a Gumbel-type distribution, consistent with a major assumption of current adaptation theory. Thus, if one-step mutational neighborhoods are essentially random samples of sequences, the distribution of beneficial fitness effects should be similar to that found for sets of random sequences.

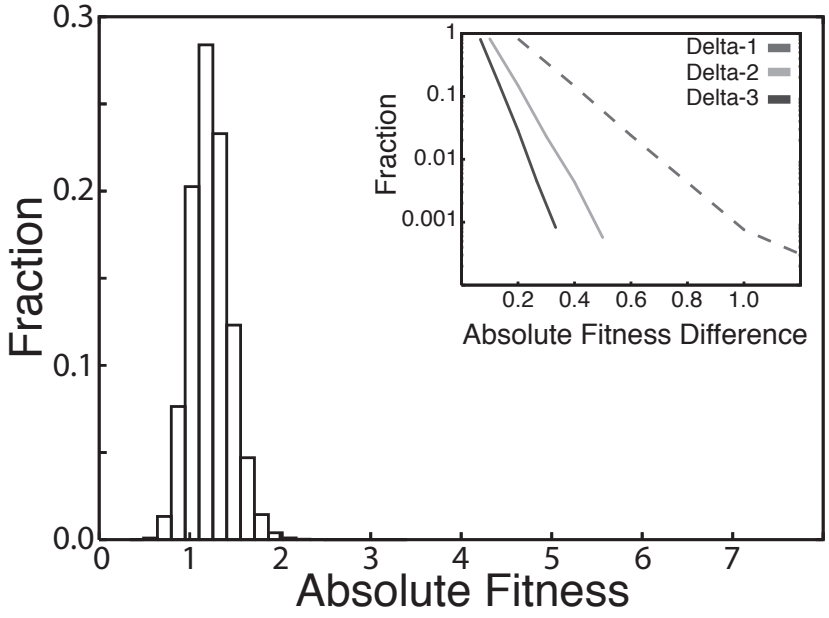

Figure 2.1: The distribution of absolute fitness of 3,636,520 random sequences. The data was divided into 10 equal-width bins and plotted so that the center of the column on the x-axis is at the upper bin bound. The y-axis is the fraction of sequences falling into a particular bin. Inset: the distribution of Δ_1, Δ_2 and Δ_3 (see text) for 15,880 sets of 229 absolute fitness values. The x-axis is the fitness effect and the y-axis is the fraction of fitnesses falling a particular bin on a log scale. The bin width is 0.2 for Δ_1, 0.1 for Δ_2, 0.67 for Δ_3.

2.2.2 Distribution of fitness effects with random starting points

The rank (i) of a genotype is defined as the position of that genotype in a set of allelic fitnesses ranked from 1 (most fit) to m (least fit), where m is the number of single-mutant sequences (Orr, 2003). An allele of rank i has $i - 1$ one-step beneficial mutations. The distribution of beneficial mutations was analyzed using sequences of rank $i \leq 4$, to be confident that they would be in the domain of EVT. The wildtype genotypes were generated with adaptive walks beginning with random starting genotypes. The mean starting fitness of the random sequences was 1.1 ($\pm$ 0.002 SE). The mean ending fitness was 3.4 ($\pm$ 0.01 SE). The distributions of beneficial effects were produced using genotypes from 5721 adaptive walks that attained a final absolute fitness between 3 and 9. The average walk accrued 84.4 ($\pm$

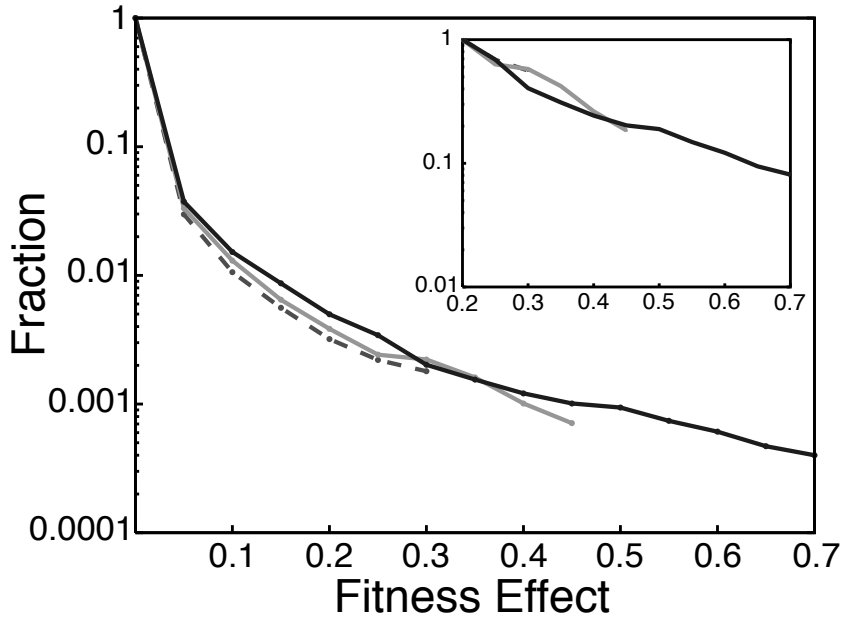

Figure 2.2: The cumulative distribution of beneficial fitness effects of wildtype alleles from random walks. Data are from 5721 adaptive walks starting from random sequences - one wildtype genotype per rank per walk. The x-axis is the size of the beneficial fitness effect and the y-axis is the fraction of mutants with fitness greater than the x-axis value on a log scale. The dashed curve is $i = 2(n = 5004)$, the light gray curve is $i = 3(n = 9908)$ and the black curve is $i = 4(n = 14871)$. Inset: exponential behavior when truncated at $S = 0.20$. Style and color of curves matches the main figure.

0.28 SE) substitutions before reaching a local optimum.

The set of genotypes used to estimate the distribution of beneficial fitness effects was produced by randomly selecting a single sequence for every rank class $i \leq 4$ from each adaptive walk. This produced a unique data set for each rank class and ensured the statistical independence of the observations within each data set. By measuring $S = W_j - W_i$, the difference between the fitnesses of each high-fitness mutant genotype and the wildtype on an absolute scale, we estimated the distribution of beneficial fitness effects for each rank class. The distributions of beneficial effects deviate from exponential by having an excess of small-sized mutations (**Figure 2.2**). For each wildtype rank examined, at least 80% of the beneficial mutations increase fitness by less than 0.01, on an absolute scale.

Inspection of **Figure 2.2** suggests that the distributions may be nearly exponential for the larger S values. Indeed, when the distribution of effects is truncated to $S > 0.2$, this class of mutations appears approximately exponential (**Figure 2.2**, inset). However, it must be emphasized that the genotypes with $S > 0.2$ are a very small fraction of the full distribution ($< 0.5\%$). Consistent with Orr's assertions, the ML estimate of the means of the truncated distributions are statistically indistinguishable for the different rank classes [$p = 0.71 (i = 2, 3)$ and $p = 0.88 (i = 3, 4)$, Wilcoxon-Mann-Whitney]. In contrast to the theory, the means of the full distributions for different ranks are significantly different [$p < 2.2 \times 10^{-16}$ $(i = 2, 3)$ and $p < 2.2 \times 10^{-16}$ $(i = 3, 4)$, Wilcoxon-Mann-Whitney].

2.2.3 Distribution of fitness effects in high-fitness space

The fitnesses attained at the end of the adaptive walks started from random genotypes were low relative to the maximum possible fitness of 100, thus these data do not represent regions of sequence space with high-fitness genotypes. To evaluate mutational effects in high-fitness regions of sequence space, we used inverse folding to generate a large set of sequences with secondary structures that nearly or perfectly matched the target structure. These sequences were used to start 8390 adaptive walks (referred to as "high-fitness walks"). We only considered walks in which the final sequence attained a fitness greater than 20, giving a subset of 6959 adaptive walks. The mean final fitness attained in this subset of walks was 56.71 ($\pm$0.21, SE).

Using a single sequence of each rank $i \leq 4$ from each walk, we generated the distribution of beneficial effects as described for the random walks (**Figure 2.3**). The entire spectrum of beneficial effects is not exponentially distributed, again because of an excess of small fitness effect mutations. Furthermore, the fitness effects for the mutants of the high-fitness genotypes are on average greater than for the mutants of the random-walk genotypes. The larger effect mutations resulted in the much faster rate of adaptation of the sequences in high-fitness space: the average size of a fixed mutation was significantly larger for the high-fitness walks than the random walks (high-fitness walks: 1.034 ± 0.004; random walks: 0.034 ± 0.0001). The rate of adaptation, however, does not correspond to a rate obtained in a truly evolutionary process, but the comparison of relative rates is meaningful nonetheless.

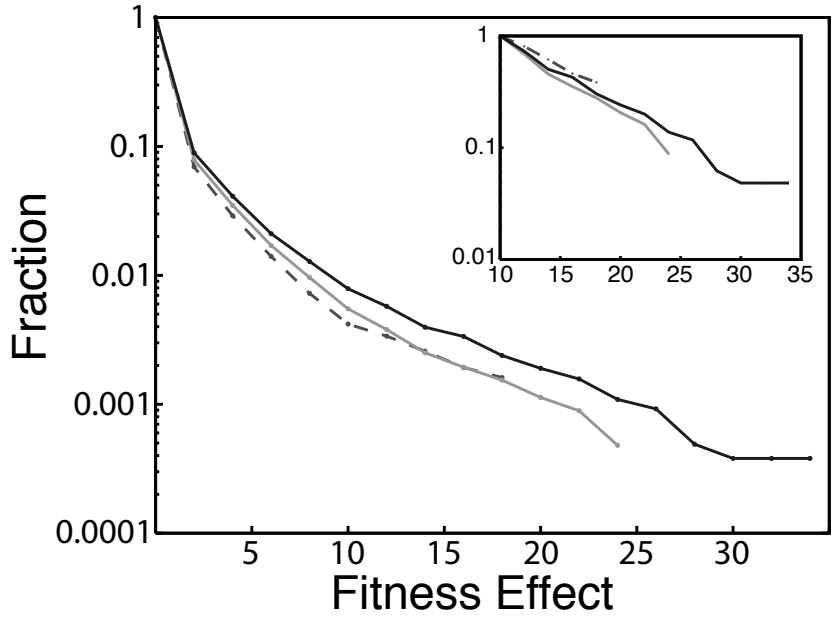

Figure 2.3: The cumulative distribution of all one-step beneficial fitness effects of wildtype alleles from the high-fitness walks. Data are from 6959 adaptive walks starting near fitness optima - one wildtype genotype per rank per walk. The x-axis is the size of the beneficial fitness effects and the y-axis is the fraction of mutants with fitness greater than the x-axis value on a log scale. The dashed curve is $i = 2(n = 6204)$, the light gray curve is $i = 3(n = 12374)$ and the black curve is $i = 4(n = 18432)$. Inset: exponential behavior when truncated at $S = 10.0$. Style and color of curves matches the main figure.

2.2.4 Deviation from exponential behavior

To compare the distributions of beneficial fitness effects in the different regions of sequence space, we progressively truncated the distributions to determine the minimum threshold required to achieve exponentiality. The motivation for this approach is that the appropriate truncation value is not obvious by inspection of the plots in **Figures 2.2** and **2.3**. Thus, for each distribution, we plotted the estimated mean S value for progressively larger truncation values and identified the point at which the estimate of the mean asymptotes. Any systematic variation in the mean and, by extension, the exponential parameters will appear as variation in the asymptotic values.

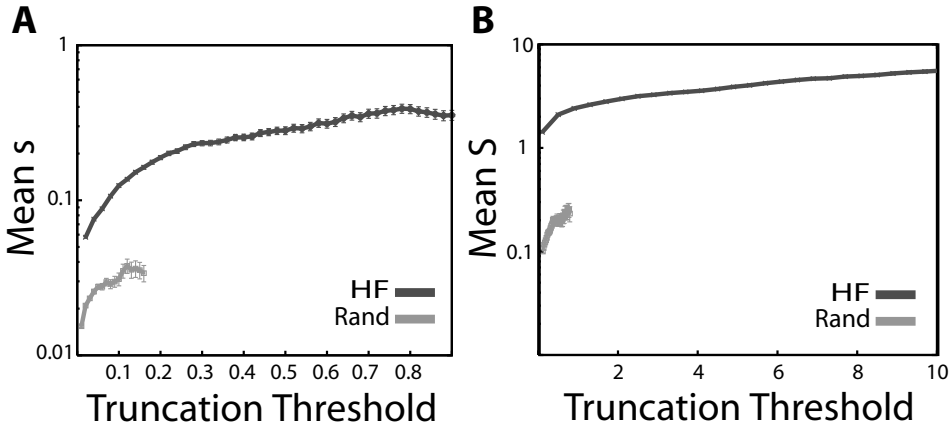

Figure 2.4: The effect of truncation on the estimated mean beneficial effect. The distributions become approximately exponential when the curve shown here asymptotes. The upper plot is the estimate of the mean using absolute fitness differences. The lower plot is the estimate based on s values.

The truncated distributions of the two sets of sequences are vastly different (**Figure 2.4**). The high-fitness sequences maintain a significantly higher mean fitness effect than the random sequences and become exponential at a significantly higher threshold ($S = 0.20$ for random walks; $S = 10.0$ for high-fitness walks). We have included the comparison between S (top panel **Figure 2.4**) and s (bottom panel **Figure 2.4**). Neither fitness measure removes the non-exponentiality nor the difference in fitness effects in the two regions of genotype space. Therefore, the distributions of beneficial fitness effects differ among the two regions of sequence space.

2.2.5 Decline in mean s during walks

So far we have considered the absolute difference in fitness (S) between the wildtype and its mutants. Now we consider the relative fitness difference between the genotypes (s), which is defined as the absolute fitness difference between the mutant and wildtype alleles normalized to the absolute fitness of the wildtype allele. We monitored the change in s during an adaptive walk by measuring the mean size of all new beneficial effects in the one-step neighborhood of the wildtype genotypes

(**Figure 2.5**). We only considered wildtype alleles with $i \leq 4$ for this analysis. The average s in the mutant neighborhood declined during the course of an adaptive walk, demonstrating that small benefit mutations come to dominate the landscape with the approach toward a local optimum. Not surprisingly, the mutants of the "high-fitness" genotypes had higher s values during most stages of the adaptive walks because of the large S values observed.

The important but perhaps obvious result is that the mean of the distribution of beneficial effects declines as the adaptive walk progresses. Early in the course of a walk, large s mutations exist permitting adaptation to proceed quickly. As the adapting sequence approaches a local optima, the possible s values become progressively smaller thus slowing adaptation. Thus, the distribution of beneficial fitness effects changes during the course of an adaptive walk, supporting recent theoretical predictions (Orr, 2002, 1998). This result is in agreement with the theoretical predictions of Fisher's geometric model of adaptation (Fisher, 1930) and empirical studies of viral adaptation (Burch and Chao, 1999).

2.3 Discussion

Gillespie (1983) pioneered a theory of adaptation for populations that are displaced from a fitness optima by an environmental change. He argued that the wildtype allele would remain sufficiently far in the extreme right-hand tail of the distribution of allelic fitnesses that the fitness of any beneficial mutants would be within the domain of extreme-value theory. This theory tells us that the differences between consecutive rank-ordered extreme values from a randomly selected set of values, should follow an exponential distribution. Orr (2002; 2003) then used this theory to argue that the distribution of beneficial fitness effects for genotypes in the extreme right-hand tail of the fitness distribution would be exponential, with a single exponential parameter governing all such genotypes (Orr, 2003).

This theory is potentially very important for both artificial and natural evolution. It offers a framework for predicting the outcome of adaptation in response to environmental challenges such as pharmaceuticals, pesticides, and herbicides. To date, the predictions of the model have received mixed experimental support (Imhof and Schlotterer, 2001; Rozen et al., 2002; Sanjuan et al., 2004), but these types of studies are generally based on small sample sizes of limited statistical power and

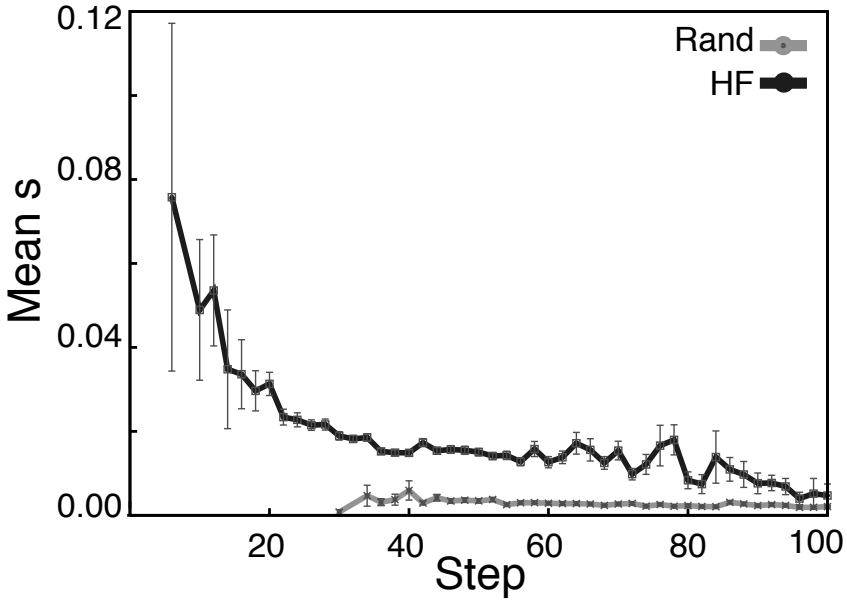

Figure 2.5: Mean s for all beneficial mutations in the neighborhood of $R \leq 4$ wild-type sequences across the length of an adaptive walk. Data are from 5721 random and 6959 high-fitness adaptive walks. The x-axis is the number of substitutions and the y-axis is the mean s of the one-step beneficial mutations from all low-rank wildtype alleles at that step.

have additional limitations, as discussed by Orr (2003). These studies are mentioned not to diminish their importance, but rather to illustrate the difficulty in testing the theory.

We have tested this theory using a quasi-empirical model of RNA evolution. RNA secondary-structure prediction by free-energy minimization gives a biologically-realistic map from a genotype (sequence) to phenotype (shape ensemble). We assigned fitnesses to individual RNA molecules based upon biologically-motivated properties of the their shape ensembles. No a priori assumptions were made regarding an underlying distribution of allelic fitnesses or fitness correlations among similar sequences.

We found that the distribution of fitness values is of the Gumbel-type. Maxima drawn from this class of distributions converge to what is often called '*the*' extreme-value distribution (for an excellent overview see Box 2 in (Orr, 2005); for a detailed treatment see (Leadbetter et al., 1983)). Current adaptation theory com-

monly assumes that distributions of fitnesses are Gumbel-type. Orr has shown that Gumbel-type distributions of fitness values arise in Fisher's geometrical model of adaptation (Orr, 2005). Yet, empirical evidence to support the assumption is limited by our ability to measure the fitness of large sets of random genotypes. To our knowledge, this is the first empirical evidence supporting the existence of Gumbel distributions in biological systems.

Although a major assumption of the theory holds up in the RNA model, we found two fundamental departures from its predictions. First, the distribution of beneficial effects depends on the fitness of the parent genotype; the average size of a beneficial effect increases with the fitness of the parent genotype. Second, for the two fitness classes we evaluated, the distributions of beneficial effects are non-exponential, though they are monotonically declining as predicted by the theory. The distributions appeared exponential and rank-invariant only after left truncations that discarded over 99% of the observations. The appropriate truncation thresholds also differed for these two classes of sequences.

A priori, two possible explanations for the discrepancy between the theory and our observations can be proposed. First, the fitness landscape in our quasi-experimental system may not satisfy the prerequisites of extreme value theory. This explanation was rejected through a large random survey of sequences in which the tail of the fitness distribution was shown to have the essential characteristics predicted by EVT (**Figure 2.1**). Thus, we turn to a second possible explanation: correlations among closely related sequences defy Gillespie and Orr's assumptions that the one-step mutations of any given genotype have i.i.d. random fitnesses from the distribution of all allelic fitnesses. In other words, the theory assumes that fitness values are distributed completely randomly throughout genotype space.

In our model, most point mutations are nearly neutral because they alter the structural repertoire, and therefore the fitness, of a molecule only slightly. Thus, the fitnesses of a sequence and its one-step mutants are correlated, implying that, on average, the fitness differences between beneficial mutants and their parent sequences will be smaller than expected if the fitnesses of the beneficial mutants had been i.i.d. random samples from an overall fitness distribution, as the theory assumes. Therefore, the correlation between the fitnesses of parental genotypes and their one-step mutants produced at least part of the discrepancy between our observations and the Orr-Gillespie theory - the excess of small effect mutations.

Fitness correlations among closely related genotypes are certainly not unique to our model. In a closely related model in which the fitness of an RNA sequence is determined by thermostability alone, Fontana et al. (1993) measured fitness correlations among genotypes and their mutants. In particular, they measured the correlation length (ρ), which is the distance d at which the fitnesses of a reference sequence and a d-mutant sequence become essentially statistically independent. They estimated $\rho = 6.25$ for a 70 nucleotide sequence suggesting that, on average, one-step mutants will have similar fitnesses to their parental genotypes, although it does not specifically address correlations between high fitness sequences and their beneficial mutants. Fitness correlations are evident in many other biological systems. For example, if stable RNA structures are important to fitness, then the interactions between the paired bases violate the assumption of independence of separate mutations: a beneficial base pairing could be restored by either of two mutations that would each achieve correlated fitness effects (Parsch et al., 2000). In β-helix-loop-helix (bHLH) proteins, structure-function relationships may produce correlation among the fitness effects of mutations (Atchley et al., 2000) and, by extension, produce distinct fitness distributions in local regions of genotype space.

The observed association between high fitness genotypes and large beneficial effects arises from both the correlation structure of the fitness landscape and the shape of the selective-value function and thus may be specific to our model. We used a hyperbolic decaying function because it models the realistic scenario in which most molecular structures are essentially unviable and very few have high fitness. This assumption is supported by remarkable structural conservation for many different classes of RNA (Doudna, 2000). By virtue of fitness correlations, a sequence with low to medium fitness (like those from the random adaptive walks), will lie near its one-step mutants in the shallow region of the selective value function. Thus any beneficial effects will likely be quite small. In contrast, high-fitness sequences (like those from the high-fitness walks) and their one-step mutants will occupy the steep region of the function, where beneficial effects may be relatively large. A preliminary survey of beneficial fitness effects using a linear selective-value function also yields non-exponential distributions of beneficial effects. In this case, however, the mean beneficial effect does not depend on the fitness of the parent sequence. This suggests that the observed anisotropy in beneficial fitness effects across sequence space may be closely linked to the shape of the selective-value function.

We offer a few caveats to this study. First, our model includes no selection for function per se; instead we use characteristics known to be important for functional RNA molecules *in vitro* and *in vivo*. Second, our fitness function is bounded both below and above, yet the theory of Orr and Gillespie was developed for unbounded distributions (Gillespie, 1983; Orr, 2003). Since our general survey of RNA sequence space was consistent with EVT (**Figure 2.1**) and even the fittest sequences in our study are quite far from the upper bound, we believe that the fitness bounds do not pose a problem. Third, in the interest of accurate structural prediction and computational tractability, we considered relatively short RNA molecules (76 nucleotides) that each has exactly 228 one-step mutants. The differences between our results and the theory may be attributed, in part, to the small number of mutants per genotype. Based on Figure 1 and Gillespies (1983) statement that 200 mutations per genotype are sufficient for the theory, however, we believe that this is not an important source of bias. Finally, our results are for one model system and other systems may yield different results.

Although this study demonstrates that the current theory might not withstand the complexity of all biological systems, some generality was evident. In particular, the distributions of fitness effects were monotonically decaying and the general shape of the distributions of beneficial fitness effects was invariant across genotype space, as predicted by the Orr-Gillepsie theory. Furthermore, after discarding the nearly-neutral beneficial mutations, the distributions of the remaining large effects were approximately exponential. This suggests that a more flexible theoretical framework may be possible in the future.

2.4 Appendix 1: Maximum Likelihood Estimation of the Exponential Parameter

The general probability density function (pdf) for an exponential distribution is: $y(x) = \lambda e^{-\lambda x}$. The likelihood L of an exponentially distributed set of values is then:

$$L = [\lambda e^{-\lambda x_1}][\lambda e^{-\lambda x_2}] \dots [\lambda e^{-\lambda x_n}] = \prod_{i=1}^{n} \lambda e^{\lambda x_i}$$

taking the log gives:

$$\begin{aligned}
\ln L &= \ln \prod_{i=1}^{n} ([\lambda e^{-\lambda x_i}]) \\
\ln L &= \sum_{i=1}^{n} (\ln[\lambda e^{-\lambda x_i}]) \\
&= \sum_{i=1}^{n} (\ln \lambda + \ln[e^{-\lambda x_i}]) \\
&= \sum_{i=1}^{n} \ln \lambda + \sum_{i=1}^{n} -\lambda x_i \\
\ln L &= n \ln \lambda + -\lambda \sum_{i=1}^{n} x_i
\end{aligned}$$

We take the maximum likelihood (ML) estimate of the exponential parameter($\hat{\lambda}$) to be $\delta lnL/\delta\lambda = 0$, :

$$\frac{\delta lnL}{\delta \lambda} = \sum_{i=1}^{n} x_i + \frac{n}{\hat{\lambda}}$$

Setting equal to zero we obtain:

$$\begin{aligned}
-\sum_{i=1}^{n} x_i + \frac{n}{\hat{\lambda}} &= 0 \\
\frac{\sum_{i=1}^{n} x_i}{n} &= \frac{1}{\hat{\lambda}}
\end{aligned} \tag{2.6}$$

Thus, the mean of the fitness values is the inverse of the exponential param-

eter defining the distribution. The mean of the distribution has the advantage of being more biologically interesting and less susceptible to fluctuation from variance in the data sets.

References

Lauren Ancel and Walter Fontana. Plasticity, Modularity and Evolvability in RNA. *Journal of Experimental Zoology*, 288(3):242–283, 2000.

William R. Atchley, Kurt R. Wollenberg, Walter M. Fitch, Werner Terhalle, and Andreas W. Dress. Correlations Among Amino Acid Sites in bHLH Protein Domains: An Information Theoretic Analysis. *Mol Biol Evol*, 17(1):164–178, 2000.

Christina L. Burch and Lin Chao. Evolution by Small Steps and Rugged Landscapes in the RNA Virus phi6. *Genetics*, 151(3):921–927, 1999.

Jennifer A. Doudna. Structural genomics of RNA. *Nature Structural Biology*, 7(11): 954–6, 2000.

AD Ellington. RNA selection. Aptamers achieve the desired recognition. *Current Biology*, 4(5):427–429, 1994.

Ronald Aylmer Fisher. *The Genetical Theory of Natural Selection*. Oxford University Press, Oxford, 1930.

Walter Fontana and Peter Schuster. Continuity in evolution: on the nature of transitions. *Science*, 280(5368):1451–1455, 1998.

Walter Fontana, Peter F. Stadler, Erich Bornberg-Bauer, Thomas Griesmacher, Ivo L. Hofacker, Manfred Tacker, Pedro Tarazona, Edward D. Weinberger, and Peter Schuster. RNA Folding and Combinatory Landscapes. *Physical Review E*, 47:2083–2099, 1993.

John H. Gillespie. A simple stochastic gene substitution model. *Theoretical Population Biology*, 23(2):202–215, 1983.

Emil Julius Gumbel. *Statistics of Extremes*. Columbia University Press, New York, 1958.

Ivo L. Hofacker, Walter Fontana, Peter F. Stadler, L. Sebastian Bonhoeffer, Manfred Tacker, and Peter Schuster. Fast Folding and Comparison of RNA Secondary Structures. *Monatshefte fur Chemie*, 125:167–188, 1994.

Martijn A. Huynen, Peter F. Stadler, and Walter Fontana. Smoothness within ruggedness: the role of neutrality in adaptation. *Proc Natl Acad Sci USA*, 93(1): 397–401, 1996.

Marianne Imhof and Christian Schlotterer. Fitness effects of advantageous mutations in evolving *Escherichia coli* populations. *Proc Natl Acad Sci USA*, 98(3):1113–1117, 2001.

M.R. Leadbetter, Georg Lindgren, and Holger Rootzen. *Extremes and Related Properties of Random Sequences and Processes*. Springer-Verlag, 1983.

JS McCaskill. The equilibrium partition function and base pair binding probabilities for RNA secondary structure. *Biopolymers*, 29(6-7):1105–1109, 1990.

Lauren Ancel Meyers, Jennifer F. Lee, Matthew Cowperthwaite, and Andrew D. Ellington. The Robustness of Naturally and Artificially Selected Nucleic Acid Secondary Structures. *Journal of Molecular Evolution*, 58(6):618–625, 2004.

R Nussinov and AB Jacboson. Fast algorithm for predicting the secondary structure of single-stranded RNA. *Proceedings of the National Academy of Sciences*, 77 (111):6309–6313, 1980.

H. Allen Orr. The Population Genetics of Adaptation: The Adaptation of DNA Sequences. *Evolution*, 56(7):1317–1330, 2002.

H. Allen Orr. The Distribution of Fitness Effects Among Beneficial Mutations. *Genetics*, 163(4):1519–1526, 2003.

H. Allen Orr. The Genetic Theory of Adaptation: A Brief History. *Nature Reviews Genetics*, 6(2):119–127, 2005.

H.A. Orr. The Population Genetics of Adaptation: The Distribution of Factors Fixed during Adaptive Evolution. *Evolution*, 52(4):935–949, 1998.

John Parsch, John M. Braverman, and Wolfgang Stephan. Comparative Sequence Analysis and Patterns of Covariation in RNA Secondary Structures. *Genetics*, 154(2):909–921, 2000.

Daniel E. Rozen, J. Arjan G. M. de Visser, and Philip J. Gerrish. Fitness Effects of Fixed Beneficial Mutations in Microbial Populations. *Current Biology*, 12(12): 1040–1045, 2002.

Rafael Sanjuan, Andres Moya, and Santiago F. Elena. The distribution of fitness effects caused by single-nucleotide substitutions in an RNA virus. *Proc Natl Acad Sci USA*, 101(22):8396–8401, 2004.

Peter Schuster, Walter Fontana, Peter F. Stadler, and Ivo L. Hofacker. From sequences to shapes and back: a case study in RNA secondary structures. *Proceedings of the Royal Society of London B*, 255(1344):279–284, 1994.

E van Nimwegen, JP Crutchfield, and M Huynen. Neutral evolution of mutational robustness. *Proc Natl Acad Sci USA*, 17(76):9716–9720, 1999.

M. Waterman. Secondary structure of single-stranded nucleic acids. In *Studies on foundations and combinatorics, Advances in mathematics supplementary studies*, volume 1, pages 167–212. Academic Press N.Y., 1978.

Ishay Weissman. Estimation of Parameters and Larger Quantiles Based on the k Largest Observations. *Journal of the American Statistical Society*, 73(364):812–815, 1978.

Claus O. Wilke and Christoph Adami. Interaction between directional epistasis and average mutational effects. *Proceedings of the Royal Society of London: Series B*, 268(1475):1469–1474, 2001.

Stephan Wuchty, Walter Fontana, Ivo L. Hofacker, and Peter Schuster. Complete suboptimal folding of RNA and the stability of secondary structures. *Biopolymers*, 49(2):145–165, 1999.

M Zuker and P Stiegler. Optimal computer folding of large RNA sequences using thermodynamics and auxiliary information. *Nucl. Acids. Res.*, 9(1):133–148, 1981.

Michael Zuker. On Finding All Suboptimal Foldings of an RNA Molecule. *Science*, 244(4900):48–52, 1989.

Chapter 3

From Bad to Good: Fitness Reversals and the Ascent of Deleterious Mutations

3.1 Introduction

Modern evolutionary theory recognizes that deleterious mutations may reduce fitness and retard adaptation (Bachtrog and Gordo, 2004; Johnson and Barton, 2002; Maynard Smith, 1978; Orr, 2000; Peck, 1994). Accumulation of deleterious mutations is expected to affect the rate and course of many biological processes such as sexual selection, development of cancer, and senescence (Charlesworth and Charlesworth, 1998). The theoretical work underlying these predictions makes an important assumption: the fitness effect of a deleterious mutation is constant until the mutation disappears or fixes.

In the standard infinite population experiencing a combination of natural selection and random mutation, deleterious mutations should not fix, but accumulate to a level perfectly balanced by mutation and selection. Some processes can lead to deleterious mutations fixing in infinite populations, however. For example, in Eigen's quasispecies model, high rates of mutation can overwhelm selection and shift the mutation-selection balance such that deleterious mutations accumulate to exceedingly high levels (Bull et al., 2005; Eigen, 1971). In finite populations, several processes may also allow deleterious mutation fixation (Charlesworth and Barton,

2004). The best studied of these is random genetic drift - the stochastic fixation of deleterious mutations in relatively small populations. Additionally, if recombination is rare and the population size is finite, then deleterious mutations can hitchhike to fixation with independently-acting beneficial mutations (Johnson, 1999; Kim and Stephan, 2000).

The fixation of deleterious mutations certainly reduces the fitness of populations. It may be possible, however, for the fitness effect of an initially deleterious mutation to change over time. In particular, compensatory mutations may evolve that reduce the negative impact of deleterious mutations or, in extreme cases, the resulting fitness may be even higher than the fitness of the ancestor in which the deleterious mutation arose (Weinreich and Chao, 2005). Such compensatory mutations may appear before (or after) the deleterious mutation has fixed. Metaphorically speaking, while fixed deleterious mutations are generally expected to be bad, they may be stepping stones to distant adaptive peaks.

Evolutionary geneticists have long considered mutations that ameliorate or compensate for the deleterious effect of a prior mutation. The literature on this subject, however, focuses almost exclusively on compensatory mutations occurring after the fixation of the initial deleterious mutation, and therefore does not address the likelihood that the initial mutation will fix in the first place (Burch and Chao, 1999; Moore et al., 2000; Poon and Chao, 2005). One possible explanation for this emphasis is convenience – both mathematical and experimental. To greatly simplify the evolutionary dynamics, population genetic models of adaptation typically assume that selection is much stronger than mutation [strong selection, weak mutation models (SSWM)]. Under this assumption, a deleterious mutation will disappear or fix before secondary mutations arise in the genome and thus the fitness effect of a deleterious mutation remains unchanged throughout its evolutionary trajectory to either fixation or loss (Gillespie, 2004).

If the mutation rate is relatively large, however, additional mutations may arise in the genome carrying the initially deleterious mutation before it fixes or is lost. Such secondary mutations change the genetic background and thus potentially change the fitness effect of the initial deleterious mutation. The background selection literature has frequently considered the scenario in which a good mutation is driven to extinction by bad mutations (see (Innan and Stephan, 2003; Kim and Stephan, 2000) and refs therein). Our interest, however, is in a process involving

epistasis between mutations that results in amelioration of the deleterious effect and, ultimately, the fixation of an initially bad mutation. Although this process seems to have been largely ignored in the population genetics literature, one notable study by Kimura shows that mutations at two linked alleles, which are singly deleterious but jointly neutral, can both fix relatively rapidly even in large populations (Kimura, 1985). There has also been recent interest in the ability of populations to escape from local optima via less fit intermediate genotypes (see (Weinreich and Chao, 2005) and refs therein).

Here we use a computational model of asexually replicating RNA molecules to study the fixation of deleterious mutations. We first observe that initially deleterious mutations fix at a far greater rate than expected for an evolving asexual population and that some populations achieve high mean fitness despite rapidly accumulating deleterious mutations. We then reconcile this paradox by systematically characterizing the processes leading to fixation, which include random genetic drift, hitchhiking upon independently acting beneficial mutations, and fitness effect reversals upon secondary (compensatory) mutations.

3.2 Materials & Methods

3.2.1 Simulation Model

We used a computational simulation of a population of replicating and evolving RNA molecules. Similar simulation models have been extensively used in previous studies of evolutionary dynamics (Ancel and Fontana, 2000; Cowperthwaite et al., 2005; Fontana and Schuster, 1998; Huynen et al., 1996; van Nimwegen et al., 1999; Wilke and Adami, 2001). The program, RNAvolver (available from M.C.C. upon request), was designed to make straightforward comparisons to existing theory by simulating a stochastic, discrete-generation, asexually replicating population with a fixed size. The fitness function is based on the folding of RNA sequences into secondary structures (Ancel and Fontana, 2000; Cowperthwaite et al., 2005; Fontana and Schuster, 1987). The fitness effect of a mutation thus stems from a biologically explicit model of molecular structure and is not simply selected from a probability distribution of mutational effects, as in simpler evolutionary models (Crow and Kimura, 1970).

In our model, the genotype of each member of the population is the primary RNA sequence of $L = 76$ nucleotides, which is similar in size to a typical tRNA molecule. The focal phenotype is RNA secondary structure ("shape", informally), which provides the scaffold for functional tertiary structure and has been highly conserved during evolution (Doudna, 2000). In the simulation program, the "fitness" of each genotype is a function of its repertoire of probable secondary structures, which we predict using thermodynamic minimization (Hofacker et al., 1994; Wuchty et al., 1999; Zuker, 1989). The folding algorithm is relatively accurate for shorter molecules, but is not able to model pseudoknots (a common tertiary structure motif) and other non-canonical interactions (Hofacker et al., 1994; Nussinov and Jacboson, 1980; Zuker and Stiegler, 1981).

Fitness depends on both similarity to a reference shape (the "target", t) and thermodynamic stability, which is believed to impose a selective constraint on both naturally and artificially evolved RNA molecules (Meyers et al., 2004). To assign fitness to a molecule, we first predict the *ensemble* of lowest free energy shapes (all shapes within 3 kcal/mol of the groundstate) using the ViennaRNA-1.5 package (Hofacker et al., 1994; Wuchty et al., 1999) and then measure the structural difference between each shape (σ) in the ensemble and the target structure t. The selective value of a shape σ is given by

$$f(\sigma) = \frac{1}{\alpha + (d(\sigma, t)/L)^{\beta}} \tag{3.1}$$

where $\alpha = 0.01$ and $\beta = 1$ are scaling constants, $d(\sigma, t)$ is the Hamming distance between σ and the target shape, and $L = 76$ is the length of the sequence. To determine the Hamming distance between two shapes, we measured the number of positions at which the parenthesized representations (e.g. ((((....)))), where matching parentheses are paired bases and dots are unpaired bases) of the shapes differ. For example, two structures that differ by exactly a base pair would have a Hamming distance of two. By setting fitness equal to a hyperbolic function of the distance to the target shape, we model strong selection for that target. That is, only molecules very close to the target are expected to function well.

The overall fitness, W, of a genotype is the average of the selective values of the shapes in its ensemble of secondary structures, each weighted by its Boltzmann probability (p_σ), $W = \sum_\sigma f(\sigma) p_\sigma$ (Ancel and Fontana, 2000; Cowperthwaite et al.,

2005). This fitness function assumes that both the structure of the molecule and its thermodynamic stability are important for function. The range of fitness values possible given our choice of parameters is 0.99 - 100.0. Prior studies show that the evolutionary dynamics are relatively robust to the particular choice of fitness function (Ancel and Fontana, 2000; Cowperthwaite et al., 2005). In our simulations, molecules replicate at each generation at a rate proportional to their fitness.

We adapted 100 replicate populations of RNA molecules under three different genomic mutation rates ($U = 0.01, 0.08, 0.32$) and 45 populations with $U = 0.95$ (this set was constrained by computational limitations). Population size was held fixed at $N = 1000$, which was a compromise between minimizing computational time and maximizing N. Mutation rates were identical for all bases in the RNA alphabet. These mutation rates spanned the range of published estimates for microorganisms including viruses and bacteria (Drake and Holland, 1999). Simulations each ran for 5000 generations except the $U = 0.95$ simulations, which were computationally limited to approximately 2500-3000 generations.

Identifying Fixed Mutations

Mutations were classified as fixed if, at any time during the simulation, they were retained by at least 95% of the extant genotypes. For each genotype containing the mutation, we verified that the mutation was always present in the lineage leading from the initial deleterious mutation, and never lost and subsequently reacquired. The subsequent analysis considers all deleterious mutations that met this 95% criteria (henceforth referred to as the "fixation threshold"). A more stringent criterion ($> 95\%$) was impractical because of the high mutations rates under which the populations evolved.

3.2.2 Expected Fixation Frequencies

Kimura derived the following probability that a unique mutation with fitness effect s will fix in a haploid population of effective size N_e: $1 - e^{-2s}/1 - e^{-2N_e s}$ (Kimura, 1957, 1962). This model assumes that there are no subsequent changes in the mutant lineage before fixation or loss. We used Kimura's equation to predict the role of drift in the ascent of deleterious mutations and defined N_e as the average number of individuals that produce progeny in each generation, which gave an upper bound

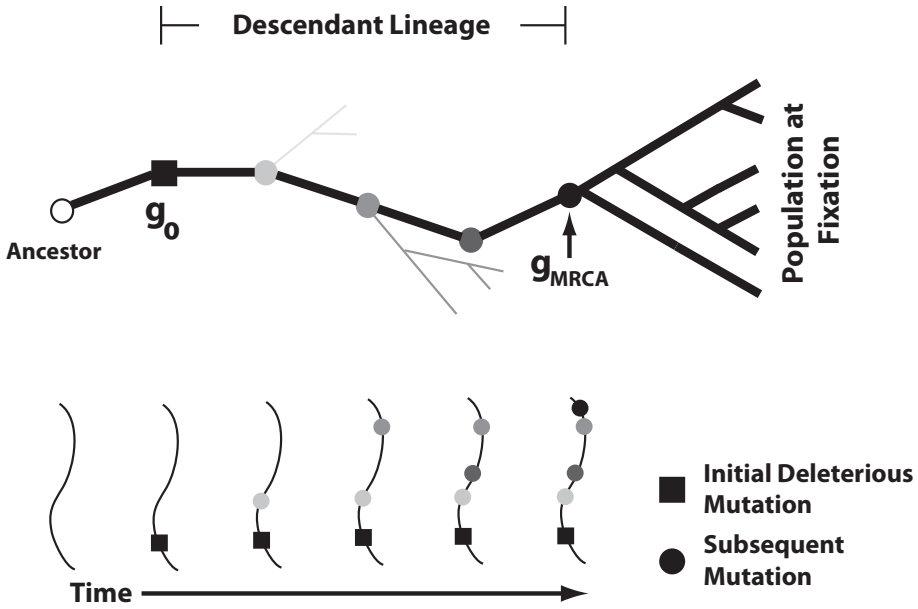

Figure 3.1: Diagram depicting a simplified "descendant lineage" for a genotype carrying a deleterious mutation (black square) that fixed in the population. The genealogy of the population present at fixation is used to determine the MRCA. The descendant lineage is the single genotypic line of descent from the initial mutant genotype to g_{MRCA}. The faint gray branches along the descendant lineage represent lineages that go extinct. The bottom half of this figure shows the accumulation of mutations in the genotypes comprising the descendant lineage.

for N_e. Individuals produced roughly equal numbers of offspring in each generation (not shown), however, so the actual value of N_e was likely close to this value. We emphasize that our populations significantly deviate from the idealized ones Kimura considered and, therefore, these calculations are only intended to serve as a rough approximation of what might be expected to occur by drift alone. For example, under the SSWM approximation, mutations necessarily arise and proceed to fixation (or loss) one at a time; in our model, multiple mutations can simultaneously proceed to fixation or loss.

3.2.3 Measuring Changes in Fitness Effect

We measured the magnitude and direction of change in the fitness effect of a deleterious mutation during its evolutionary lifetime as follows. Consider a deleterious mutation δ that creates a new mutant genotype, which we call g_0. The genotype g_0 is the entire set of 76 bases in the molecule, including δ. If δ is not excessively severe, then g_0 may reproduce and its descendants possibly acquire mutation(s) at other sites. As these descendent genotypes arise, there will be a tree-like genealogy emanating from g_0 (**Figure 3.1**). We use g_i to refer to a descendent genotype of g_0 containing δ and i subsequent mutational events at other sites (where a mutational "event" occurs during replication and creates one or more base changes). We measured the fitness effect of δ in g_i by creating new genotypes in which δ was reverted back to its ancestral state, but the i mutational events subsequent to δ were retained. This δ-free genotype is designated g_i'. The fitness effect of δ in the descendent genotypes g_i's is then $s_i = (W_{g_i} - W_{g_i'})/W_{g_i'}$, where W_{g_i} is the absolute fitness of the descendent genotype and $W_{g_i'}$ is the absolute fitness of the δ-free genotype. Informally, the fitness effect of δ is the fitness difference between the descendent genotype with and without δ.

For comparison to the fixed mutations, we selected 10 deleterious mutations from each simulation (1000 mutations for each mutation rate) and tracked the fitness effect of each mutation in the descendant genotypes, up to six subsequent mutational events. We selected these deleterious mutations at random from the subset of all deleterious mutations that met the following criteria: (1) the mutation had at least one descendant genotype, (2) the mutation did not fix and (3) the mutation did not arise on genotypes that had one of the (eventually) fixed deleterious mutations appear within six subsequent mutations. We defined these criteria because most deleterious mutations have no descendants and therefore we cannot measure a change in fitness effect. We also modified the first criteria by increasing the required number of descendants, but this did not qualitatively change our results (not shown).

3.2.4 Determining the MRCA of the Final Population

For each simulation, we identified the most recent common ancestor (MRCA) of the sequences present at the end of the simulation. The MRCA was exactly determined

from a genotypic pedigree. It is a unique genotype; it is not, however, a consensus genotype. Typically, additional mutations arise between the origin of the MRCA and the end of the simulation that lead to divergence from the MRCA genotype. This divergence is expected given that we are evolving populations under moderately high mutation rates.

We then identified the history of mutation events on the genealogical branches leading from the founder genotype to the MRCA, thereby ignoring mutations on lineages that ultimately extinguished. We refer to the mutational events on the MRCA lineage as *ancestral* mutations. Note that these ancestral mutations may be ephemeral, never reaching substantial frequencies in the population and perhaps disappearing upon subsequent mutations at the same site occurring before the MRCA. The only requirement for an ancestral mutation is that the initial mutational event creates a genotype from which the MRCA directly descended.

3.3 Results

3.3.1 Adaptation despite frequent incorporation of deleterious mutations

We followed the mean fitness of n replicate populations during 5000 generations of evolution ($n = 100, U = 0.01, U = 0.08, U = 0.32$; $n = 45, U = 0.95$). The average fitness of the populations increased with U up to $U = 0.32$ and then crashed at the highest rate of $U = 0.95$ (**Figure 3.2**, dark bars). At $U = 0.95$, populations were overwhelmed by deleterious mutations and may have experienced an error catastrophe (Ancel and Fontana, 2000; Bull et al., 2005; Eigen, 1971), though we did not investigate this possibility. In contrast to the other mutation rates, the mean final fitness achieved in the $U = 0.32$ runs was not only highest but was highly variable, with about 20% of the runs achieving extremely high fitness (> 40, on a scale from 0.99 to 100) and the remaining runs achieving more modest fitness ($\approx$ 7-9). We rejected the possibility that adaptation occasionally proceeded faster due to rare simultaneous double mutations because such events were, on average, deleterious and simultaneous double mutants never fixed (not shown).

We tallied the cumulative numbers of deleterious and beneficial *ancestral* mutations during the time leading to the most-recent common ancestor (MRCA) of

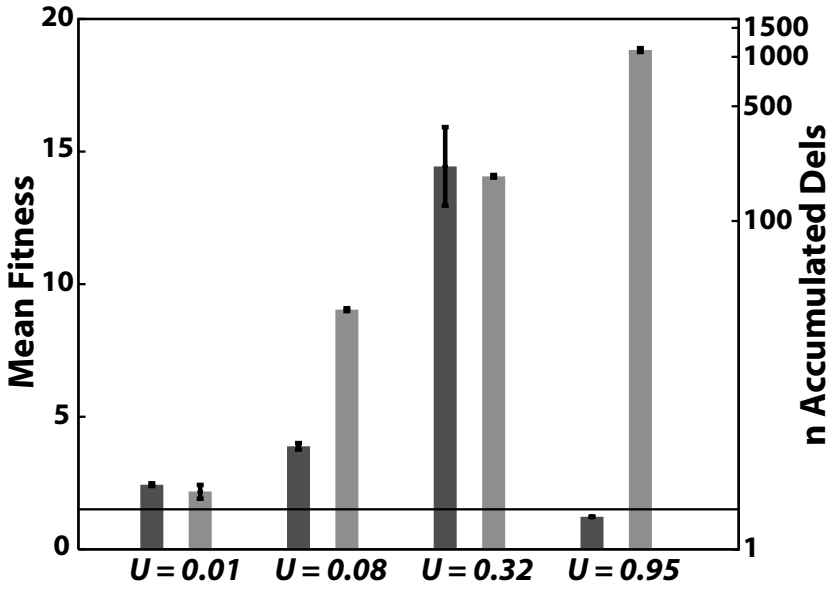

Figure 3.2: The mean fitness of evolved populations increases with mutation rate (up to $U = 0.32$) despite accumulating greater numbers of deleterious mutations. The dark grey bars (left-hand axis) represent the mean final fitness of populations that evolve under each mutation rate. The light gray bars (right-hand axis) show the mean number of deleterious mutations that accumulate during the time to the MRCA of the final population. The error bars represent one standard error from the sample mean.

all extant sequences at the end of each simulation. Ancestral mutations are those that occur along the single dominant genotypic lineage from the founding genotype to the MRCA and define a history of sequential mutational events. A relative minority of the total ancestral mutations ultimately reached the fixation threshold - about 10% under $U = 0.32$ and 15% under $U = 0.08$ (data not shown). **Figure 3.3** shows the maximum frequency attained by each ancestral mutation that did not fix. Several forces may operate to preclude mutations arising on the MRCA lineage from fixing such as drift, clonal interference and selection for other mutations at the same site.

Each mutation in this historical sequence was classified as deleterious or beneficial according to its relative fitness effect at the time it arose. Deleterious mutations were those with a fitness effect that was less than the reciprocal of the

actual population size ($s < -1/N$), while beneficial mutations were those with a fitness effect that was greater than the reciprocal of the actual population size ($s > 1/N$). Intuitively, the incidence of MRCA ancestral deleterious mutations increased with the genomic mutation rate (**Figure 3.2**, light bars). One might also expect that the rate of adaptation (change in mean fitness) would be inversely related to the rate at which deleterious mutations impact the dominant lineage. In fact, we found the opposite across all but the highest mutation rate: higher mutation rates yielded both increased accumulation of deleterious mutations and higher mean fitness (up to $U = 0.95$). In **Figure 3.2** (dark bars), populations with $U = 0.32$ achieved higher mean fitness, on average, than those with $U = 0.08$ or $U = 0.01$, despite incorporating a greater number of deleterious mutations.

Figure 3.4 illustrates three unintuitive properties for the fitness and ancestral mutation trajectories for populations experiencing $U = 0.08$ and $U = 0.32$. First, $U = 0.32$ populations experienced substantially greater incorporation of deleterious mutations than $U = 0.08$ populations, yet enjoyed consistently higher mean fitness. Second, ancestral deleterious and beneficial mutations occurred in

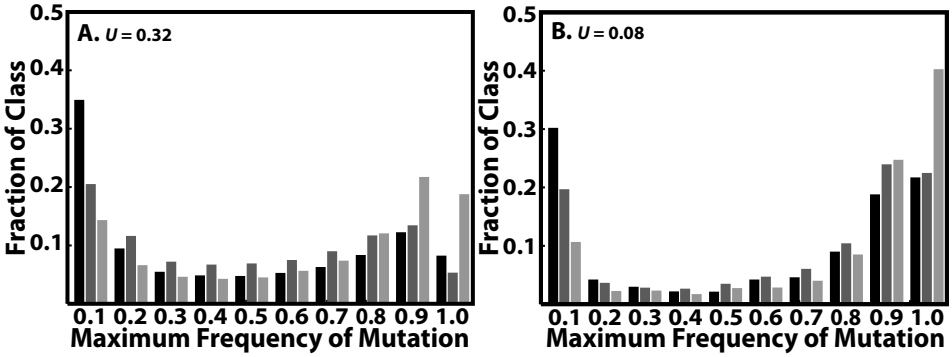

Figure 3.3: The maximum frequency of ancestral mutations (those forming the dominant mutational lineage from the founding population to the MRCA of the ending population) that did not fix. The black, dark gray and light gray bars correspond to mutations with initial fitness effects that are deleterious, neutral and beneficial, respectively. The x-axis is the upper bin bound for the frequency attained (e.g. 0.20 includes those mutations whose maximum frequency is greater than 0.10 and less than or equal to 0.20). The y-axis is the fraction of mutations in each class that attained each frequency range. The top pane (**A**) shows the frequency distribution for $U = 0.32$ and the bottom pane (**B**) depicts $U = 0.08$.

the MRCA lineages at nearly equal rates. The correlation between mutation rate and mean fitness may be explained, in part, by the more rapid accumulation of beneficial mutations under moderately high mutation rates. Third, during periods of relatively stable mean fitness, deleterious mutations impacted the MRCA lineage at the same rate as during periods of rapid adaptation. These observations taken together suggest that initially deleterious mutations may not strictly impede adaptation, in contrast to theoretical predictions (Johnson and Barton, 2002; Maynard Smith, 1978; Orr, 2000; Peck, 1994).

3.3.2 Processes enabling the fixation of deleterious mutations

We now consider the relative importance of several forces that might produce these counterintuitive observations. We focused our attention on the smaller subset of deleterious mutations that fixed in the populations. Three distinct processes ac-

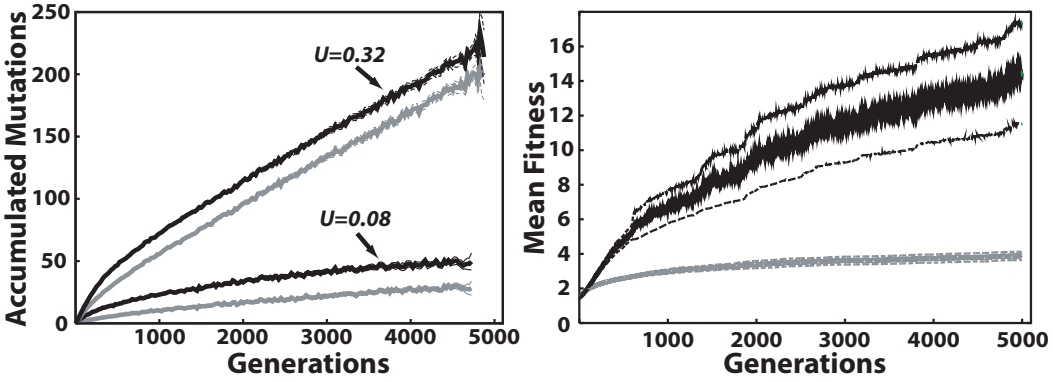

Figure 3.4: Mutation accumulation and mean fitness of evolving populations. The top pane shows the accumulation of beneficial and deleterious mutations in the lineage leading to the most-recent common ancestor, while the bottom pane shows the mean fitness of the populations over time. In both panes, the thicker lines represent the mean value and the thin, dotted lines represent bounds for 95% confidence intervals. In the top pane, the dark lines represent beneficial mutations and the light lines represent deleterious mutations (see text for definition). The jaggedness in the lines is the result of averaging over all simulations, which frequently differ in the length of their MRCA lineages. Within any single run the number of mutations monotonically increases. In the lower pane, the dark lines correspond to $U = 0.32$ and the light lines correspond to $U = 0.08$.

counted for the success of these mutations: (1) random genetic drift, (2) hitchhiking, and (3) fitness reversals, i.e. the fitness effect changed from bad to good.

We discuss these processes in reverse order, beginning with the most prevalent and unexpected of the three: fitness reversals driven by compensatory mutations. Suppose a deleterious mutation arises and decreases the fitness of the genotype carrying it by a factor s. Population genetic models of adaptation generally assume conditions of strong-selection and weak-mutation (SSWM) and therefore, during the trajectory to either fixation or loss, no additional change occurs in the genotype carrying the deleterious mutation. Under the SSWM assumptions, s would not be expected to change during the evolutionary trajectory of the mutation. If the SSWM assumptions are relaxed, however, a genome carrying the deleterious mutation may experience additional mutations before it fixes or is lost from the population, and thus the s-value of the initial mutation may change.

For each genome experiencing a deleterious mutation (g_0), a complete genealogy was kept of every genotype that descended from it. A deleterious mutation (δ) was considered fixed when at least 95% of the genotypes in the extant population retained δ throughout their evolutionary histories. Starting with the extant population in which δ was first fixed, we searched backwards to identify the most recent common ancestor genotype (g_{MRCA}) of all genotypes that retained δ. Since the populations were evolved under moderately high mutation rates, g_{MRCA} often contained δ plus several subsequent mutations at other sites that arose after δ and before the fixation of δ.

We identified the single descendant lineage of genotypes that captured the history of mutations beginning at g_0 and ending at g_{MRCA}: $\{g_0, g_1, \ldots, g_i, g_{MRCA}\}$, which we referred to as the "descendant lineage" of δ. The typical number of subsequent mutations in the descendant lineage was 2-10 (2-40) in populations experiencing $U = 0.08$ ($U = 0.32$). Each subsequent mutation could have altered the fitness effect of δ before its fixation and, therefore, we measured the fitness effect (s_i) of δ at each "step" along this single descendant lineage from g_0 to g_{MRCA} (δ was necessarily present at each step). We used this temporal series of s_i's to capture the changing fitness effect of δ.

Many of the deleterious mutation fixation events were characterized by dramatic fitness reversals before fixation occurred as the genotypes containing δ accumulated additional mutations. These subsequent mutations rapidly transformed

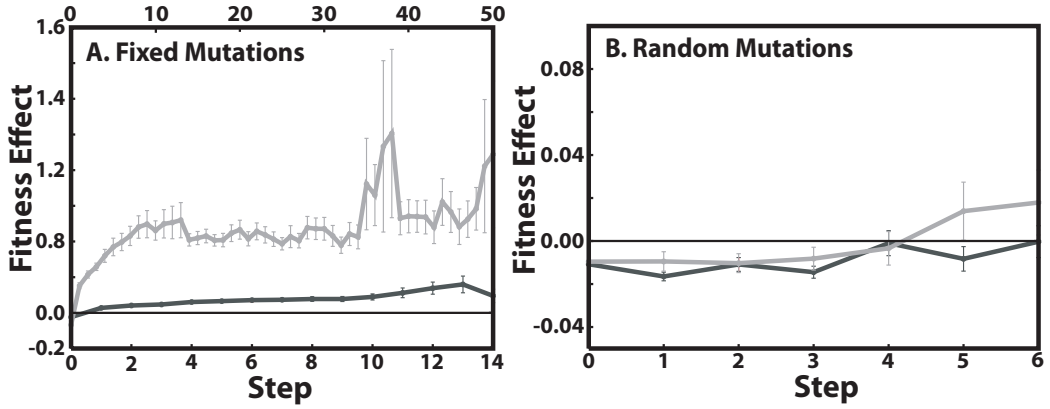

Figure 3.5: Fixed deleterious mutations interact positively with subsequent substitutions, while random deleterious mutations generally remain deleterious (see text). **A**: Mutations that were initially deleterious and ultimately fixed tended to become beneficial before their fixation. It is apparent that the largest increases in fitness occurred in the first few subsequent mutations. **B**: In contrast, random deleterious mutations generally remained deleterious with subsequent mutations. In both graphs, the black lines correspond to $U = 0.08$ and the light lines to $U = 0.32$ (error bars represent one standard error of the mean). The horizontal lines separate the beneficial (above) and deleterious (below) fitness effects. The fitness effect of a mutation is calculated as $(W_{g_i} - W_{g'_i})/W_{g'_i}$, where $W_{g'_i}$ is the fitness effect of the descendent lineage without the fixed mutation and W_{g_i} is the fitness effect of the descendent lineage *with* the fixed lineage

δ from a liability into an asset and, thereby, increased its probability of success (**Figure 3.5A**). Both the rate and magnitude of the fitness effect reversals appeared to increase with mutation rate. For a random sample of deleterious mutations that never fixed, the pattern was markedly different. These mutations typically remained a liability upon subsequent mutation (**Figure 3.5B**), though the few deleterious mutations that persisted for five or six steps appeared to have acquired some small effect compensatory mutations. Thus, most deleterious mutations remained deleterious throughout their evolutionary lifetime; only a notable few became beneficial through positive interactions with their changing genetic backgrounds. Even at $U = 0.01$, some fitness reversals were observed (not shown), indicating that a much lower mutation rate is required to meet the SSWM assumptions of population genetics models.

A fitness effect reversal does not imply that the fitness of the genotype as a

whole will rise from below the ancestor to above the ancestor or, furthermore, that the reversal explains the ultimate fixation of the initial mutation. It merely means that a genotype is better off with the mutation than without it. In **Figure 3.6A & B**, we show that, indeed, the fitnesses of the genotypes containing the fixed deleterious mutations (g_i's, light lines) rose to levels above that of the ancestor, and that without the initial mutation (g_i''s, dark lines), the fitnesses of the genotypes were significantly lower. Notably, under both the high and low mutation rates, the average fitness of the g_i''s remained below that of the ancestor. For the randomly chosen deleterious mutations that did not fix (**Figure 3.6C & D**), the fitness of the descendant genotypes (with and without the initial mutation) continually declined relative to that of the ancestor and the fitness of the g_i''s is greater than that of the g_i's. These figures indicate that fitness reversals via interactions with compensatory mutations played an important role in the ascent of these deleterious mutations. In fact, we found that about 80% of the initially deleterious mutations that fixed did so as a result of a fitness effect reversal (**Table 3.1**) - a process not considered by most population genetics theory, with a few notable exceptions (Kimura, 1985; Weinreich et al., 2005). For comparison, ancestral mutations (those in the MRCA lineage) that did not fix in the population only reversed their fitness effect about 25% of the time (data not shown).

We next consider the second process contributing to fixation of deleterious mutations: evolutionary hitchhiking. We say that a deleterious mutation hitchhikes to fixation when it fixes on a genetic background that attains fitness at or above the ancestor (g_0), but the fixed deleterious mutation remains deleterious (or neutral) in every genotype leading to g_{MRCA}. We determined the number of fixed deleterious mutations that did not undergo a fitness-effect reversal and existed on genotypes that evolved to higher fitness than the ancestor before the deleterious mutation fixed. Finally, we assumed that the remaining fixation events were the result of random genetic drift. These were the fixed deleterious mutations that maintained a negative (or neutral) fitness effect and were found on genotypes with fitness below the ancestor (**Table 3.1**).

We finally ask whether the number of fixation events that we attribute to fitness effect reversals and hitchhiking might be within the range predicted to occur by drift alone. Populations experiencing genomic mutation rates of $U = 0.08$ and $U = 0.32$ fixed, on average, 9.8 and 15.2 initially deleterious mutations, during 5000

generations of evolution, respectively. This corresponds to actual fixation rates for deleterious mutations of 3.09×10^{-5} (95%CI: $[2.90 \times 10^{-5}, 3.29 \times 10^{-5}]$) and 1.11×10^{-4} (95%CI: $[1.05 \times 10^{-5}, 1.16 \times 10^{-5}]$), for $U = 0.08$ and $U = 0.32$ respectively (**Table 3.2**). Kimura's approximation yields expected fixation probabilities of 3.27×10^{-5} ($U = 0.08$) and 1.21×10^{-31} ($U = 0.08$) when calculated using the mean fitness effect of the fixed deleterious mutations in our simulations [$s = -0.0239$ ($U = 0.08$); $s = -0.0672$ ($U = 0.32$)]. A comparison of the observed and expected rates of fixation suggests that, under $U = 0.32$, fitness reversals may lead to rates of deleterious mutation fixation that are higher than expected by drift alone, while, under $U = 0.08$ the rates of deleterious fixation do not exceed the expected rates from Kimura's model. We stress, however, that our populations are significantly different from the idealized ones Kimura envisioned and thus there may be multiple reasons for the observed discrepancies.

In summary, a complicated mix of forces allowed initially deleterious muta-

Type of Fixation Event	High Mutation Rate (U=0.32)	Low Mutation Rate (U=0.08)
Fitness Reversal	0.815	0.636
Hitchhiking	0.113	0.279
Random Drift	0.072	0.085

Table 3.1: Forces leading to the fixation of deleterious mutations. We categorize all fixation events (n=981, $U = 0.08$; n=1523, $U = 0.32$) of initially deleterious mutations into one of three types: fitness reversals, hitchhiking, or drift. Fitness reversals occurred when fixed deleterious mutations attain a beneficial fitness effect ($S > 1/N$) in the "descendant lineage" (see text). Hitchhiking occurs when deleterious mutations do not become beneficial ($S < 1/N$) in the "descendant lineage" and are carried to fixation on good genetic backgrounds. Fixation by drift occurs when deleterious mutations do not become beneficial ($S < 1/N$) along the "descendant lineage" and are carried to fixation on genetic backgrounds that remain less fit than the ancestor. We classify each event based on the maximum benefit attained in the "descendant lineage".

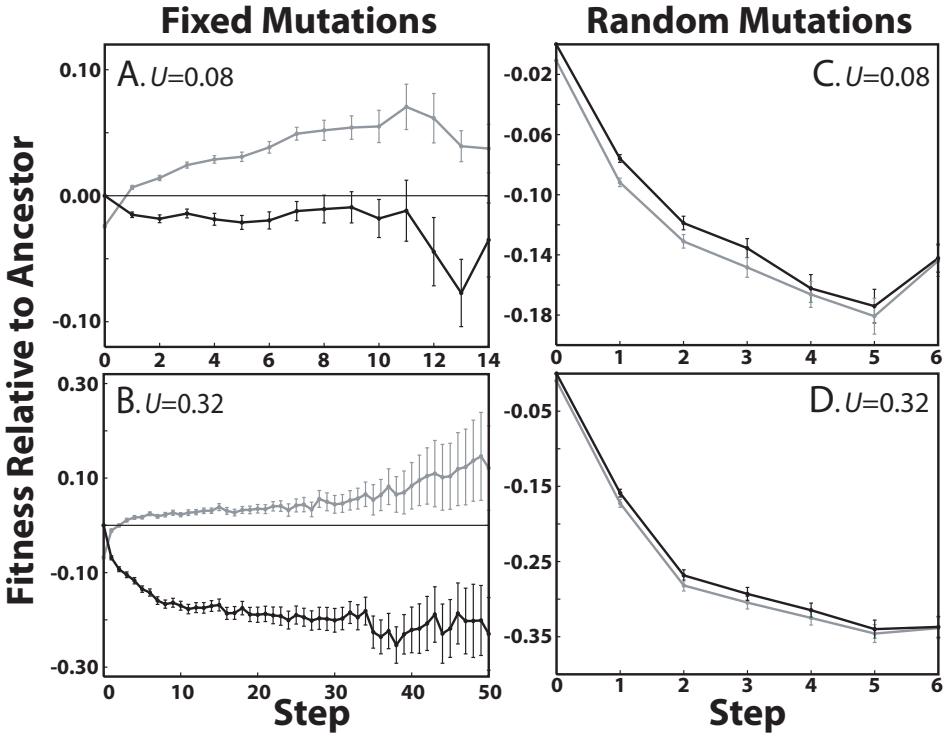

Figure 3.6: Fixed deleterious mutations are found in genotypes that are more fit than the ancestral genotype in which the deleterious mutation arose. In each graph, the gray lines correspond to g_i and the black lines g_i'. We define the fitness of descendent genotypes relative to the ancestor as $((W_{desc} - W_{anc})/W_{anc})$, where W_{anc} is the fitness of the parent genotype that gave rise to the deleterious mutation and W_{desc} may mean the fitness of g_i or g_i'. The error bars depict one standard error of the mean. **A & B** show the change in fitness of the genetic backgrounds harboring the fixed deleterious mutations in the $U = 0.08$ and $U = 0.32$ runs, respectively. **C & D** show the change in fitness of the genetic backgrounds of random deleterious mutations that did not fix in the $U = 0.08$ and $U = 0.32$ runs, respectively.

tions to occasionally rise to fixation. Hitchhiking may work in concert with fitness effect reversals, and therefore our estimates of the contributions of these two processes may be low (**Table 3.1**). Furthermore, the incidence of fitness reversals increased with mutation rate (from $U = 0.01$ to $U = 0.08$ to $U = 0.32$), perhaps contributing to the evolution of higher mean fitnesses across these mutation rates. Fitness-effect reversals are only part of the story, however, as the initial deleterious effects of fixed deleterious mutations were much larger in the $U = 0.32$ populations

Mutation Rate	Fixation Threshold	Number Deleterious	Number Fixed	Observed Fixation Probability	Expected Fixation Probability
$U = 0.08$	0.95	317,745	9.81	3.09×10^{-05}	3.27×10^{-05}
$U = 0.32$	0.95	1,375,005	15.23	1.11×10^{-05}	1.21×10^{-31}

Table 3.2: The probability of fixation of deleterious mutations in our simulations compared to theoretical predictions of Kimura (1957). For the theoretical calculations, we estimated N_e as the average number of reproducing individuals each generation, which we find to be 153.0 ($U = 0.08$) and 514.9 ($U = 0.32$), and estimate s as the mean size of the fixed mutations.

than the $U = 0.08$ populations.

3.4 Discussion

In this study, we offer a new perspective on the effect and role of deleterious mutations in adaptation. We simulated the adaptation of asexual populations of 1000 individual RNA genomes that each coded for a phenotype, which consisted of a set thermodynamically probable secondary structures. In turn, fitness depended on the overall similarity of a molecule's phenotype to a target shape. The effect of a mutation was determined by measuring its impact on the shape of the molecule (it's phenotype), and thus the distribution of fitness effects behaved as might be expected of a biological system.

The novel result is that nearly one-third of the mutations that evolve in the MRCA lineage (the single genealogical history from the starting genotype to the MRCA of the ending population) arise with deleterious effects, yet this apparent load of deleterious mutations does not impede adaptation. This can be explained by the frequent occurrence of fitness reversals, that is, more than half of these deleterious mutations do not stay deleterious, but become neutral or beneficial through interactions with compensatory mutations. Importantly, the compensatory mutation(s) arise and reverse the deleterious effect well before the deleterious mutation fixes, and the beneficial combination of mutations then ascends together to fixation.

Kimura described a special case of our process in a model of neutral com-

pensatory mutations (Kimura, 1985). He derived the time for transition between a wildtype genotype (AB) to a double mutant (A′B′), which has fitness identical to the wildtype. To create the double mutant, however, the population needed to pass through the deleterious intermediates AB′ or A′B, which each had fitness $1 - s$. He showed that under continuous mutation pressure, the double mutant can fix relatively rapidly, even in large populations. The fixation time for the double mutant was not unreasonably long, being slightly longer than the fixation time for a pair of neutral mutations and much shorter than the fixation time for a pair of unconditionally deleterious mutations.

A major question is whether this process occurs in nature. There is abundant experimental evidence that the fitness effect of a mutation can depend on genetic background (Lunzer et al., 2005; Weinreich et al., 2005, 2006). There is also evidence that compensated deleterious mutations are present in the genomes of flies (Kulathinal et al., 2004) and humans (Kondrashov et al., 2002). There is, however, a lack of empirical evidence (as opposed to negative evidence) for the full process we describe, although it would be difficult to observe without detailed histories of the substitution events. In a study using the AVIDA software, Lenski and colleagues observed a moderate number (∼15 %) of initially deleterious mutations that ultimately fixed. One of those deleterious mutations reversed its fitness effect and provided the basis for further fitness gains, though it was not stated whether the reversal occurred before fixation (Lenski et al., 2003).

Two factors may be necessary for this process to occur: a high mutation rate and epistasis. The mutation rate must be high enough that a second, interacting mutation arises in the genome before the first mutation is lost or fixed. While background selection typically refers to pairs of mutations (one beneficial and one deleterious) that have net negative fitness effects and no epistatic interactions, here we focus on pairs of mutations (with at least one deleterious) that epistatically interact to yield net positive fitness effects. We conjecture that, to the extent background selection is occurring, fitness reversals may likewise be important to the evolutionary dynamics. Furthermore, the mutation rate of interacting sites must be high enough to have a reasonable probability of creating the right combinations. Some natural systems are characterized by high mutation rates, including RNA viruses. Additionally, there is a sense that the self-replicating molecules present at the origin of life may have had high error rates, and so may fit this model. In the early stages

of the process, a small population size may be important to the extent that it affects the rate of drift.

Ascent via fitness reversals also requires a rugged (epistatic) fitness landscape. Although epistasis is widely recognized in genetics and evolution, the process described here requires an extreme form of it: the fitness effect of a mutation actually reverses (from bad to good) in the presence of a second mutation. Most studies of epistasis focus on the weaker form in which the fitness effect of a first mutation undergoes small changes in response to a second interacting mutation.

Recent theoretical and experimental efforts, however, are beginning to elucidate additional details of these stronger epistatic interactions (so called, "sign epistasis") (Weinreich et al., 2005, 2006). For instance, one recent study of cefotaxime resistance demonstrated strong epistatic interactions between mutations (Weinreich et al., 2006). Their findings, however, were interpreted within the same strong-selection, weak-mutation (SSWM) assumptions previously mentioned. As a result, they reached the conclusion that the evolutionary optimization process is limited to a succession of individual mutations that each increase fitness. If the SSWM assumptions are relaxed, however, then many more evolutionary trajectories may be possible, in particular those that involve deleterious mutations followed by compensatory mutations that reverse the initial deleterious effect.

Other studies suggest that compensatory mutations occur at relatively high frequencies (Poon and Chao, 2005; Poon et al., 2005). For example, in the virus ϕX174, Poon and Chao estimated that fitness recovery following a deleterious mutation proceeded by compensatory mutation (as opposed to back mutation) in about 70% of the cases examined (Poon and Chao, 2005). As another example, Poon et al. estimated, using data from 129 deleterious mutations in a wide range of organisms and genes, that approximately 12 compensatory mutations exist for each deleterious mutation (Poon et al., 2005). Compensatory evolution, as we observed in simulated RNA, may therefore be a general general feature of more complex organisms.

Our results are a natural extension of previous work examining compensatory evolution in viruses and bacteria. As noted above, those studies almost exclusively considered compensatory beneficial mutations appearing after the fixation of a deleterious mutation and demonstrated that the compensatory effect depends on the presence of the initial deleterious mutation (Burch and Chao, 1999, 2004; Moore et al., 2000; Poon and Chao, 2005). The compensatory interactions we observe occur

prior to fixation (or loss) of the deleterious mutation, and thus have a fundamentally different evolutionary implication: they alter the fitness effect of a deleterious mutation sufficiently early to sway its ultimate evolutionary fate.

While it is recognized that asexuality poses several problems to adaptation through processes such as clonal interference, background selection and Muller's ratchet (Orr, 2005), the relative contributions of each to the "cost of asexuality" is not known. A natural extension of this study is, therefore, to partition the fates of beneficial and deleterious mutations into this broader set of mechanisms. Classifying just the processes preventing fixation of beneficial mutations, however, would be non-trivial. In our model, all processes that affect the fates of beneficial mutations are occurring simultaneously and, furthermore, epistasis is rampant and a mutation will typically be followed by others before fixation or loss.

In our study, deleterious mutations accumulated rapidly without impeding adaptation - a result counter to most theoretical predictions. We attribute our results, at least in part, to the fact that the fitness effect of a mutation can change dramatically and rapidly upon additional mutations. It remains unclear whether these reversions are sufficient to not only ensure fixation of the original mutation, but to constitute major adaptive steps.

References

Lauren Ancel and Walter Fontana. Plasticity, Modularity and Evolvability in RNA. *Journal of Experimental Zoology*, 288(3):242–283, 2000.

D Bachtrog and I Gordo. Adaptive evolution of asexual populations under Muller's ratchet. *Evolution Int J Org Evolution*, 58(7):1403–1413, 2004.

J. J. Bull, Lauren Ancel Meyers, and Michael Lachmann. Quasispecies Made Simple. *PLoS Computational Biology*, 1(6):0450–0460, 2005.

Christina L. Burch and Lin Chao. Evolution by Small Steps and Rugged Landscapes in the RNA Virus phi6. *Genetics*, 151(3):921–927, 1999.

Christina L. Burch and Lin Chao. Epistasis and Its Relationship to Canalization in the RNA Virus ϕ6. *Genetics*, 167(2):559–567, 2004.

Brian Charlesworth and Nick Barton. Genome Size: Does Bigger Mean Worse? *Current Biology*, 14(6):R233–R235, 2004.

Brian Charlesworth and Deborah Charlesworth. Some evolutionary consequences of deleterious mutations. *Genetica*, 102/103:3–19, 1998.

Matthew C. Cowperthwaite, J. J. Bull, and Lauren Ancel Meyers. Distributions of Beneficial Fitness Effects in RNA. *Genetics*, 170(4):1449–1457, 2005.

James F. Crow and Motoo Kimura. *An Introduction to Population Genetics Theory.* Burgess Publishing Company, 1970.

Jennifer A. Doudna. Structural genomics of RNA. *Nature Structural Biology*, 7(11): 954–6, 2000.

John W. Drake and John J. Holland. Mutation rates among RNA viruses. *Proc Natl Acad Sci USA*, 96(24):13910–13913, 1999.

M Eigen. Selforganization of matter and the evolution of biological macromolecules. *Naturwissenschaften*, 58(10):465–523, 1971.

Walter Fontana and Peter Schuster. A computer model of evolutionary optimization. *Biophysical Chemistry*, 26(2-3):123–147, 1987.

Walter Fontana and Peter Schuster. Continuity in evolution: on the nature of transitions. *Science*, 280(5368):1451–1455, 1998.

John H. Gillespie. *Population Genetics: A Concise Guide*. Johns Hopkins University Press, Baltimore, 2004.

Ivo L. Hofacker, Walter Fontana, Peter F. Stadler, L. Sebastian Bonhoeffer, Manfred Tacker, and Peter Schuster. Fast Folding and Comparison of RNA Secondary Structures. *Monatshefte fur Chemie*, 125:167–188, 1994.

Martijn A. Huynen, Peter F. Stadler, and Walter Fontana. Smoothness within ruggedness: the role of neutrality in adaptation. *Proc Natl Acad Sci USA*, 93(1): 397–401, 1996.

Hideki Innan and Wolfgang Stephan. Distinguishing the Hitchhiking and Background Selection Models. *Genetics*, 165(4):2307–2312, 2003.

Toby Johnson. Beneficial Mutations, Hitchhiking and the Evolution of Mutation Rates in Sexual Populations. *Genetics*, 151(4):1621–1631, 1999.

Toby Johnson and Nick H. Barton. The Effect of Deleterious Alleles on Adaptation in Asexual Populations. *Genetics*, 162(1):395–411, 2002.

Yuseob Kim and Wolfgang Stephan. Joint Effects of Genetic Hitchhiking and Background Selection on Neutral Variation. *Genetics*, 155(3):1415–1427, 2000.

M. Kimura. The role of compensatory neutral mutations in molecular evolution. *Journal of Genetics*, 64(1):7–19, 1985.

Motoo Kimura. Some problems of stochastic processes in genetics. *Annals of Mathematical Statistics*, 28:882–901, 1957.

Motoo Kimura. On the Probability of Fixation of Mutant Genes in a Population. *Genetics*, 47(6):713–719, 1962.

Alexey S. Kondrashov, Shamil Sunyaev, and Fyodor A. Kondrashov. Dobzhansky-Muller incompatibilities in protein evolution. *Proc Natl Acad Sci USA*, 99(23): 14878–14883, 2002.

Rob J. Kulathinal, Brian R. Bettencourt, and Daniel L. Hartl. Compensated Deleterious Mutations in Insect Genomes. *Science*, 306(5701):1553–1554, 2004.

Richard E. Lenski, Charles Ofria, Robert T. Pennock, and Christoph Adami. The evolutionary origin of complex features. *Nature*, 423(6936):139–144, 2003.

Mark Lunzer, Stephen P. Miller, Roderick Felsheim, and Antony M. Dean. The Biochemical Architecture of an Ancient Adaptive Landscape. *Science*, 310(5747): 499–501, 2005.

J. Maynard Smith. *The Evolution of Sex*. Cambridge University Press, 1978.

Lauren Ancel Meyers, Jennifer F. Lee, Matthew Cowperthwaite, and Andrew D. Ellington. The Robustness of Naturally and Artificially Selected Nucleic Acid Secondary Structures. *Journal of Molecular Evolution*, 58(6):618–625, 2004.

Francisco B.-G. Moore, Daniel E. Rozen, and Richard E. Lenski. Pervasive compensatory adaptation in *Escherichia coli*. *Proceedings of the Royal Society of London: Series B*, 267(1442):515–522, 2000.

R Nussinov and AB Jacboson. Fast algorithm for predicting the secondary structure of single-stranded RNA. *Proceedings of the National Academy of Sciences*, 77 (111):6309–6313, 1980.

H. Allen Orr. The Rate of Adaptation in Asexuals. *Genetics*, 155(2):961–968, 2000.

H. Allen Orr. The Genetic Theory of Adaptation: A Brief History. *Nature Reviews Genetics*, 6(2):119–127, 2005.

J. R. Peck. A Ruby in the Rubbish: Beneficial Mutations, Deleterious Mutations and the Evolution of Sex. *Genetics*, 137(2):597–606, 1994.

Art Poon and Lin Chao. The Rate of Compensatory Mutation in the DNA Bacteriophage ϕX174. *Genetics*, 170(3):989–999, 2005.

Art Poon, Bradley H. Davis, and Lin Chao. The Coupon Collector and the Suppressor Mutation: Estimating the Number of Compensatory Mutations by Maximum Likelihood. *Genetics*, 170(3):1323–1332, 2005.

E van Nimwegen, JP Crutchfield, and M Huynen. Neutral evolution of mutational robustness. *Proc Natl Acad Sci USA*, 17(76):9716–9720, 1999.

Daniel M Weinreich and Lin Chao. Rapid evolutionary escape by large populations from local fitness peaks is likely in nature. *Evolution*, 59(6):1175–82, 2005.

Daniel M. Weinreich, Richard A. Watson, and Lin Chao. Perspective: Sign Epistasis and Genetic Constraint on Evolutionary Trajectories. *Evolution*, 59(6):1165–1174, 2005.

Daniel M. Weinreich, Nigel F. Delaney, Mark A. DePristo, and Daniel L. Hartl. Darwinian Evolution Can Follow Only Very Few Mutational Paths to Fitter Proteins. *Science*, 312(5770):111–114, 2006.

Claus O. Wilke and Christoph Adami. Interaction between directional epistasis and average mutational effects. *Proceedings of the Royal Society of London: Series B*, 268(1475):1469–1474, 2001.

Stephan Wuchty, Walter Fontana, Ivo L. Hofacker, and Peter Schuster. Complete suboptimal folding of RNA and the stability of secondary structures. *Biopolymers*, 49(2):145–165, 1999.

M Zuker and P Stiegler. Optimal computer folding of large RNA sequences using thermodynamics and auxiliary information. *Nucl. Acids. Res.*, 9(1):133–148, 1981.

Michael Zuker. On Finding All Suboptimal Foldings of an RNA Molecule. *Science*, 244(4900):48–52, 1989.

Chapter 4

A Simple Rule Shapes Phenotypic Evolution

4.1 Introduction

Despite its familiar slogan – "survival of the fittest" – evolution by natural selection may not always yield optimal organisms. In particular, it will be fundamentally constrained by the variation introduced into populations by mutation or migration. If better traits never arise, then natural selection will never have the opportunity to favor them. Whereas adaptive constraints are central to evolutionary theory (Arthur, 2003; Beldade and Brakefield, 2003; Pigliucci and Kaplan, 2000), there have been relatively few empirical characterizations of them (Beldade et al., 2002; Frankino et al., 2005; Miller et al., 2006; Teotonio and Rose, 2000; Travisano et al., 1995). Several of these studies suggest that selection can overcome putative constraints (Beldade et al., 2002; Frankino et al., 2005). Yet, one study of the enzyme beta-isopropylmalate dehydrogenase (IMDH) concludes that adaptation is constrained by its spectrum of mutations (Miller et al., 2006).

With the introduction of the fitness landscape metaphor, Sewell Wright was one of the first to argue for the importance of adaptive constraints (Wright, 1932). In contrast to Fisher's panselectionist views (Fisher, 1930), Wright suggested that fitness valleys – low-fitness genotypes separating high-fitness genotypes – may preclude simple incremental evolution (Wright, 1932). He argued that adaptation depends on both the structure of the fitness landscape (that is, the spectrum of possible mu-

tations) and demographic conditions. Since the 1930's, the theory of evolutionary constraints has matured, but is largely premised on hypothetical fitness landscapes or very local estimates of mutational effects (Gavrilets, 2004; Stadler, 1995).

For most phenotypes of interest, we cannot yet model complete fitness landscapes. It requires knowing the fitnesses across large sets of genotypes, typically too vast to exhaustively study either empirically or computationally. There are, however, a few biologically important phenotypes for which this is tractable. In particular, Eigen and Schuster pioneered the study of RNA molecules, using RNA secondary-structure folding algorithms as tractable genotype-to-phenotype maps (Fontana, 2002; Stadler, 1995). In their model, the genotype of a molecule is its primary sequence and the phenotype is its predicted minimum free energy secondary structure; fitness is based entirely on the similarity of a phenotype to an ideal target structure. Through extensive sampling (that is, folding many diverse sequences) and evolutionary simulations, this system has motivated and clarified several important ideas in modern evolutionary theory, including error catastrophes, quasispecies, neutral networks, and punctuated equilibria (Ancel and Fontana, 2000; Cowperthwaite et al., 2005, 2006; Eigen, 1971; Fontana and Schuster, 1998b; Gruner et al., 1996a,b; Huynen et al., 1996; Schuster et al., 1994; van Nimwegen et al., 1999).

The most influential concept to emerge from these RNA studies is that of "neutral networks", which are sets of genotypes with identical fitness that are interconnected by neutral mutations (Schuster et al., 1994). In the RNA model, the genotypes in a neutral network are sequences that fold into the same shape and are connected to each other by paths of neutral point mutations. The neutral networks of RNA and protein molecules appear to share three basic characteristics: (i) most neutral networks are small (contain few genotypes), whereas relatively few are large (contain many genotypes); (ii) large neutral networks are mutationally adjacent to a greater diversity of phenotypes than small neutral networks; and (iii) large neutral networks span the entire sequence space (Fontana and Schuster, 1998a; Reidys et al., 1997; Schuster et al., 1994; Wagner, 2008).

Based on these characteristics, researchers have proposed that large neutral networks should facilitate evolution by allowing populations to explore vast regions of regions of fitness landscapes through neutral drift (Huynen et al., 1996; Reidys et al., 1997; Schuster et al., 1994; Wagner, 2005, 2008). There is some evidence to support this assertion, though it is largely based on sampling studies (Reidys

et al., 1997; Schuster et al., 1994; Wagner, 2008) or simulation studies with strong assumptions about the fitness landscape (Wagner, 2008). Most recently, Wagner (2008) showed that populations evolving on large neutral networks sample more alternative phenotypes than those evolving on small neutral networks, yet these populations were constrained to explore a single neutral network.

Whether large neutral networks actually facilitate the evolution of optimal phenotypes fundamentally depends on the global structure of mutational connections between different neutral networks. If large neutral networks are almost exclusively connected to other large neutral networks, then populations will easily move among common phenotypes, but be unable to evolve rare phenotypes. Theoretical and computational characterizations of RNA fitness landscapes suggest that this may, in fact, be the case. Yet, these predictions are largely based on relatively small samples of sequences which may include only the most common phenotypes in the fitness landscape (Reidys et al., 1997; Schuster et al., 1994).

Here, we use the RNA folding model to determine the complete structure of fitness landscapes and how neutral network size and adjacencies constrain evolutionary dynamics (for better or for worse). Specifically, we fold all RNA molecules of lengths 12 to 18 nucleotides, and then develop a network model describing the patterns of mutational connectivity among the phenotypes produced by molecules of the same length. We build on previous characterizations of RNA neutral network structure (Fontana and Schuster, 1998a; Li et al., 1996; Schuster et al., 1994; Stadler et al., 2001), and argue that the mutational connectivity among phenotypes follows simple predictable patterns that fundamentally constrain evolution.

4.2 Materials and Methods

RNA Folding Model RNA molecules fold into secondary structures that are the essential scaffolds for functional tertiary structures and are evolutionarily conserved for most functional RNA molecules (Higgs, 2001). The formation of secondary structures is relatively well understood and can be rapidly predicted using thermodynamic minimization (Hofacker et al., 1994; Waterman, 1978; Wuchty et al., 1999; Zuker, 1989). We used the Vienna RNA folding software [version 1.6.1 with the default parameter set; (Hofacker et al., 1994)] to predict the lowest free energy shapes of all RNA molecules of lengths 12-18 nucleotides. We assume that the shape

of a molecule is a reasonable proxy for its fitness (Ancel and Fontana, 2000; Cowperthwaite et al., 2006; Fontana and Schuster, 1998b) and refer to each map from sequences of length n to their predicted shapes as an n-mer fitness landscape.

Simulation Model We studied evolutionary dynamics on the 12-mer fitness landscape by computationally simulating a population of evolving RNA molecules. The molecules stochastically replicate at each discrete generation in proportion to their fitnesses, and evolve by point mutations. We and others have used similar models to study many aspects of RNA evolutionary dynamics (Ancel and Fontana, 2000; Cowperthwaite et al., 2005, 2006; Fontana and Schuster, 1998b; Huynen et al., 1996; van Nimwegen et al., 1999; Wilke and Adami, 2001). An important feature of the RNA system is that the fitness effect of a point mutation stems from a biologically explicit model of molecular structure and is not simply selected from a probability distribution of mutational effects, as in simpler evolutionary models.

To compute the fitness of a molecule, we first predict its minimum free energy secondary structure (that is, its groundstate), and then compare this predicted structure with a pre-specified target structure. Specifically, if σ is the groundstate of a molecule m and t is the target structure, then the fitness of the molecule W is given by

$$W(m) = \frac{1}{\alpha + (d(\sigma, t)/L)^{\beta}} \tag{4.1}$$

where $\alpha = 0.01$ and $\beta = 1$ are scaling constants, $d(\sigma, t)$ is the Hamming distance between the parenthetical representations of σ and t [1], and $L = 12$ is the length of the sequence. The range of fitness values possible given our choice of parameters is 0.99 - 100.0; except the open-chain shape, which was assigned a fitness of zero. Several other studies using this computational model have shown that the qualitative results are largely insensitive to the choice of parameters and even the shape of the fitness function (Ancel and Fontana, 2000; Cowperthwaite et al., 2006; Fontana and Schuster, 1998b; Huynen et al., 1996; van Nimwegen et al., 1999).

For every starting structure-target structure combination, we adapted 20 replicate populations for $\tau = 1,000,000$ generations. The population size was held fixed at $N = 1000$, which was chosen both for computational tractability and to

[1] Parenthetical notation represents paired bases with pairs of parentheses and unpaired bases with dots (e.g. `(((....)))` is a simple stem-loop structure)

limit the effects of genetic drift. The genomic mutation rate was maintained at $U = 0.0003$ ($NU = 0.3$) for all bases in the RNA alphabet. We used soft-selection (constant N) to maintain the population size when genotypes that fold into the open-chain shape occasionally appear.

The expansive and intertwining neutral networks smooth the fitness landscape so that virtually every phenotype can mutate to at least one fitter phenotype, except, of course, the optimal (target) phenotype. Yet the likelihood of finding a more fit mutation while drifting on a large neutral network may be exceedingly small. Specifically, 96.7% of all neutral networks have at least one beneficial mutation (across all fitness functions considered in this study), and there always exists a path of beneficial and neutral mutations leading to the target phenotype.

In our simulations, the average time to target was 339111.7 generations; and there is no significant correlation between time to target and the abundance of the target. The simulations were allowed to run for approximately three times longer than the typical time to acquire the target, and 100 times longer than the evolutionary simulations reported in other studies using this system (Ancel and Fontana, 2000; Cowperthwaite et al., 2006; Fontana and Schuster, 1998b; Huynen et al., 1996; van Nimwegen et al., 1999). Two sets of simulations with different parameter sets ($N = 500, U = 0.05, \tau = 5,000$; $N = 1000, U = 0.005, \tau = 250,000$) produced similar results to those reported here (not shown). The parameters were selected to be biologically reasonable and do not appear to strongly affect the outcome. Although even the most unlikely phenotype can evolve given infinite time, we believe that our results reflect the likely course of evolution.

Rfam Informatics Analysis Rfam is a curated database of functional RNA genes, which are those genes in which the RNA molecule itself takes parts in a biological reaction (Griffiths-Jones et al., 2005). Here, we used version 7 (2006) of the database. We restricted our analysis to families in which the predicted shape of each sequence in the family was at least 60% identical to the consensus structure, thereby minimizing the effects of folding inaccuracies. This included 239 Rfam families (about 50% of the entire database) with representatives of every functional class in the database.

Abundance estimates were obtained by calculating contiguity statistics for the secondary structures predicted by thermodynamic minimization of each sequence

in a family. We then determined the rank percentiles of these abundance estimates in a null distribution of abundance estimates from random sequences. To generate the null distributions, we randomized each sequence in a family 500 times (preserving nucleotide composition), and then calculated the contiguity statistics of the ground-state shapes of these random molecules. We finally determined the fraction of contiguity statistics in the null distributions that were less than the contiguity statistic from the naturally occurring molecule (**Fig. 4.8**).

Receiver Operating Curves Receiver operating curve (ROC) analysis is a technique for assessing the performance of classifier models (Fawcett, 2003). The area under an ROC gives the probability that a model correctly assigns a binary variable (in this case, natural or random molecule) to its proper group. We used ROC analysis to assess relative accuracies of thermostability and contiguity for classifying sequences as natural (taken from the Rfam database) or random, under the assumption that natural molecules will have higher contiguity and thermostability than random permutations of those molecules.

Specifically, we performed logistic regressions of molecule class (natural or random permutation) on contiguity statistic and thermostability, and compute the area (A) under the ROC as:

$$A = \frac{\sum_i ((\mathrm{TP}_j - \mathrm{TP}_i) \times (\mathrm{FP}_j - \mathrm{FP}_i)}{P \times N}$$

where P and N are the numbers of positive and negative instances in the data set, TP and FP are the counts of true positive and false positive classifications between indices i and j. We used the ROCR package to perform all such calculations in R 2.5.0 (Sing et al., 2005).

4.3 Results

4.3.1 Characteristics of RNA fitness landscapes

We have predicted the groundstate structures of all RNA molecules of lengths 12 through 18 nucleotides; we refer to length n RNA molecules as n-mers. The map from sequences to shapes is extremely degenerate with large numbers of sequences (genotypes) giving rise to identical shapes (phenotypes), as previously observed

(Gruner et al., 1996a,b; Schuster et al., 1994). We found that the number of unique phenotypes approximately doubles with each single-base addition, from 59 unique 12-mer shapes to 3211 unique 18-mer shapes. Some of these shapes are quite common, with many unique genotypes folding into them, while others are quite rare, formed by few unique genotypes.

We define *abundance* as the number of genotypes that produce a particular phenotype. The distributions of phenotype abundances appear similar across all lengths of molecules (roughly exponential without the 10% of extreme values in each tail), with relatively few highly abundant phenotypes and many rare ones **Figure 4.1**. This is qualitatively similar to the distributions reported previously for both protein and larger RNA molecules (Gruner et al., 1996a,b; Li et al., 1996; Schuster et al., 1994).

Figure 4.1 shows a portion of the abundance distribution and a sample of shapes present in the 12-mer fitness landscape. For the 12-mer to 16-mer sequence lengths, the landscapes are composed entirely of variations on stem-loop-structures. In the 17- and 18-mer landscapes, we observe the emergence of sequences folding into multi-loop shapes, albeit at very low frequencies (on the order of 0.001% of all sequences). The relatively low structural diversity is consistent with known constraints on RNA structural motifs, for example, loops must contain at least three nucleotides (Hofacker et al., 1994; Waterman, 1978).

A set of genotypes that shares a common phenotype is called the *neutral network* of that phenotype (**Fig. 4.2**) (Schuster et al., 1994). Neutral networks may be composed of one or more components. Within any component, all genotypes are connected to each other by a sequence of point mutations that remain within the component; these mutations are, by definition, neutral. For example, in the bottom network of **Fig. 4.2B**, the red phenotype has a neutral network with two components, each of which consists of a set of red nodes interconnected by red edges. The abundance of a phenotype is precisely the size of its neutral network.

Counterintuitively, there is only a weak positive relationship between the abundance of a phenotype and the number of distinct components in its neutral network ($r^2 = 0.11, P \approx 0.01$). The majority of the 12-mer RNA neutral networks are dominated by relatively few large components, which each contain approximately 8-10% of the sequences in the neutral network; together these large components account for at least 80% of the neutral network. Importantly, the large components

Rank	Abundance	Nc	Dhamm	Dspl
1	14325304	nd	nd	nd
2	218567	16	11	36
3	183791	10	12	32
4	162009	26	12	39
5	152393	9	12	25
6	151705	15	12	29
7	122332	8	12	32
8	117213	21	12	35
9	113896	8	12	33
10	110509	8	11	32
11	105538	8	12	47
12	93866	7	8	24
. . . .				
38	2260	12	9	18
39	2208	1	6	12
40	1525	16	9	21
41	1379	15	7	14
42	1368	2	5	10
43	1299	22	8	16
44	1188	34	7	12
45	1139	23	8	18
46	860	3	7	13
47	800	3	6	15
48	713	3	7	17
49	665	15	8	15
50	411	11	5	8
51	314	3	4	6
52	240	3	4	6
53	220	4	4	8
54	197	5	3	6
55	165	4	6	10
56	153	4	6	10
57	109	6	6	12
58	54	1	4	6
59	20	1	4	8

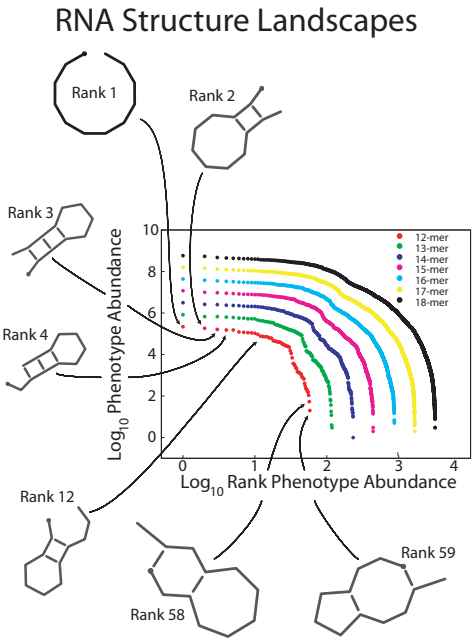

Figure 4.1: Phenotype abundance distributions for all fitness landscapes. The graph shows the phenotype abundances (y-axis) for each phenotype, ranked in order of abundance (x-axis). The most common phenotype is rank 1, the second most common is rank 2, and so on. Shown at left is the distribution of abundances, the number of components (Nc), the maximum hamming distance between a pair of sequences in a component (Dmax), and the length of the maximal shortest neutral path between a pair of sequences in a component (Dspl) for each shape in the 12-mer RNA landscape. The figure also depicts a sample of the secondary structures from this landscape. The number of components and maximum diameter of the open chain shape was not determined.

share many of the same characteristics as the entire neutral network. In particular, they are each mutationally connected to the majority of the shapes that are adjacent to the entire neutral network (typically $> 75\%$). **Figure 4.1** also reports the number of components (Nc), the maximum Hamming distance between a pair of sequences in a single component (Dmax), and the maximum shortest path length between a pair of sequences in a single component (Dspl) for the neutral networks in the 12-mer landscape. The neutral networks for the most abundant phenotypes percolate through the entire space of genotypes.

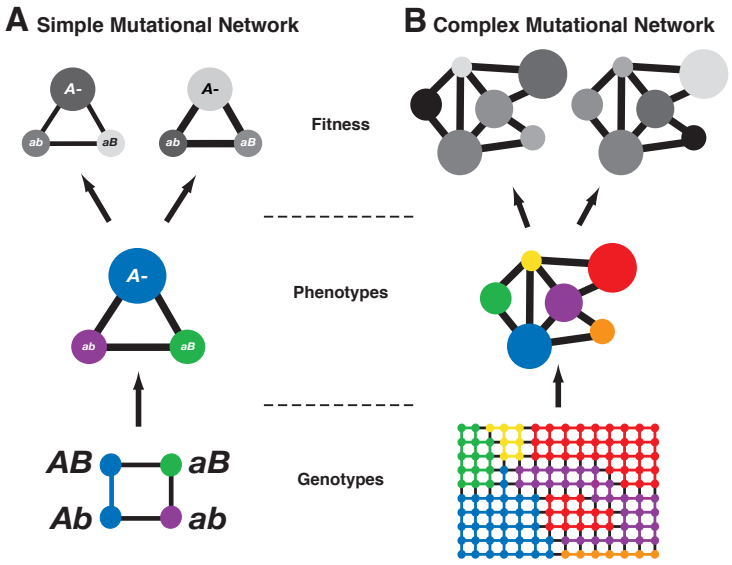

Figure 4.2: Simple mutational networks - (A) a two-locus, two-allele network and (B) a more complex (hypothetical) mutational network. The lower networks show mutational connections among genotypes; vertices are unique genotypes and edges are point mutations. Colored edges represent neutral mutations, which connect genotypes with the same phenotype (color); black edges represent non-neutral mutations, which lead to a change in phenotype. The middle networks show mutational connections among phenotypes. The size of a phenotype vertex is proportional to the number of genotypes that produce it. Pairs of vertices are connected if there is at least one point mutation that converts one phenotype to the other. The top networks show possible fitness landscapes in which each phenotype is assigned a fitness value, indicated in grayscale.

4.3.2 Characteristics of RNA mutational networks

The various phenotypes within a fitness landscape are connected to each other by mutations. If we aggregate all genotypes into their respective neutral networks, we create a *mutational network* in which each vertex represents a distinct phenotype and edges connect pairs of vertices when there is at least one point mutation that converts one phenotype to the other (**Fig. 4.2**). For example, consider a two-locus, two-allele, haploid model with genotypes AB, Ab, aB, and ab (**Fig. 4.2A**). There are three unique phenotypes - the two (A-) genotypes produce one phenotype (blue), aB produces another phenotype (green), and ab produces a third phenotype (purple).

Mutational networks, in turn, form the underpinnings for fitness landscapes, which depend on the map from phenotype to fitness. **Fig. 4.2B** caricatures a higher dimensional genotype network and its projections to phenotype and fitness networks. For RNA molecules, the vertices in a mutational network represent unique shapes and the edges represent point mutations that cause a molecule to fold into a new shape.

Roughly speaking, evolution by natural selection moves populations along the edges in a mutational network from one phenotype vertex to another. We are therefore interested in how the structure of mutational networks influences evolutionary dynamics. Intuitively, the structure of a mutational network may influence (i) the likelihood that a given phenotype will arise and, (ii) if it arises, the likelihood that the population can further evolve other, better phenotypes. Hereafter, we use *accessibility* to refer to the likelihood that a phenotype will arise, and *evolvability* as the likelihood that a phenotype can further evolve other, better phenotypes.

The most straightforward measure of a phenotype's mutational connectivity is its *degree* in the mutational network, that is, the number of other phenotype that can be reached by a single mutation. For the 12-mer through 18-mer RNA molecules, there are significant positive correlations between phenotype abundance and degree [$R = 0.88$(12-mer) to $R = 0.91$(18-mer); $P < 2 \times 10^{-16}$]. This has been observed previously and suggests that abundant phenotypes should be both more evolvable and more accessible than rare phenotypes (Reidys et al., 1997; Wagner, 2005, 2008).

The degree of a phenotype is, however, a crude indicator of its mutational connectivity to other phenotypes. It does not reflect the probability that a mutation will actually yield a new phenotype; this probability typically declines as the size of the neutral network increases. Furthermore, the degree does not quantify whether the non-neutral mutations off a neutral network are evenly divided among the set alternative phenotypes, or are biased towards a select few of these phenotypes.

We therefore developed two novel statistics, which provide a more nuanced perspective on mutational connectivity. Both of these statistics use the quantity $f_{ij} = \frac{\nu_{ij}}{\sum_{k \neq i} \nu_{ik}}$, where ν_{ij} is the number of point mutations to genotypes in the neutral network for phenotype i that create a genotype in the neutral network for phenotype j, and $\sum_{k \neq i} \nu_{ik}$ is the total number of non-neutral point mutations to genotypes in the neutral network for phenotype i. Thus, f_{ij} is the fraction of

non-neutral point mutations to genotypes in the neutral network for phenotype i that create genotypes in the neutral network for phenotype j. Large values of this fraction indicate that phenotype j is relatively easy to find (via random mutations) from phenotype i. Mutational proximity is often not symmetric (that is, $f_{ij} \neq f_{ji}$), because the denominators differ.

The first statistic estimates the overall accessibility of phenotype i from other phenotypes in the landscape using $A_i = \sum_j f_{ji}$. Large values of A_i indicate that phenotype i is relatively accessible from throughout the landscape. The second statistic quantifies the potential for evolution away from phenotype i using a variation on Simpson's diversity index: $E_i = 1 - \sum_j f_{ij}^2$. This index indicates the diversity of other phenotypes that can be easily produced by mutations from a given phenotype, and thus may indicate the potential for further adaptation away from that phenotype. Specifically, it gives the probability that two randomly chosen *non-neutral* mutations to genotypes within a given neutral network will result in the same phenotype. The index is large for phenotypes that are adjacent to many other phenotypes, and its non-neutral mutations are fairly evenly divided among the adjacent phenotypes; it is small for phenotypes that primarily mutate to one or very few alternate phenotypes.

In the 12-mer landscape, A increases significantly with the abundance of a phenotype (**Fig. 4.3,top pane**). In other words, random mutations are more likely to move genotypes to a large neutral network than to a small neutral network. In contrast, E decays significantly with phenotype abundance (**Fig. 4.3,middle pane**), suggesting that it may be more difficult to evolve away from large neutral networks than small neutral networks. To provide more insight into the mutational networks, we also calculated the average abundance of phenotypes reached by mutation from phenotype i using $B_i = \sum_j \frac{\nu_{ij}}{\sum_{k \neq i} \nu_{ik}} \times |p_j|$. We find that the average abundance of neighboring phenotypes significantly increases with the abundance of a phenotype (**Figure 4.3,bottom pane**), meaning that the majority of non-neutral mutations to abundant phenotypes produce other abundant phenotypes.

Thus far we have characterized the mutational networks formed by single point mutations. If we instead considered the mutational networks formed by all combinations of one, two or three mutations, then the phenotype network becomes highly interconnected. The number of adjacent phenotypes significantly increases with multiplicity of mutations considered (mean node degrees are 42.7, 53.6, and

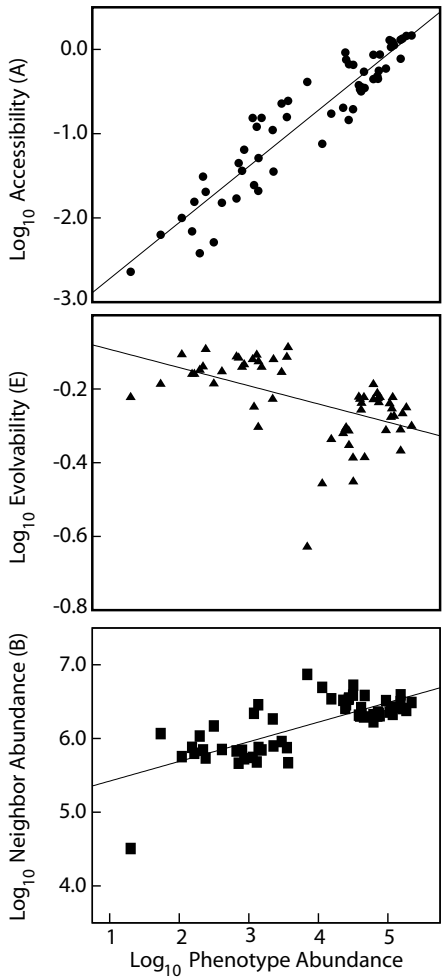

Figure 4.3: Mutational connectivity among RNA phenotypes. (Top) The A statistic (described in text) indicates the likelihood that a given phenotype will arise through point mutation. Random mutations are more likely to hit upon larger neutral networks that smaller neutral networks ($r^2 = 0.886, P < 2.2 \times 10^{-16}$; calculated on log-transformed data). (Middle) The E statistic (described in text) indicates the likelihood of given phenotype will produce diverse alternative phenotypes upon mutation. Point mutations to sequences in large neutral networks are less likely to yield novelty than point mutations to sequences in small neutral networks ($r^2 = 0.265, P = 3.56 \times 10^{-5}$). (Bottom) The B statistic (described in text) suggests that point mutations to abundant phenotypes create other abundant phenotypes ($r^2 = 0.559, P = 1.58 \times 10^{-11}$).

57.2 for the one, two, and three mutant adjacencies, respectively; $P < 5 \times 10^{-3}$), and the network is nearly completely connected for triple mutations. Thus, under elevated mutation rates, populations may be able to attain rare phenotypes easier than expected based on point mutation adjacencies.

In summary, these observations suggest that abundant phenotypes may be easy to find but difficult to escape, and thus the structure of a fitness landscape may significantly constrain evolutionary dynamics. Whereas the accessibility of abundant shapes is rather intuitive, the prediction that their vast neutral networks can hinder further evolution contradicts a large body of theory, which suggests that large neutral networks should enhance evolvability Huynen et al. (1996); Wagner (2005, 2008). We note that this evolutionary constraint was previously proposed for a simple fitness landscape model (van Nimwegen and Crutchfield, 2000).

4.3.3 Mutational networks provide novel insights into evolutionary dynamics

To test the hypothesis that highly abundant phenotypes are readily accessible, yet poorly poised for further evolution, we ran stochastic simulations of an adapting population of 12-mer RNA molecules using an established model (see Materials and Methods for details) (Ancel and Fontana, 2000; Cowperthwaite et al., 2006; Fontana and Schuster, 1998b; Huynen et al., 1996; van Nimwegen et al., 1999). Since we are interested in the effect of phenotype abundance on the capacity of selection to acquire the optimal phenotype, we selected the phenotypes of the founding populations (henceforth, founding phenotypes) and target shapes to span the range of abundances found among the 12-mer phenotypes. We chose ten founding phenotypes [ranks (abundance): 3 (183,791), 8 (117,213), 13 (76,478), 18 (61,699), 23 (39,740), 28 (27,312), 33 (11,354), 38 (2,260), 43 (1,299), 48 (713)] and randomly selected 20 genotypes from the neutral network of each founding phenotype to form 200 isogenic founding populations. Each founding population was composed of a single genotype and, therefore, a single phenotype. In essence, we simulated adaptation starting from 20 random points in the neutral network of each founding phenotype.

We separately adapted each founding population to twelve target phenotypes [ranks (abundance): 2 (218,576), 7 (122,332), 12 (93,866), 17 (61,895), 22 (41,092), 27 (27,522), 32 (15,348), 37 (2,963), 42 (1,368), 47 (800), 52 (240), 57 (109)]. We

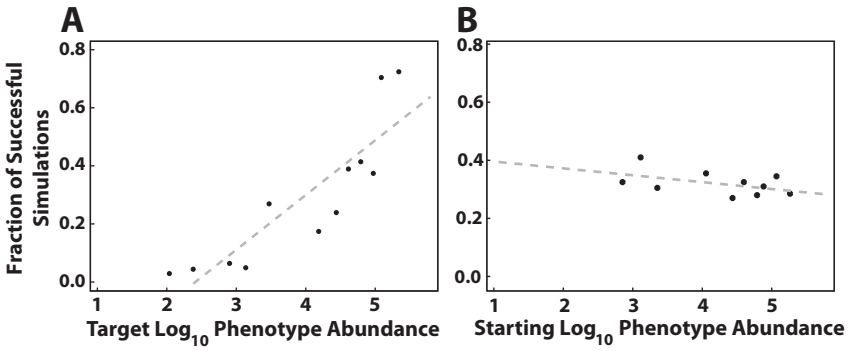

Figure 4.4: Stochastic evolutionary simulation in the 12-mer fitness landscape. (A) The phenotype abundance of the target strongly affects the success of adaptation ($r = 0.76$, $P = 2.2 \times 10^{-4}$). (B) The phenotype abundance at the start of the simulation has no effect on the evolutionary outcome ($r = -0.023$, $P = 0.17$). We simulated adaptation over one million generations with a genomic mutation rate of $U = 0.0003$ and a constant population size of N = 1000.

considered adaptation successful if the population ever acquired the target phenotype, regardless of its frequency in the population. In the successful runs, however, the target phenotype quickly dominates the populations and rises to frequencies of nearly N (the population size).

The mutational connectivity statistics described above (A_i and E_i) will only be good indicators of evolutionary dynamics if the probability of mutating from phenotype i to phenotype j correlates with the fraction of mutations to i that produce j (f_{ij}). To test this basic assumption, we compared the phenotype mutation rates observed in the simulations (fraction of mutations to i that produce j) to f_{ij} (the fraction of non-neutral point mutations to genotypes in the neutral network for phenotype i that create genotypes in the neutral network for phenotype j). In fact, we find an almost perfect relationship between the two quantities (**Fig. 4.6A**), suggesting that mutational network structure fundamentally constrains evolution and that A_i and E_i are good indicators of these constraints.

Across the 2400 simulations, we observed a significant positive correlation between the abundance of the target phenotype and the likelihood that a population successfully evolved to the target (**Fig. 4.4A**). This is consistent with the positive relationship between phenotype abundance and mutational accessibility, as indicated by the A statistic (**Fig. 4.3A**). Phenotype abundance also positively correlates with

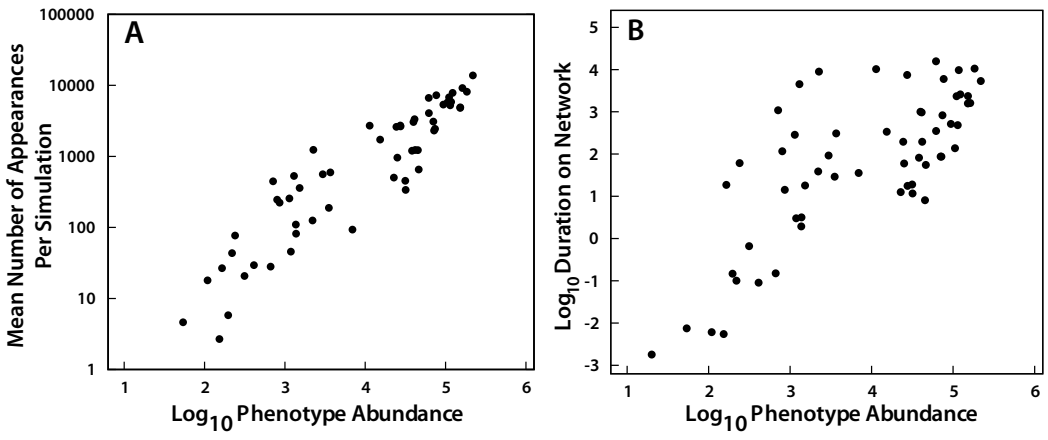

Figure 4.5: Populations exploring the 12-mer fitness landscape. (A) The number of appearances of a phenotype is strongly correlated with the abundance of that phenotype ($r = 0.92$, $P = 2.2 \times 10^{-16}$, calculated on log-transformed data). (B) The total number of time steps that a phenotype occurs in the evolving populations is positively correlated with its abundance ($r = 0.75, P = 1.5 \times 10^{-11}$, calculated on log-transformed data).

the number of times a phenotype arises in the evolving populations (**Fig. 4.5A**). Taken together, these results support our hypothesis that abundant shapes are more likely to appear via mutation in evolving populations than are rare shapes.

We did not, however, observe a relationship between the founding phenotype abundance and the ultimate evolutionary outcome (**Fig. 4.4B**). When a simulation failed to acquire the target, the population was primarily composed of phenotypes of greater abundance than both the target phenotype and the average abundance of a random phenotype, demonstrating that the structure of mutational networks can steer populations towards abundant, but non-optimal, phenotypes. As suggested by the negative relationship between abundance and the E statistic, evolution away from abundant phenotypes appears to be limited by the improbability of beneficial mutations. In support of this explanation, we also find a significant positive correlation between the abundance of a phenotype and the duration of the phenotype in the evolving populations (**Fig. 4.5B**).

These observations appear to be inconsistent with the widely-held belief that neutral networks facilitate evolution by allowing populations to traverse large regions of fitness landscapes without reducing fitness (Bornberg-Bauer and Chan,

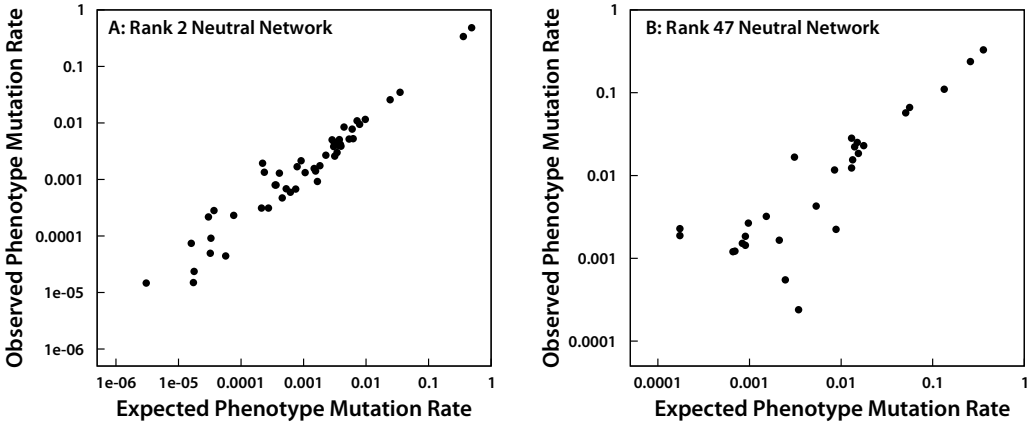

Figure 4.6: Network connectivity correlates with mutation frequency in the 12-mer fitness landscape. The rates of mutation between phenotype i and phenotype j in simulations is nearly identical to the fraction of non-neutral mutations to i that produce j (f_{ij}). The top pane depicts this correlation for an abundant phenotype (rank 2, 218567 sequences), whereas the bottom pane shows this for a small neutral network (rank 47, sequences). The mean slope of the regression line (taken over all 52 of 59 neutral networks that arose in simulation) was $r^2 = 0.978$ with 95% confidence interval $[0.945, 1.011]$, which is statistically indistinguishable from one.

1999; Fontana and Schuster, 1998b; Huynen et al., 1996; Schuster et al., 1994; van Nimwegen et al., 1999; Wagner, 2005, 2008). In our simulations, populations readily evolve from one abundant shape to another (that is, from one large neutral network to another), but are often unable to evolve rare phenotypes. Thus, while the hypothesis that neutrality (the fraction of mutations that are neutral) allows populations to explore phenotype space is true, the evolutionary outcome of such exploration is generally confined to other abundant phenotypes. Most of the prior studies addressing this hypothesis are based on relatively small random samples of sequences from large genotype spaces, which may consist of exclusively abundant phenotypes. The conclusion that neutrality facilitates evolution is reasonable when considering only abundant subsets of fitness landscapes, but is somewhat misleading when one considers the fitness landscapes in their entirety.

4.3.4 The "ascent of the abundant" and the evolution of natural RNA molecules

These results suggest the following hypothesis: the evolution of phenotypes, whether complex whole-organism phenotypes or RNA shapes, may be biased toward abundant phenotypes, even if those phenotypes are not optimal. We cannot, however, test this hypothesis by directly measuring the abundances of complex organism-level phenotypes since we cannot yet completely characterize their fitness landscapes. As a first step in this direction, we have developed a simple structural statistic that allows us to indirectly estimate the abundances of naturally occurring RNA shapes, which are much larger and more complex than those considered thus far.

Across the n-mer phenotypes, we observed that longer contiguous helical stacks (stems) form more frequently than shorter contiguous stacks and stacks that contain bulges (which break up helices). We quantify this with a new statistic (**Fig 4.7**) given by

$$C_s = \log\left(\frac{\text{total length stem-loop regions} + \text{number of base pairs}}{\text{number of contiguous stacks}}\right)$$

This *contiguity statistic* significantly correlates with log phenotype abundance in the 12- through 18-mer landscapes [r ranges from $r = 0.71$ ($P = 3.6 \times 10^{-10}$) in the 12-mer landscape to $r = 0.69$ ($P < 2.2 \times 10^{-16}$) in the 18-mer landscape]. The utility of the contiguity statistic is that one genotype is sufficient to estimate the abundance of its phenotype. We conjecture, therefore, that we can use the contiguity statistic to ask whether naturally occurring RNA molecules are biased towards abundant shapes.

We used the contiguity statistic to estimate the abundances of the RNA molecules in Rfam, a curated database of functional RNA genes (Griffiths-Jones et al., 2005). The Rfam molecules are grouped into families, and every sequence in a family is thought to code for the same functional RNA. We compared the contiguity statistics calculated for the Rfam sequences to null distributions generated by calculating contiguity statistics for thousands of random permutations of those sequences. Specifically, for each naturally evolved molecule, we determined whether the contiguity statistics of their predicted shapes were significantly larger than the contiguity statistics of random molecules from the same fitness landscape

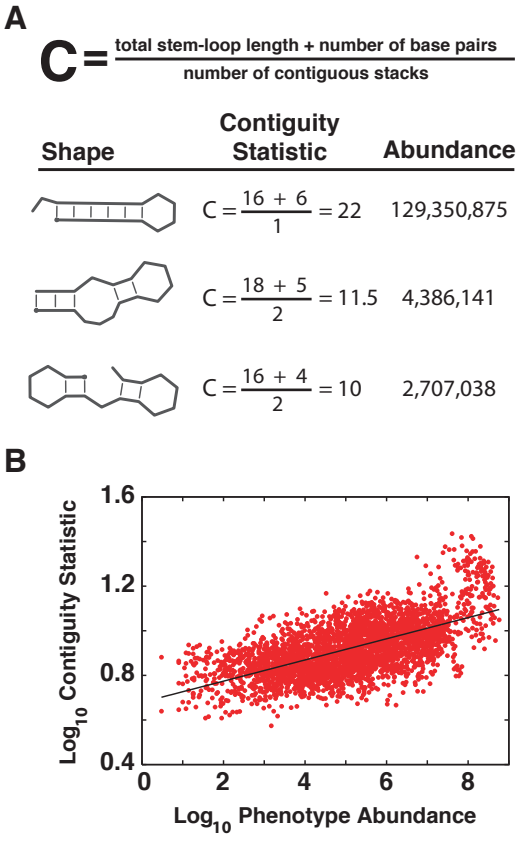

Figure 4.7: Calculation of the contiguity statistic. **A.** Sample calculations of the contiguity statistic for three 18-mer shapes. **B.** The contiguity statistic is strongly correlated with abundance for all lengths of RNA molecules studied; example shown is the 18-mer landscape ($r^2 = 0.69, P < 2.2 \times 10^{-16}$). Minimal Gaussian noise was added to reduce granularity in the data.

(see Methods for details).

The structures of the natural RNA molecules indeed have larger contiguity statistics than randomly chosen structures from the same fitness landscapes (**Fig. 4.8**). This observation supports an "ascent of the abundant" hypothesis in which the mutational networks connecting diverse phenotypes may steer populations toward abundant, though not necessarily optimal, phenotypes. Yet, **Fig. 4.8** (red squares) shows that natural molecules are also significantly more thermostable than random molecules. Thus one must ask whether the high contiguity values of natural

molecules are simply byproducts of the evolution of thermostability (or some other advantageous structural property) or, in fact, exist because of mutational biases towards abundant shapes, or both.

The abundances of the natural molecules (as estimated by their contiguity statistics) are even more statistically pronounced than their thermostabilities. We used logistic regression analysis to ask which of contiguity or thermostability better distinguishes naturally occurring molecules from their random permutations. We regressed molecule class (natural or random permutation) on contiguity statistic and (separately) on thermostability. The area under a receiver operating curve (ROC) gives the probability that a model correctly assigns a binary variable (natural or random molecule) to its proper group. The logistic model for contiguity yielded an area under the ROC of 0.82, which is good; the model for thermodynamic stability yielded an area under the ROC of 0.62, which is poor. Our results are therefore consistent with an apparent biases towards abundant phenotypes in both the small RNA landscapes and natural RNAs are not simply byproducts of natural selection for thermostability.

4.4 Discussion

Evolutionary biologists have long appreciated that the evolutionary potential of a phenotype depends on the breadth of its neutral network. Eigen's error catastrophe theory, an extension of classic mutation-selection balance theory, argues that the evolutionary potential of a phenotype depends on both its fitness relative to alternative phenotypes and its robustness to mutations (Bull et al., 2005). Under high mutation rates, only phenotypes with sufficiently large and connected neutral networks can persist. The phrase "survival of flattest" has been used to refer to the evolutionary success of low-fitness phenotypes with large neutral networks over higher-fitness phenotypes with small neutral networks (Wilke et al., 2001). Critically, this idea assumes that these diverse phenotypes compete directly with one another in an evolving population.

The relationship between abundance and evolvability that we have described here is not a simple restatement of this idea. Instead, the evolutionary tendency towards abundant phenotypes results from a biased exploration of phenotype space. Abundant phenotypes are more discoverable (random mutations are more likely to

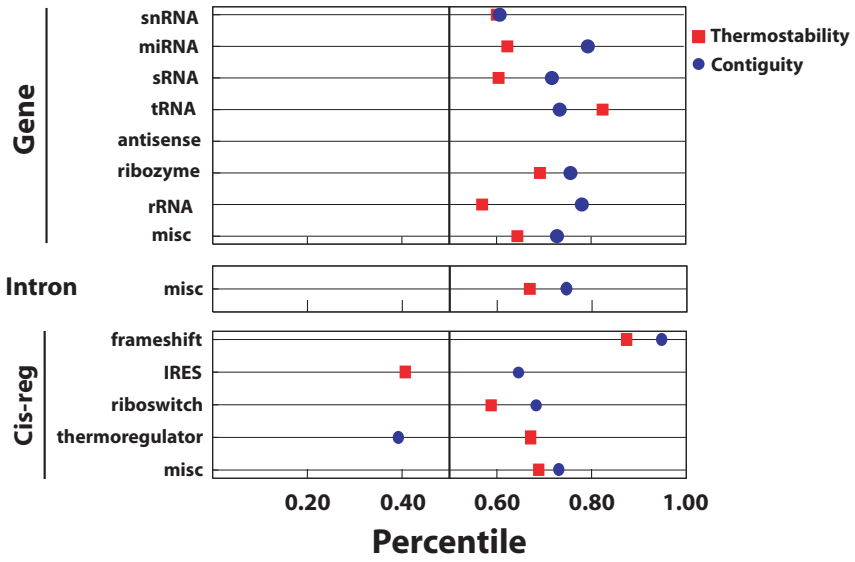

Figure 4.8: Contiguity statistic and thermostability percentiles for natural functional molecules from the Rfam database. The blue and green circles represent percentiles calculated from consensus structures and individual sequences, respectively. The red squares represent percentiles for thermostability predictions of molecules folding into the wild-type structures. We used 239 families in which the consensus structure was relatively well conserved among the individual genotypes. The x-axis gives the fraction of random phenotypes that are predicted to be less abundant (or less thermostable) than the actual phenotype, based on a comparison to 500 randomized molecules. The functional taxonomy is determined by the Rfam database.

produce abundant phenotypes) and more inescapable (once abundant phenotypes evolve, it is very hard to mutate to other phenotypes). In our simulations, we observed that, when the populations failed to acquire the target phenotype, it was not due to the target shape being lost to mutation pressure or other forces. In the failed simulations, the target phenotype never appeared in the first place (not shown).

Our results extend ideas developed in prior studies of both RNA and protein structural evolution (Li et al., 1996; Schuster et al., 1994). In particular, Schuster et al. argued that abundant RNA phenotypes are within a few mutations of almost any genotype in the landscape (Schuster et al., 1994), and Reidys et al. further demonstrated that only abundant phenotypes have neutral networks that percolate through the entire sequence space Reidys et al. (1997). As a result, evolutionary bi-

ologists have proposed that large neutral networks greatly enhance the evolutionary potential of evolving populations (Huynen et al., 1996; Reidys et al., 1997; Schuster et al., 1994; Wagner, 2005, 2008). Yet, these studies largely focused on the local structure of neutral networks and not global patterns of mutational connectivity.

Here we have taken a global perspective and found that large neutral networks are more likely to impede than enable evolution. The probability of a non-neutral mutation and the diversity of phenotypes produced by such mutations both decline as neutral network size increases (**Fig. 4.3,middle**). In our simulations, populations on large neutral networks were no more likely to evolve better phenotypes than populations on small neutral networks (**Fig. 4.4**). Furthermore, these populations spent more time on large neutral networks than small neutral networks (**Fig. 4.5B**).

Our results more generally suggest that the structure of RNA mutational networks favors the evolution of abundant phenotypes, even when rare phenotypes are more fit. Abundant phenotypes are more likely to arise via a random mutation than rare phenotypes, and, once established in the population, are more difficult to escape via subsequent mutations. This gives a new perspective on the widely-accepted hypothesis that large neutral networks facilitate evolution (Huynen et al., 1996; Reidys et al., 1997; Schuster et al., 1994; Wagner, 2005, 2008). While large neutral networks enable populations to *explore* large regions of fitness landscapes via mutation, the outcome of such exploration is almost always evolution to another abundant phenotype rather than to a rare phenotype. Thus, in the larger scheme of things, neutrality may serve as a trap rather than a catalyst for evolution.

While our study suggests that naturally occurring RNA molecules are biased towards abundant shapes, we recognize that abundance may have evolved as a byproduct of correlated biophysical or biochemical properties that enhance the functionality of molecules. We specifically address the possibility that the abundance bias may be driven by thermostability. Our simulation study shows that abundant shapes will evolve in the absence of natural selection for thermostability, and our analysis of natural RNA molecules indirectly suggests that thermostability alone cannot account for the bias toward abundant shapes. We believe that both processes have probably contributed to the prevalence of abundant shapes: (i) natural selection for thermostability and/or other beneficial molecular properties that correlate with abundance and (ii) the underlying structure of the mutational network.

We contend that the second process is important and perhaps has precluded the evolution of functionally optimal molecules.

In closing, we have further characterized the relationship between phenotype abundance and mutational connectivity, and explored its evolutionary implications. The abundance of a phenotype positively correlates with the probability of randomly mutating to that phenotype and negatively correlates with the probability of randomly mutating away from that phenotype to alternative phenotypes. Consequently, the evolutionary potential of a phenotype critically depends on its abundance, and mutational networks therefore can fundamentally constrain evolution. As we learn more about the structure of mutational networks, we can gain new perspectives on the history and function of natural systems and better methods for artificially selecting molecules with desired functions. Characterizing mutational networks remains a formidable challenge, particularly when we consider more complex phenotypes and sources of variation beyond simple point mutations. We can approach these larger landscapes using statistical shortcuts, like the contiguity statistic introduced here, that indirectly provide information about the global structure of the fitness landscape, or by designing farther-reaching mutagenesis experiments.

References

Lauren Ancel and Walter Fontana. Plasticity, Modularity and Evolvability in RNA. *Journal of Experimental Zoology*, 288(3):242–283, 2000.

Wallace Arthur. Developmental constraint and natural selection. *Evolution & Development*, 5(2):117–118, 2003.

Patricia Beldade and Paul M. Brakefield. The difficulty of agreeing about constraints. *Evolution & Development*, 5(2):119–120, 2003.

PatrIcia Beldade, Kees Koops, and Paul M. Brakefield. Developmental constraints versus flexibility in morphological evolution. *Nature*, 416(6883):844–847, 2002.

Erich Bornberg-Bauer and Hue Sun Chan. Modeling evolutionary landscapes: Mutational stability, topology, and superfunnels in sequence space. *Proc Natl Acad Sci USA*, 96(19):10689–10694, 1999.

J. J. Bull, Lauren Ancel Meyers, and Michael Lachmann. Quasispecies Made Simple. *PLoS Computational Biology*, 1(6):0450–0460, 2005.

Matthew C. Cowperthwaite, J. J. Bull, and Lauren Ancel Meyers. Distributions of Beneficial Fitness Effects in RNA. *Genetics*, 170(4):1449–1457, 2005.

Matthew C. Cowperthwaite, J. J. Bull, and Lauren Ancel Meyers. From bad to good: Fitness reversals and the ascent of deleterious mutations. *PLoS Computational Biology*, 2(10):1292–1300, 2006.

M Eigen. Selforganization of matter and the evolution of biological macromolecules. *Naturwissenschaften*, 58(10):465–523, 1971.

T. Fawcett. ROC Graphs: Notes and Practical Considerations for Data Mining Researchers. Technical Report HPL-2003-4, HP Labs, 2003, 2003.

Ronald Aylmer Fisher. *The Genetical Theory of Natural Selection*. Oxford University Press, Oxford, 1930.

Walter Fontana. Modeling 'evo-devo' with RNA. *Bioessays*, 24(12):1164–1177, 2002.

Walter Fontana and Peter Schuster. Shaping Space: the Possible and the Attainable in RNA Genotype-Phenotype Mapping. *Journal of Theoretical Biology*, 194(4): 491–515, 1998a.

Walter Fontana and Peter Schuster. Continuity in evolution: on the nature of transitions. *Science*, 280(5368):1451–1455, 1998b.

W. Anthony Frankino, Bas J. Zwaan, David L. Stern, and Paul M. Brakefield. Natural Selection and Developmental Constraints in the Evolution of Allometries. *Science*, 307(5710):718–720, 2005.

Sergey Gavrilets. *Fitness Landscapes and the Origin of Species*, volume 41 of *Monographs in Population Biology*. Princeton University Press, 2004.

Sam Griffiths-Jones, Simon Moxon, Mhairi Marshall, Ajay Khanna, Sean R. Eddy, and Alex Bateman. Rfam: annotating non-coding RNAs in complete genomes. *Nucl. Acids Res.*, 33(Supp1):D121–124, 2005.

W. Gruner, U. Giegerich, D. Strothmann, C. Reidys, J. Weber, I. Hofacker, P. Stadler, and P. Schuster. Analysis of RNA sequence structure maps by exhaustive enumeration. I. Neutral Networks. *Monatshefte fur Chemie*, 127:355–374, 1996a.

W. Gruner, U. Giegerich, D. Strothmann, C. Reidys, J. Weber, I. Hofacker, P. Stadler, and P. Schuster. Analysis of RNA sequence structure maps by exhaustive enumeration. II. Structure of neutral networks and shape space covering. *Monatshefte fur Chemie*, 127:375–389, 1996b.

Paul G. Higgs. RNA secondary structure: physical and computational aspects. *Quarterly Reviews of Biophysics*, 33(03):199–253, 2001.

Ivo L. Hofacker, Walter Fontana, Peter F. Stadler, L. Sebastian Bonhoeffer, Manfred Tacker, and Peter Schuster. Fast Folding and Comparison of RNA Secondary Structures. *Monatshefte fur Chemie*, 125:167–188, 1994.

Martijn A. Huynen, Peter F. Stadler, and Walter Fontana. Smoothness within ruggedness: the role of neutrality in adaptation. *Proc Natl Acad Sci USA*, 93(1): 397–401, 1996.

Hao Li, Robert Helling, Chao Tang, and Ned Wingreen. Emergence of preferred structures in a simple model of protein folding. *Science*, 273(5275):666–669, 1996.

Stephen P. Miller, Mark Lunzer, and Antony M. Dean. Direct Demonstration of an Adaptive Constraint. *Science*, 314(5798):458–461, 2006.

Massimo Pigliucci and Jonathan Kaplan. The fall and rise of Dr Pangloss: adaptationism and the Spandrels paper 20 years later. *Trends in Ecology & Evolution*, 15(2):66–70, 2000.

Christian Reidys, Peter F. Stadler, and Peter Schuster. Generic properties of combinatory maps: Neutral networks of RNA secondary structures. *Bulletin of Mathematical Biology*, 59(2):339–397, 1997.

Peter Schuster, Walter Fontana, Peter F. Stadler, and Ivo L. Hofacker. From sequences to shapes and back: a case study in RNA secondary structures. *Proceedings of the Royal Society of London B*, 255(1344):279–284, 1994.

Tobias Sing, Oliver Sander, Niko Beerenwinkel, and Thomas Lengauer. ROCR: visualizing classifier performance in R. *Bioinformatics*, 21(20):3940–3941, 2005.

Barbel M. R. Stadler, Peter Stadler, Gunter P. Wagner, and Walter Fontana. The topology of the possible: Formal spaces underlying patterns of evolutionary change. *Journal of Theoretical Biology*, 213(2):241–74, 2001.

Peter F Stadler. Towards a general theory of landscapes. In R. Lopéz-Peña, R. Capovilla, R. Garcia-Pelayo, H. Waelbroeck, and F. Zertuche, editors, *Complex Systems and Binary Networks*, pages 77–163. Springer-Verlag, 1995.

Henrique Teotonio and Michael R. Rose. Variation in the reversibility of evolution. *Nature*, 408(6811):463–466, 2000.

M Travisano, JA Mongold, AF Bennett, and RE Lenski. Experimental tests of the roles of adaptation, chance, and history in evolution. *Science*, 267(5194):87–90, 1995.

E van Nimwegen, JP Crutchfield, and M Huynen. Neutral evolution of mutational robustness. *Proc Natl Acad Sci USA*, 17(76):9716–9720, 1999.

Erik van Nimwegen and James P. Crutchfield. Metastable evolutionary dynamics: Crossing fitness barriers or escaping via neutral paths? *Bulletin of Mathematical Biology*, 62(5):799–848, 2000.

Andreas Wagner. Robustness, evolvability, and neutrality. *FEBS Letters*, 579(8): 1772–1778, 2005.

Andreas Wagner. Robustness and evolvability: a paradox resolved. *Proc Biol Sci*, 275(1630):91–100, 2008.

M. Waterman. Secondary structure of single-stranded nucleic acids. In *Studies on foundations and combinatorics, Advances in mathematics supplementary studies*, volume 1, pages 167–212. Academic Press N.Y., 1978.

Claus O. Wilke and Christoph Adami. Interaction between directional epistasis and average mutational effects. *Proceedings of the Royal Society of London: Series B*, 268(1475):1469–1474, 2001.

Claus O. Wilke, Jia Lan Wang, Charles Ofria, Richard E. Lenski, and Christoph Adami. Evolution of digital organisms at high mutation rates leads to survival of the flattest. *Nature*, 412(6844):331–333, 2001.

S. Wright. The roles of mutation, inbreeding, crossbreeding and selection in evolution. *Proceedings of the VI International Congress of Genetrics*, 1:356–366, 1932.

Stephan Wuchty, Walter Fontana, Ivo L. Hofacker, and Peter Schuster. Complete suboptimal folding of RNA and the stability of secondary structures. *Biopolymers*, 49(2):145–165, 1999.

Michael Zuker. On Finding All Suboptimal Foldings of an RNA Molecule. *Science*, 244(4900):48–52, 1989.

Chapter 5

Evolution of Mutation Rates in Finite Asexual Populations

The mutation rate is a fundamental evolutionary parameter. It determines the amount of genetic variation entering populations and thus affects the rate of molecular evolution, the speed of adaptation, the fitness achieved by evolving populations, rates of speciation, and evolution of biological robustness. Both theoretical and empirical studies have yielded progress in understanding how various factors affect evolution of the mutation rate. At the same time, these studies provide only a limited view. The difficulty is that mutation has two faces. Beneficial mutations improve fitness, and are necessary for adaptation. Yet, most mutations are harmful, and thus any mutation rate imposes a 'load' on populations that works against adaptation and high fitness. The difficulty is in understanding the balance between these two opposing effects and, especially, how that balance depends on the environment, the fitness landscape, and the movement of the population across that landscape.

For mathematical tractability, previous models have assumed simple properties of fitness landscapes. The most important of these assumptions are to specify the fitness effects of mutations, and to assign a distribution of deleterious fitness effects that is unchanging, even as the population evolves (Andre and Godelle, 2006; Ishii et al., 1989; Johnson and Barton, 2002; Kimura and Ota, 1974; Kirschner and Gerhart, 1998; Leigh, 1970; Liberman and Feldman, 1986; Orr, 2000; Sniegowski et al., 2000). At best, only the rate is allowed to change. These simplifications follow from the fact that the individual is assigned only a fitness value, not a phenotype

that determines fitness.

Recent advances in computational and structural biology have enabled the development of simulation models based on predicting molecular structures from RNA or protein sequences (Chan and Bornberg-Bauer, 2002; Cowperthwaite and Meyers, 2007). The sequence-to-structure prediction models can serve as tractable, biologically motivated genotype-to-phenotype maps, which create complex fitness landscapes over which populations are allowed to adapt and evolve. This type of model has been used to address a wide array of questions in evolutionary biology that are not easily addressed with classical models (see Cowperthwaite and Meyers (2007) for a recent review).

In contrast to the simple landscapes in population genetic models, biological fitness landscapes are believed to be complex and highly irregular (Gavrilets, 2004). The primary source of the irregularity is the complicated mapping from genotype to phenotype. This irregularity causes the distribution of the fitness effects of mutations (both beneficial and deleterious) to vary across the fitness landscape. Given recent evidence suggesting that fitness landscapes strongly affect the dynamics of mutation rate evolution (Johnson and Barton, 2002; Orr, 2000; Tenaillon et al., 1999), prior studies may not be well equipped to understand some aspects of mutation rate evolution in natural organisms.

Here, we studied the evolution of mutation rate in finite asexual populations, using an RNA folding based simulation model. We investigated the influence of several factors that have previously been proposed to influence the dynamics of mutation rate evolution: population size, fluctuating environment, deleterious mutations and genome size. We also studied the effect of the fitness function on the evolution of mutation rate.

5.1 Model

5.1.1 RNA simulation

We study finite, asexual populations using a simulation model based on the prediction of RNA secondary structures from simulated RNA molecules. This model is similar to those used in prior studies [such as in (Ancel and Fontana, 2000; Cowperthwaite et al., 2006; Fontana and Schuster, 1987)], except that here we allow the

mutation rate to freely evolve (see below; **Figure 5.1**). Following Cowperthwaite et al. (2006), the simulation model matches assumptions commonly made in analytical population genetics models: individuals reproduce in discrete generations and the population size of adults (N) is held constant. At each generation, N individual's are selected to replicate in proportion to their fitness, and, during replication, mutations may occur in their progeny's RNA genome and/or their progeny's mutation rate modifier locus. The N offspring are retained for the next generation, and the N parents die.

In the present study, an individual's phenotype is its "shape", which is the predicted minimum free energy (mfe) secondary structure of its RNA genome. The mfe shape is the most thermodynamically stable secondary structure, as predicted by the folding algorithm in the Vienna RNA folding software [version 1.6.3; (Hofacker et al., 1994)]. The Vienna RNA software uses principles of thermodynamic minimization to predict RNA secondary structure, and is reasonably accurate for short RNA molecules, as determined by similarity to known secondary structures obtained from extensive comparative analyses (Mathews et al., 1999, 2004). However, the folding algorithms cannot account for non-canonical pairing interactions, including pseudoknot structures (Eddy, 2004).

An individual's fitness was calculated from the deviation of it's shape from the target shape, and was measured using the Hamming distance. To measure the Hamming distance, the target shape and an individual's phenotype shape are first transformed into parenthetical notation where '(' and ')' represent paired bases and '.' represent unpaired bases. For instance, a simple hairpin structure can be written as "((((....))))", in which the stem consists of four pairs of bases, and the hairpin loop consists of four unpaired bases. The Hamming distance between this hairpin and the shape "(((.....)))" is two, which is the smallest amount by which two shapes may differ. We also note that there is not a one-to-one relationship between the genetic distance and structural distance, even a single mutation may cause a large structural difference (Fontana et al., 1993a,b). The genome length is fixed at 76 nucleotides in our simulations and thus there is no ambiguity in measuring the Hamming distance between different shapes.

The simulations used two distinct fitness functions, which differ in how they penalize the structural difference between an individual's phenotype and the target

shape (**Figure 5.2A**). One fitness function is hyperbolic:

$$W_h = \frac{1}{0.01 + (d/L)^2} \tag{5.1}$$

where $\alpha = 0.01$ and $\beta = 1$ are scaling constants, d is the Hamming distance between an individual's phenotype and the target shape, and $L = 76$ is the length of the RNA genome. The hyperbolic function models strong selection for target structure; in other words, relatively few shapes are predicted to function well. For example, the smallest deviation from the target structure (a Hamming distance of two) causes the largest reduction in fitness ($s = (27.54 - 100.0)/100.0 = -0.72$); further deviations from the target cause additional declines in fitness.

The other function scales fitness linearly:

$$W_l = 100 - \left[\frac{100}{L} \times d\right] \tag{5.2}$$

where the terms are the same as described in the hyperbolic case. Under the linear fitness function, fitness decreases linearly with Hamming distance from the target shape. The strength of selection for the target structure is therefore much weaker when fitness is high (small deviation from the target shape), and much weaker when fitness is low (large deviation from the target shape).

The fitness effects of mutations are determined only through the biological model of molecular structure and its interaction with the fitness function. To measure the fitness effect of a mutation, we first predict the phenotype of a new mutant genotype and re-compute its fitness. The fitness effect of a mutation is then calculated as the difference in fitness between the genome with the mutation and the genome without the mutation:

$$s = \frac{(w_{mut} - w_{wt})}{w_{wt}} \tag{5.3}$$

where w_{mut} and w_{wt} are the fitnesses of the mutant and wild-type genotypes, respectively. Clearly, the fitness effect of a mutation varies with genetic background, but this dependence is also known to operate in biological systems (Wolf et al., 2000).

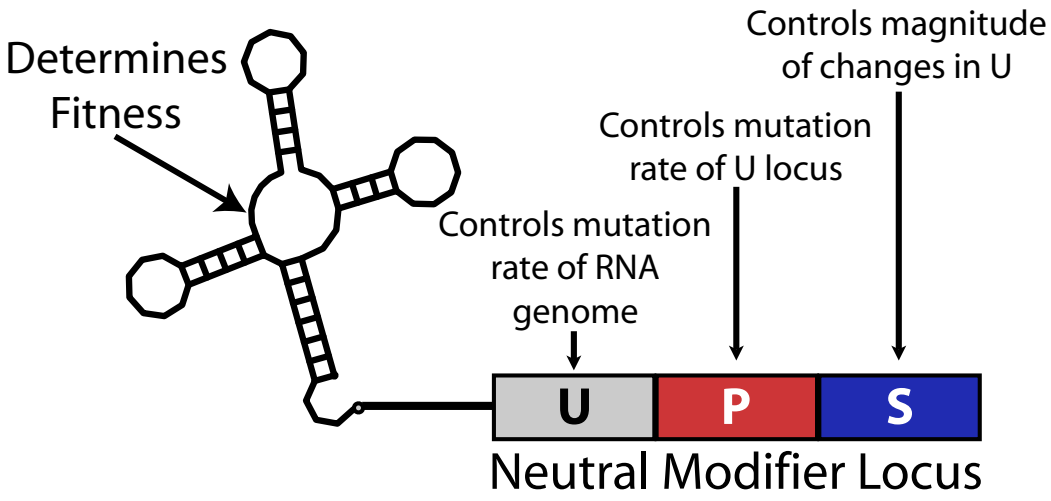

Figure 5.1: Cartoon of individuals in RNA simulation model. The fitness of an individual is based solely on the shape of it's RNA genome. A mutation-rate modifier locus is linked to each RNA genome, and controls the rate of evolution of the RNA genome. The modifier locus is composed of three genes: (i) U controls the rate of evolution of the RNA genome, (ii) P controls the probability that U mutates, and (iii) S sets the magnitude of changes in U (see text for details).

5.1.2 Mutation rate evolution

The mutation rate of an individual's RNA genome is controlled by a linked modifier locus (**Figure 5.1**). This modifier imparts no direct effect on fitness; it only sets the evolutionary rates of itself and the particular RNA genome to which it is linked. Each individual/genome maintains a modifier locus, which is vertically transmitted to offspring as part of its genome. The modifier locus can mutate during transmission, but its state does not factor into an individual's fitness. There is also no recombination of modifier loci between individuals.

A modifier locus is composed of three genes: $U, S,$ & P. The U gene controls the mutation rate of the RNA genome, and it's value determines the average number of mutations per genome per replication. U is bounded by zero at the low end, but

with no upper bound. The S and P genes control different properties of the rate of evolution of U. P is the probability that U mutates between a parent and offspring's genome, thereby controlling the evolutionary rate of U; P is a probability and therefore is confined to the interval between zero and one ($0 \leq P \leq 1$). S controls the magnitude of changes in U; it is the variance term for the normal distribution from which new values of U are drawn.

Mutation rate evolution during the course of a simulation occurs as follows. When an individual is selected to reproduce, we first determine if its modifier locus mutates. If the modifier locus mutates (as controlled by P), new values of $U, S,$ & P are drawn from normal distributions. A new value for U is drawn from a normal distribution with the current value of U as the mean and the current value of S as the variance. New values for S and P are subsequently drawn from normal distributions with their respective current values as means and the variance fixed at 0.001. If the modifier locus mutates, the RNA genome is then replicated using the new values for $U, S,$ & P; otherwise, the RNA genome replicates using an exact copy of the parent's modifier locus.

5.2 Results

5.2.1 The fitness landscape

We simulated populations of RNA molecules evolving under a variety of conditions. Our model assigns genotypic fitnesses based on RNA folding in the context of a fitness function. As a result, the fitness effects of mutations depend on the background genotype and change during the course of evolution. We therefore begin with an analysis of the fitness landscape itself.

Figure 5.2A shows the shape of both fitness functions as distance from the target increases. The effect of a shape-altering mutation depends on how far the folded shape is from the target shape, and this effect depends profoundly on the fitness function. In particular, it may be difficult to evolve high fitness under the hyperbolic function unless fitness starts high, because the benefit of a mutation that improves the fold is small until the target is approached closely. Another interpretation of the same phenomenon is that most genotypes in the hyperbolic fitness landscape are of very low fitness.

Figure 5.2B shows the distribution of fitnesses for one million random genotypes (with equal base frequencies) under the hyperbolic (red line) and linear (green line) fitness functions. The fitness distributions support the notion that, under the hyperbolic fitness function, most genotypes have low fitness. The fitness of an average random genotype is indeed much lower under the hyperbolic function (hyperbolic: 1.66, linear: 40.09; $P < 2.2 \times 10^{-16}$), and consequently, high fitness genotypes in that landscape are rare. These observations are in line with observations from a previous study (Cowperthwaite et al., 2005).

To gain further insight into the evolutionary process under these fitness functions, we measured the fitness effects of random point mutations to randomly selected genotypes in both low- and high-fitness regions of the landscape. To produce a sample of random mutations in low-fitness regions of the landscape, we introduced a single random point mutation into each of one million randomly generated genotypes. A separate set of one million random mutations was created for each fitness function. The distributions are similar for the two functions, with modes near zero and long, positive tails, suggesting abundant beneficial mutations (**Figure 5.2C**).

Inverse folding was used to produce a set of one million random genotypes that closely match the target shape. The inverse folding algorithms in the ViennaRNA package optimize a sequence to fold into a target shape. We used the same target shape as in the stochastic simulations discussed in the next section. Random sequences (with equal base frequencies) served as the starting genotypes, and the final, inverse-folded genotypes were retained if their shape perfectly matched the target shape. A random point mutation was introduced into each inverse-folded genotype; separate sets of one million random mutations (one random mutation per inverse-folded genotype) were produced for each fitness function.

In high-fitness regions of the fitness landscape, the two fitness-effects distributions are vastly different (**Figure 5.2D**). As expected, on average, a point mutation confers larger detrimental effects under the hyperbolic fitness function than the linear fitness function. Also, under the same fitness function, the distributions of mutational effects differ between high and low fitness regions of the landscape (compare the same-colored lines in **Figures 5.2C** and **Figures 5.2D**). Indeed, this last observation is likely the most significant aspect of the fitness landscape for the current study.

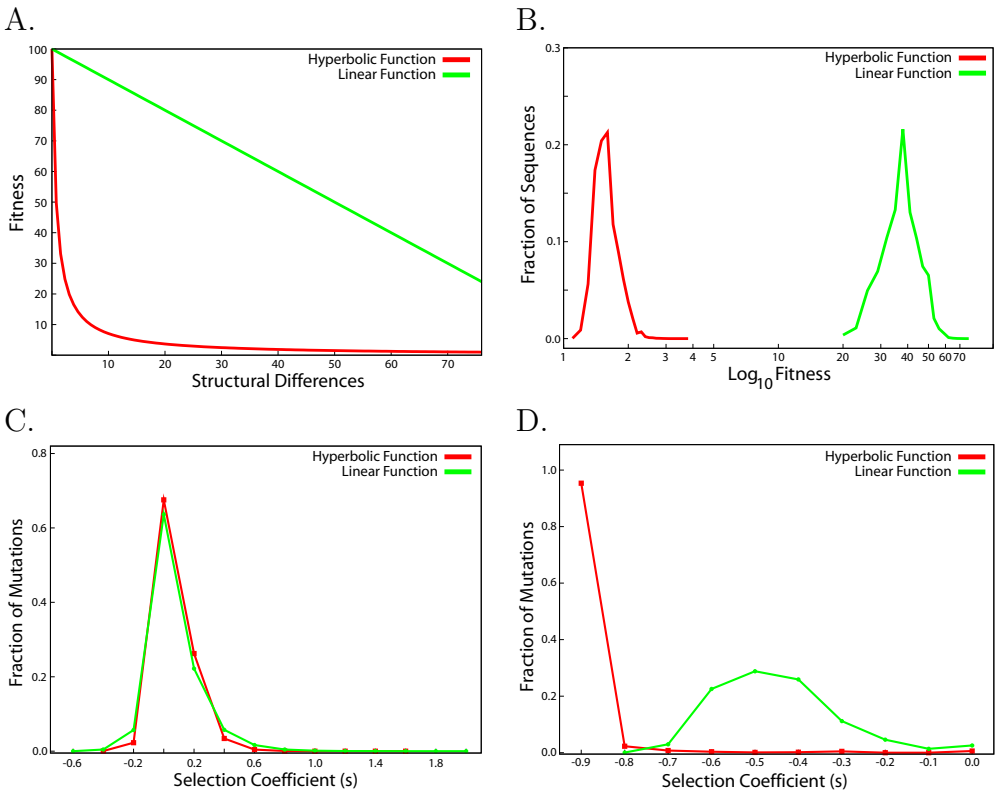

Figure 5.2: Characterization of the RNA fitness landscape in this study. **A.** shows the shape of the two fitness functions used in this study. **B.** the distribution of genotypic fitness values across each fitness landscape from one-million randomly selected genotypes. **C** shows the distribution of mutation fitness effects in low-fitness regions of each fitness landscape, whereas **D** shows the distribution of mutation fitness effects in high-fitness regions the same landscapes. Both **C** and **D** include one-million random point mutations. Note that the range of values along the abscissa is different between **C** and **D**.

5.2.2 Effect of population size on evolved fitness and mutation rate

What will influence the evolution of mutation rates in these different fitness landscapes? One factor likely to affect mutation rate evolution is population size. Small populations fix deleterious mutations by random genetic drift faster than large populations. Thus small populations are less likely to remain at a fitness peak, assuming they arrive there in the first place. This may have an effect of providing continual

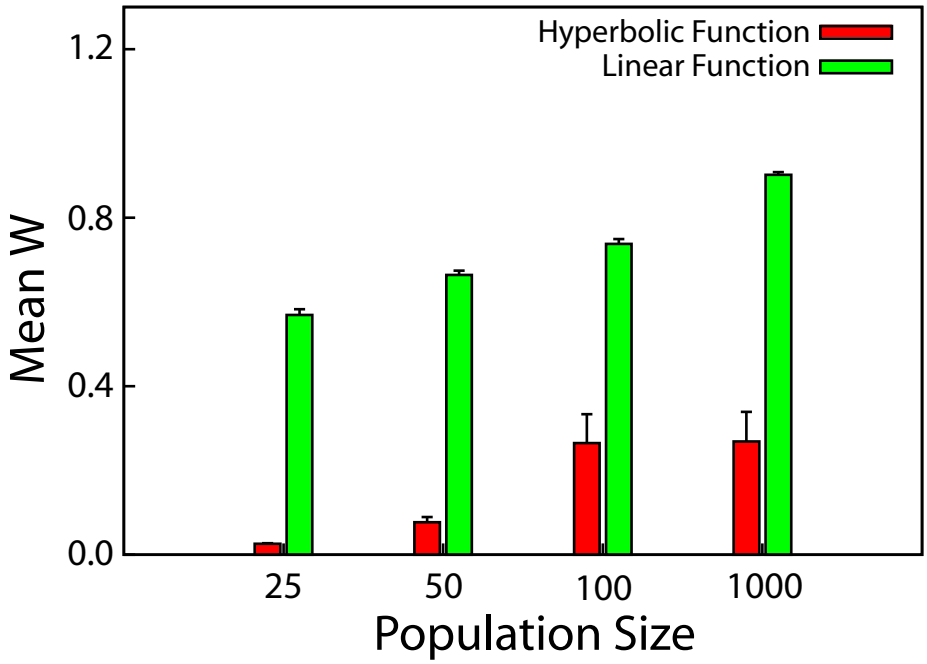

Figure 5.3: Mean W evolved under both fitness functions and across the range of population sizes. The red and green bars depict populations evolved under the hyperbolic and linear fitness functions, respectively. Each datapoint reflects the mean of twenty simulations. For each simulation, the mean W is the average population W measured over the final 5,000 generations of evolution. The mean population mutation rate was measured every five generations.

opportunities for beneficial mutations to arise, which suggests that small populations should maintain higher mutation rates than large populations.

Populations of $N = 25, 50, 100,$ and 1000 individuals were evolved for 100,000 generations. Twenty replicate populations were simulated for each set of conditions (population size, fitness function, etc.). The initial mutation rate was $U = 0.10$, and the S and P values started at 0.001. The qualitative behavior of the simulations was robust to the choice of initial parameters (not shown), although the initial U was chosen from the lower range of published estimates of genomic rates for RNA viruses (Drake and Holland, 1999).

On average, mean fitness increased with population size under both fitness functions, and populations evolving under the linear fitness function attained higher

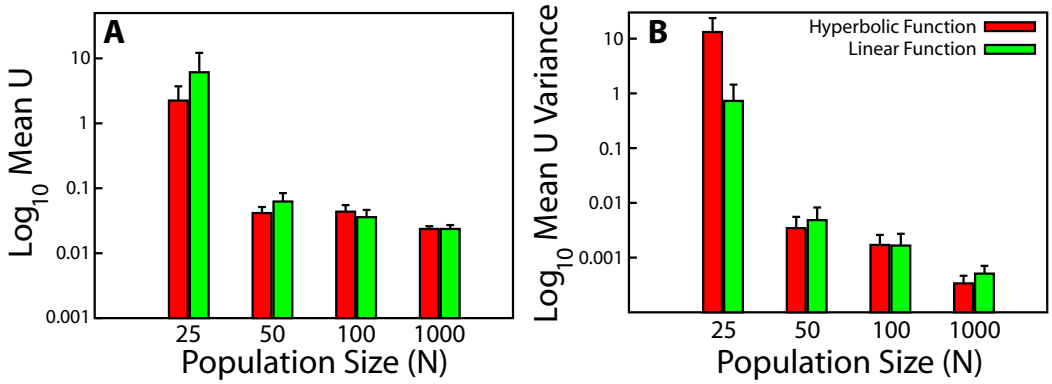

Figure 5.4: Final evolved U and (B) U variance under both fitness functions and across the range of population sizes. The red and green bars depict populations evolved under the hyperbolic and linear fitness functions, respectively. Each data-point reflects the mean of twenty simulations. For each simulation, the mean W is the average population W measured over the final 5,000 generations of evolution.

mean fitness than those evolved under the hyperbolic fitness function (**Figure 5.3**). The higher evolved fitness under the linear fitness function is expected, given that the mean fitness of random genotypes is also higher under this model (see **Figure 5.2B**). It is thus also interesting to consider relative measures of fitness evolution. The fitness increase, whether expressed relative to the starting fitness or relative to the mean fitness of a random genotype, was greater under the hyperbolic than the linear fitness function across the range of population sizes. Yet, the fitness increase in an absolute sense (final fitness minus the starting fitness), was higher under the linear fitness function.

The mean U measured over the final 5,000 generations of each simulation provides a measure of the equilibrium U to which the populations evolve. We emphasize that we are not measuring a strict equilibrium because, as discussed later, U remains volatile during the course of a simulation. Overall, U evolves lower values at larger population sizes, which generally attain higher mean fitness (**Figure 5.4A**).

In small populations, there is a striking dependence of the evolved U on the fitness function. At the smallest population size, higher U evolved under the linear fitness function than under the hyperbolic fitness function; above the smallest N, U

evolved to roughly similar values under both fitness functions. In larger populations, U evolves to be within the range of previously published estimates of mutation rates among RNA viruses ($U \approx 1$) and those of DNA organisms ($U = 1/300 \approx 0.003$) (Drake et al., 1998). Interestingly, at the largest population size, U evolves to within an order of magnitude of the lowest estimates of Drake [0.02 (here) vs 0.003 Drake et al. (1998)].

The population U averaged over time does not provide all of the interesting details. At the largest population size, only about 25% of the population has a U that is above the population mean; there is no discernible directionality (consistent increase/decrease) over time. The individuals with above-average mutation rate are, on average, about 3 standard deviations above the population mean. This class of individuals may be reasonably considered to be a mutator subpopulation.

The variance in the mean mutation rate was also measured over the final 5,000 generations. The variance captures the variability of the mean mutation rate over time, and may be an indicator of the frequency of invasions by mutator lineages; though we acknowledge that the variance of almost all population characteristics increases in small populations, so this observation should be interpreted with caution. **Figure 5.4B** shows that, as population size increases, the variance decreases. This observation is consistent with two explanations: (i) drift is rapidly fixing large-effect mutator alleles, and/or (ii) the population constantly adapting to local optima.

5.2.3 Strength of Deleterious Mutations

We now turn our attention to how deleterious mutation strength shapes the dynamics of mutation rate evolution. Deleterious mutations may be the single most important determinant of mutation rate evolution, and, according to the "reductionist" principle, are expected to strongly favor reduced mutation rates (Liberman and Feldman, 1986).

In traditional mathematical models, the strength and frequency of deleterious mutations typically remains static, whereas, in our simulations, the strength and frequency of deleterious mutations increased over the course of a run (not shown). To quantify the strength of deleterious mutations experienced over the time interval in which the mutation rate was measured, we also measured the mean fitness effect of deleterious mutations during the final 5,000 generations of evolution.

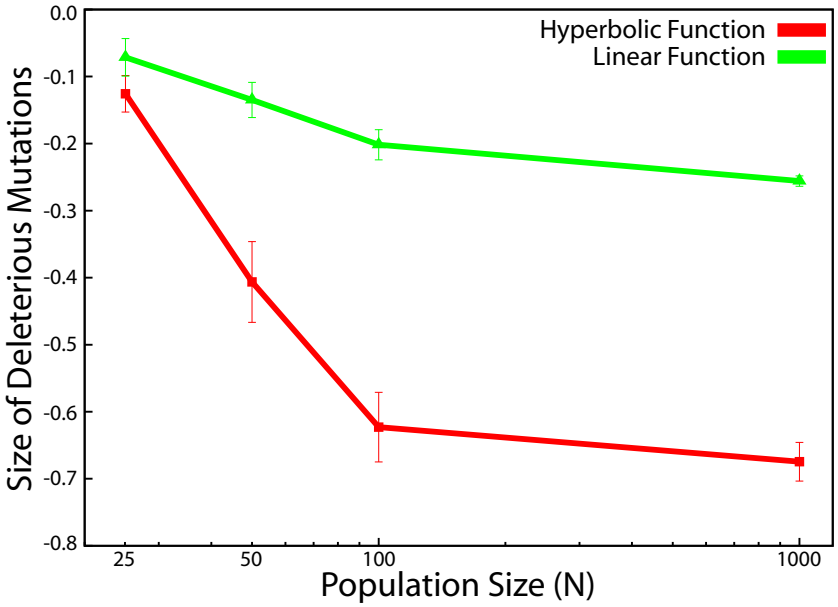

Figure 5.5: Mean magnitude of deleterious mutations under the hyperbolic (red line) and linear (green line) fitness functions. The mean s_d was measured over the final 5,000 generations of evolution, and each datapoint represents the mean of twenty independent simulations. The population size was held fixed at $N = 1000$, and the populations evolved for 100,000 generations.

For both fitness functions, the mean magnitude of deleterious mutations increased with population size (**Figure 5.5**). This increase corresponds with the higher mean fitness that evolved in larger populations. The increase in deleterious mutation strength is significantly greater under the hyperbolic fitness function, though populations achieved lower mean fitness under this fitness function.

5.2.4 Effects of Fluctuating Environment on U Evolution

In nature, organisms are constantly exposed to a variety of biotic and abiotic changes in their environment (Meyers and Bull, 2002). Environmental heterogeneity effectively changes the fitness landscape thereby offering a nearly constant opportunity for adaptive evolution, and for selection to favor higher mutation rates. Evolutionary theory has therefore long predicted environmental fluctuations to strongly affect

the dynamics of mutation rate evolution (Ishii et al., 1989; Leigh, 1970).

We simulated a fluctuating environment by periodically switching the target phenotype. Each target switch alters the fitness landscape because fitness is now based on the new optimum shape. The fitness value of every individual in the population was therefore reassign fitness (relative to the new optimal shape) following each target switch. The constant rescaling of fitness values means that once-fit genotypes may become much less fit.

We simulated twenty populations of size $N = 1000$ at each environmental fluctuation rate of $r = 1, 2, 4, 8, 16, 32, 64, 128, 256, 512,$ and 1024 generations between target shape changes; a suite of five structurally diverse shapes was used during each run. We simulated a complete set of 220 runs for each fitness function. The populations evolved for a total of 100,000 generations, during which the mutation rate was free to evolve.

Only intermediate rates of environmental change show an elevated, evolved U (**Figure 5.6**). The mutation rate remained low on average at the slowest and fastest rates of environmental changes, similar to those evolved in a static environment. The logic of this pattern appears to be simple: high rates of environmental change do not allow significant adaptation because the environment changes before beneficial mutations have time to ascend; low rates of environmental change are merely similar to constant environments in providing only a short-term benefit to high mutation rates.

5.2.5 Genome-length effects on U evolution

Drake (1991) published some of the earliest estimates of mutation rates in natural populations of DNA-based microorganisms. One striking observation to emerge from this and later studies was that genomic mutation rates seemed relatively constant across a wide range of organisms, despite orders of magnitude differences in genome size (Drake et al., 1998; Drake, 1991). The genome length and mutation rate seemed independent of one another, as if there is an evolutionary equilibrium value of the genomic mutation rate (Sniegowski et al., 2000).

These simulations can be used to address the impact of genome length on mutation evolution. The accuracy of the RNA-folding algorithms decreases with sequence length, which restricts the range of genome lengths that may be considered.

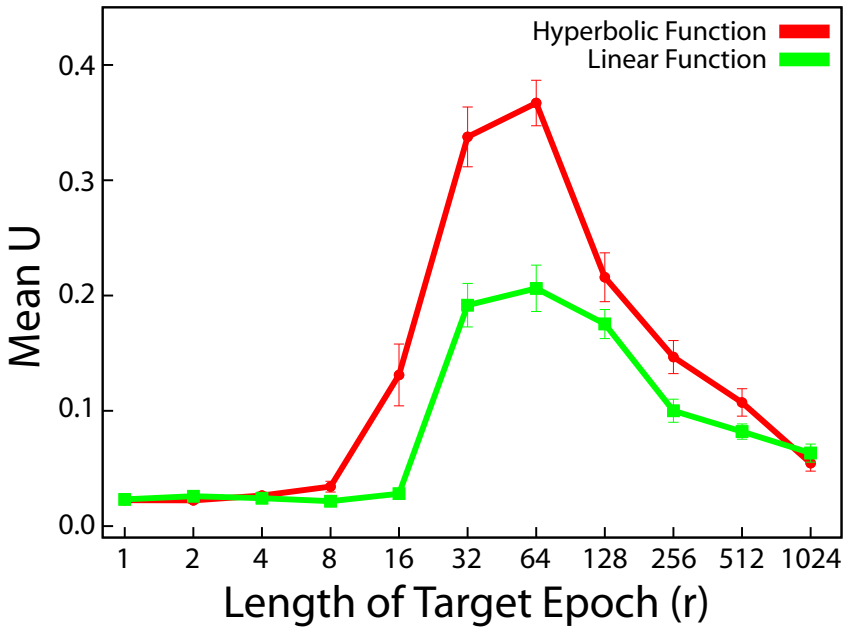

Figure 5.6: Effect of fluctuating environment on the stable evolved values of U. The x-axis (plotted on a base-2 logarithmic scale) shows the duration of selection for a particular target. The population size was held fixed at $N = 1000$, and the populations evolved for 100,000 generations. Each datapoint represents a mean taken from twenty replicate simulations. The means for each simulation were taken as the average over the final 5,000 generations of evolution.

Longer genomes were therefore created in pieces. This approach exploits the speed and accuracy of folding short molecules, while also increasing genome size. We used long genomes of length 380 nucleotides, modeled as five separate 76 nucleotide molecules (five 'chromosomes').

Populations of five-chromosome individuals were allowed to evolve for 100,000 generations under both fitness functions and across the range of population sizes $N = 25, 50, 100,$ and 1000. To assign fitness to a five-chromosome individual, we first compute a separate fitness value for each of its five chromosomes, and log-transform (base 10) these fitness values. The overall fitness is then the product of the log-transformed fitnesses, or specifically, the geometric mean fitness of the five chromosomes. The fitness values of five-chromosome individuals are therefore not comparable with those from single-chromosome individuals.

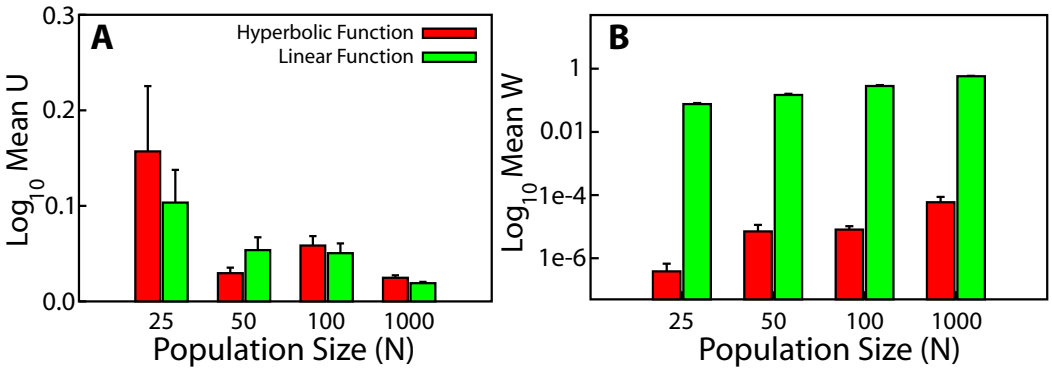

Figure 5.7: Stable evolved values of W and U in populations of individuals with 380 nucleotide genomes. The mean U (A, upper pane) and mean W (B, bottom pane) that evolved over the range of population sizes. The red and green bars depict populations evolved under the hyperbolic and linear fitness functions, respectively. Each bar depicts the mean taken from twenty replicate simulations. The mean U and W for each simulation was taken as the average over the final 5,000 generations of evolution.

At larger population size, the evolved U was largely independent of genome size and of fitness function (**Figure 5.7A**). Genome length did, however, have an effect on the evolved U at the smallest population size: U evolved to a value that was almost 20 (hyperbolic) and 60 (linear) times larger with a shorter genome length. Lastly, we note that mean fitness generally increased with population size, which agrees with our earlier results from single-chromosome individuals.

5.2.6 Trajectory of U Evolution

We conclude by addressing the dynamics of mutation rate evolution over the course of a simulation. **Figure 5.8** shows representative trajectories of mean U, W, and S_d during a typical simulation with each fitness function. There are two main observations: (i) U never approaches any sort of stable equilibrium under either fitness function, rather U remains highly volatile throughout the simulations; and (ii) over long time periods, U settles into generally similar ranges across both fitness functions. We also note that U initially spikes during the earliest phases of adaptation (first 10-20 generations) while beneficial mutations are abundant, and then rapidly

drops to be near its evolved value (not shown).

Much of the observed dynamics of U is correlated with change in the strength and frequency of deleterious mutations. The strength of deleterious mutations rapidly increases, and, by generation 50, more than half of all available mutations are deleterious under both fitness functions (**Figure 5.8, lower pane**). In the long term, deleterious mutations were always stronger under the hyperbolic fitness function than under the linear fitness function, as expected, which partly explains why the populations evolved under the hyperbolic fitness function are significantly less well adapted than those evolved under the linear fitness function (**Figure 5.3**).

5.3 Discussion

Mutation is one of the most fundamental processes in evolution. As a result, both theoretical and empirical evolutionary biologists have tried to determine the evolutionary forces that set the mutation rate. The result of these efforts is a rich body of theory that proposes a number of interesting concepts. Yet, this body of theory is largely built upon simple fitness landscape models that make many limiting assumptions, the most common being to fix the frequency and fitness effects of deleterious mutations across the fitness landscape.

The motivation for this study was therefore to ascertain how well these predictions hold when evolution occurs across a rich fitness landscape. We studied the evolution of mutation rates in finite asexual populations, using a simulation model that is based upon a biologically motivated genotype-phenotype-fitness model. Importantly, in this model, the fitness effects of mutations are not assigned, rather they are measured as the difference in fitness between a parent genotype and it's mutant offspring. The fitness effects of mutations are thus free to vary across the fitness landscape.

In many prior studies of mutation-rate evolution, mutator alleles increment the mutation rate in static, fixed intervals (e.g. mutator alleles always increase the mutation rate by a factor of 10) (Andre and Godelle, 2006; Gerrish et al., 2007; Ishii et al., 1989; Orr, 2000; Taddei et al., 1997; Tenaillon et al., 1999). Whereas, in our model, the mutation-rate could potentially change gradually because the mutation rate was allowed to evolve over a continuous interval. In fact we observed the opposite. The mutation rate changed episodically in the evolving populations;

relatively short periods of lower mutation rates were constantly interrupted by brief bursts of extremely high mutation rates.

Population size. Prior studies are not entirely consistent on how population size should affect mutation rate evolution. One perspective suggests that moderately strong mutators should achieve considerable success in larger populations, which are more likely to produce beneficial mutations with which mutators may hitchhike to fixation (Tenaillon et al., 1999). An alternative viewpoint is the 'invasion threshold', which proposes that a mutator is not likely to be successful until it is moderately common in the population (Chao and Cox, 1983).

The invasion threshold model acknowledges that there is a small chance that any *individual* with a mutator genotype will happen upon a beneficial mutation, and therefore the mutator subpopulation must be large enough for the collective probability of finding a beneficial mutation to be appreciable; empirical tests were highly supportive of this principle (Chao and Cox, 1983). Thus, a mutator genotype faces a catch-22: it must be abundant enough to experience a beneficial mutation, yet it can only become abundant by hitchhiking with a beneficial mutation. Our model may offer somewhat of an escape from this trap, in that, at times, there are lots of (mildly) beneficial mutations to be had, and thus even rare mutator genotypes can experience beneficial mutations.

The relative importance of a threshold invasion frequency is not clear. It has recently been suggested that the threshold invasion frequencies predicted by Chao and Cox (1983) are unreasonably high (Sniegowski et al., 2000). Indeed, simulation models have suggested that even rare mutators can successfully invade evolving populations, given sufficient time (Taddei et al., 1997; Tenaillon et al., 1999). Furthermore, Taddei et al. (1997) suggest that mutator genotypes can impart a substantial benefit to evolving populations, even when quite rare.

In the study here, the smallest population size maintained the highest average mutation rate, and those evolved under the linear fitness function maintained higher mutation rates than those evolved under the hyperbolic fitness function. The highest mutation rates evolved in the smallest populations might be argued on several grounds: i) Genetic drift facilitates the fixation of mutator alleles. However, this model contradicts a recent study which concluded that mutator alleles will not fix with substantial frequency in small populations (Tenaillon et al., 1999).; ii) Muta-

tors more easily achieved the minimum threshold frequency required to successfully invade in small populations. In view of the challenges to the threshold frequency model noted above, it is not clear how much support to attach to this idea.; iii) In the long term, small populations fix deleterious alleles at a higher rate than large populations, and are thus evolving adaptive substitutions more frequently than large populations (addressed more fully below).

Deleterious mutations. Deleterious mutations are thought to impose a significant pressure on evolving populations (Andre and Godelle, 2006; Johnson and Barton, 2002; Liberman and Feldman, 1986; Orr, 2000; Sniegowski et al., 2000). Yet, the expected effect of deleterious mutations on mutation rate evolution depends on the time frame under consideration. In the short term, the maximum rate of adaptation has been proposed to occur when the mutation rate evolves to match the strength of deleterious mutations (Johnson and Barton, 2002; Orr, 2000). For example, if the mean selection coefficient of deleterious mutations $s_d = -0.1$, then the mutation rate should evolve to $U = 0.1$. In the long term, the conventional wisdom is that deleterious mutations should drive the mutation rate downwards, an effect termed the "reduction" principle (Liberman and Feldman, 1986). There may be a "cost of fidelity" associated with evolving very low mutation rates, however, and this cost would preclude the mutation rate from evolving to zero (Kimura, 1967).

During the initial bout of rapid adaptation, we observed a sharp, brief burst in the mutation rate, while beneficial mutations are strong and plentiful, and deleterious mutations are weak and relatively rare. This observation thus contradicts the prediction that the maximally adaptive mutation rate is higher when deleterious mutations are stronger (Johnson and Barton, 2002; Orr, 2000), and supports other grounds for questioning the adaptive benefit of an elevated mutation rate (Elena and Sanjuan, 2005; Sniegowski et al., 2000)

One interesting question is whether the mutation rate evolves to maximize the rate of fitness increase; other factors, such as deleterious mutation load may be more significant in shaping mutation rate evolution. The pattern in the simulations here was that the strength of deleterious mutations increased as mean fitness increased, and the mutation rate evolved downwards at the same time. Furthermore, although the populations were never perfectly adapted to the target shape, the mutation rate remained low during most of the evolution relative to the mutation rate

that would maximize fitness. Our earlier work (Cowperthwaite et al., 2006), also with a population size of $N = 1000$, fixed the mutation rate at an arbitrarily high value of $U = 0.32\%$, and the populations attained much greater fitness than those evolved in this study (the fitness function was slightly different than those used here, but our results here suggest the fitness function does not have much impact on the mutation rate). Taken together, these results are consistent with deleterious mutations exerting a powerful effect on the evolution of mutation rates, and that mutation rate does not evolve to maximize population mean fitness.

An intriguing recent proposal concerns the evolution of mutation rates sufficient to cause extinction. Specifically, some models of finite, asexual populations exhibit 'runaway' mutation rate evolution that ultimately causes extinction through the accumulation of deleterious, non-lethal mutations (Andre and Godelle, 2006; Gerrish et al., 2007). Importantly, these models require that the mutator subpopulation does not experience a significant deleterious mutation load while the mutator allele is ascending to fixation. Accordingly, those models are structured such that the time to achieve mutation-selection balance is relatively long. We observed no 'runaway' escalation of mutation rate in our simulations (extinction was not possible in our model, hence the absence of extinction is not a useful criterion), which is consistent with the mutator subpopulations rapidly experiencing the load induced by deleterious mutations.

Fluctuating environments. Organisms exist in a constantly changing world (Meyers and Bull, 2002), and environmental heterogeneity has been suggested to profoundly influence the mutation rates that evolve in populations (Ishii et al., 1989; Kamp et al., 2002; Leigh, 1970). We therefore investigated the effects of environmental heterogeneity on mutation rate evolution in our RNA model. An important feature of our model is that most mutations are beneficial for some target phenotypes and deleterious for others; in other words, there is abundant antagonistic pleiotropy. There is evidence for antagonistic pleiotropy in natural organisms (Cooper and Lenski, 2000; Ostrowski et al., 2005), and therefore this may be a general factor affecting the dynamics of mutator alleles in fluctuating environments.

We observed that the pace of environmental change affected the evolved mutation rate. We did not, however, observe a direct relationship between the mutation rate and the pace of environmental change, as predicted by (Ishii et al.,

1989; Kamp et al., 2002; Leigh, 1970). In fact, the highest mutation rates were maintained at an intermediate rate of environmental change; at the slowest and fastest rates of environmental change, the evolved mutation rate was similar to those in the constant-environment simulations. The analytical study by Travis and Travis (2002) also found that intermediate rates of environmental change fostered maintenance of the highest mutation rates.

At extremely fast rates of environmental change, there is insufficient time for beneficial mutations to arise and attain significant frequencies. The fitness landscape used here likely compounds this effect. When fitness is low (at the start of a simulation), the fitness effects of mutations are small, and hitchhiking may have limited capacity to raise the mutation rate. Thus, timing of the generation of beneficial mutations is critical, which is in agreement with predictions that mutators can only invade following an environmental shift if their sub-population generates beneficial mutations almost immediately following the shift (Tanaka et al., 2003).

Genome length. Drake and Holland (1999) produced some of the earliest estimates of mutation rates in natural populations of DNA-based organisms. The genome sizes of these organisms varied by many orders of magnitude, yet the genomic mutation rate (mutations per genome per generation) was nearly the same. It seems therefore that genome size does not directly affect the evolved mutation rate. It should be noted that these estimates were largely based on phenotypic mutation rates, and thus could underestimate the genomic mutation rate.

Here, we varied the genome size by a factor of five, by allowing individuals to consist of multiple short chromosomes. One caveat is therefore that, though we were able to dramatically change the genome length, we are still measured the fitness of small sequences. Furthermore, mutations in different chromosomes did not interact epistatically. Nonetheless, our approach provided a straightforward means to investigate the effect of genome length on mutation rate evolution.

Our results qualitatively agreed with the empirical observations: genome length did not strongly influence the evolved genomic mutation rates. In large to moderately large populations, the evolved mutation rate did not depend on genome size. We did observe, however that significantly higher mutation rates were maintained in the smallest populations with shorter genomes. The consistency of evolved mutation rates has been suggested by some to imply a sort of evolutionary constant

(Sniegowski et al., 2000). Perhaps the size of the genetic alphabet (nucleotides) plays a significant role in the evolution of mutation rates, regardless of the number of words (genes).

Conclusion. There is a rich history of models to explain the evolution of mutation rate. Our approach differs from those predecessors in assuming a biologically-motivated, complex fitness landscape. As such, analytical results are not feasible, and results are based on simulations. Yet the results are easily compared to those of prior studies. In general our results are in mixed agreement with the theory. We found that population size profoundly affects the mutation rate, and this effect depends on the shape of the fitness function only at small population sizes. We have also shown that fluctuating environments strongly affect the mutation rate, but genome size does not.

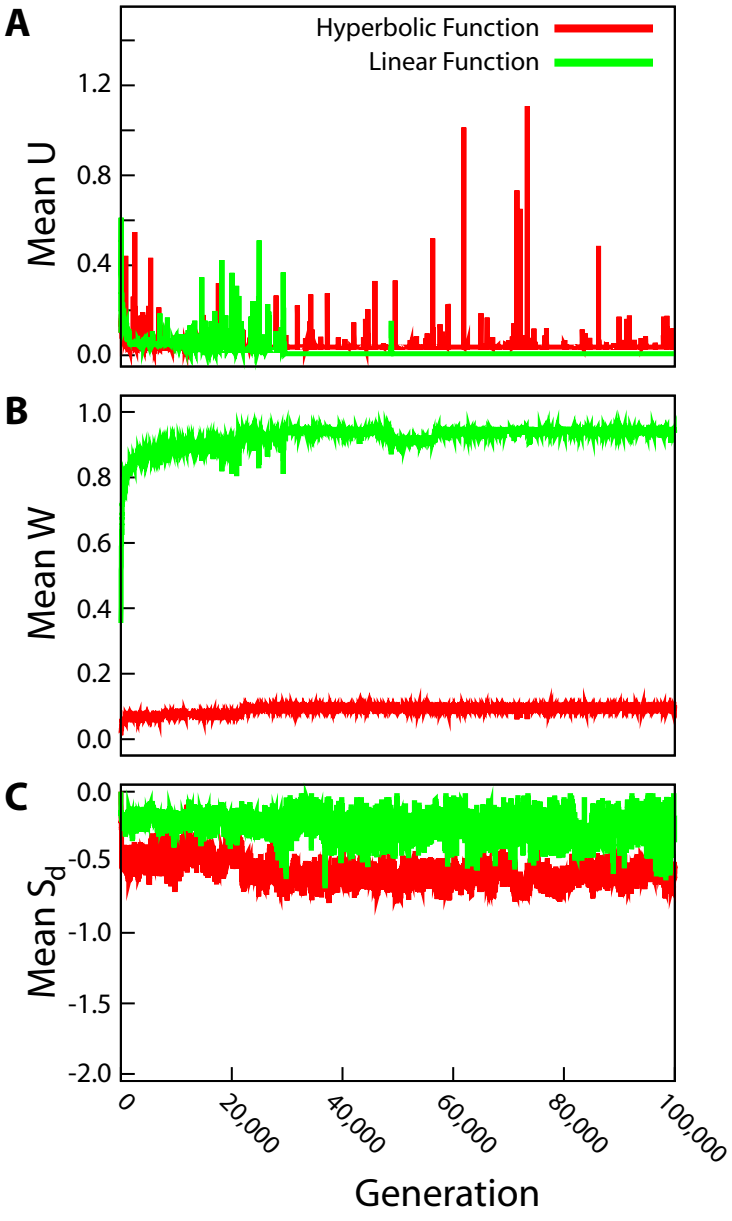

Figure 5.8: Typical trajectories of U (top pane), W (middle pane), and S_d (bottom pane) evolution. The red and green lines show typical trajectories under the hyperbolic and linear fitness functions, respectively. The population size was $N = 1000$, and the population means of each quantity were measured every five generations.

References

Lauren Ancel and Walter Fontana. Plasticity, Modularity and Evolvability in RNA. *Journal of Experimental Zoology*, 288(3):242–283, 2000.

Jean-Baptiste Andre and Bernard Godelle. The Evolution of Mutation Rate in Finite Asexual Populations. *Genetics*, 172(1):611–626, 2006.

Hue Sun Chan and Erich. Bornberg-Bauer. Perspectives on protein evolution from simple exact models. *Applied Bioinformatics*, 1(3):121–144, 2002.

Lin Chao and Edward C. Cox. Competition Between High and Low Mutating Strains of *Escherichia coli*. *Evolution*, 37(1):125–134, 1983.

V.S. Cooper and R.E. Lenski. The population genetics of ecological specialization in evolving *escherichia coli* populations. *Nature*, 407(6805):736–739, 2000.

Matthew C. Cowperthwaite and Lauren Ancel Meyers. How mutational networks shape evolution: Lessons from RNA models. *Annual Review of Ecology, Evolution and Systematics*, 38(1):203–230, 2007.

Matthew C. Cowperthwaite, J. J. Bull, and Lauren Ancel Meyers. Distributions of Beneficial Fitness Effects in RNA. *Genetics*, 170(4):1449–1457, 2005.

Matthew C. Cowperthwaite, J. J. Bull, and Lauren Ancel Meyers. From bad to good: Fitness reversals and the ascent of deleterious mutations. *PLoS Computational Biology*, 2(10):1292–1300, 2006.

John W. Drake and John J. Holland. Mutation rates among RNA viruses. *Proc Natl Acad Sci USA*, 96(24):13910–13913, 1999.

John W. Drake, Brian Charlesworth, Deborah Charlesworth, and James F. Crow. Rates of Spontaneous Mutation. *Genetics*, 148(4):1667–1686, 1998.

JW Drake. A Constant Rate of Spontaneous Mutation in DNA-Based Microbes. *PNAS*, 88(16):7160–7164, 1991.

Sean R Eddy. How do RNA folding algorithms work? *Nature Biotech*, 22(11): 1457–1458, 2004.

Santiago F. Elena and Rafael Sanjuan. Adaptive Value of High Mutation Rates of RNA Viruses: Separating Causes from Consequences. *J. Virol.*, 79(18):11555–11558, 2005.

Walter Fontana and Peter Schuster. A computer model of evolutionary optimization. *Biophysical Chemistry*, 26(2-3):123–147, 1987.

Walter Fontana, Danielle A.M. Konings, Peter F. Stadler, and Peter Schuster. Statistics of RNA secondary structures. *Biopolymers*, 33(9):1389–1404, 1993a.

Walter Fontana, Peter F. Stadler, Erich Bornberg-Bauer, Thomas Griesmacher, Ivo L. Hofacker, Manfred Tacker, Pedro Tarazona, Edward D. Weinberger, and Peter Schuster. RNA Folding and Combinatory Landscapes. *Physical Review E*, 47:2083–2099, 1993b.

Sergey Gavrilets. *Fitness Landscapes and the Origin of Species*, volume 41 of *Monographs in Population Biology*. Princeton University Press, 2004.

Philip J. Gerrish, Alexandre Colato, Alan S. Perelson, and Paul D. Sniegowski. Complete genetic linkage can subvert natural selection. *Proceedings of the National Academy of Sciences*, 104(15):6266–6271, 2007.

Ivo L. Hofacker, Walter Fontana, Peter F. Stadler, L. Sebastian Bonhoeffer, Manfred Tacker, and Peter Schuster. Fast Folding and Comparison of RNA Secondary Structures. *Monatshefte fur Chemie*, 125:167–188, 1994.

K. Ishii, H. Matsuda, Y. Iwasa, and A. Sasaki. Evolutionarily Stable Mutation Rate in a Periodically Changing Environment. *Genetics*, 121(1):163–174, 1989.

Toby Johnson and Nick H. Barton. The Effect of Deleterious Alleles on Adaptation in Asexual Populations. *Genetics*, 162(1):395–411, 2002.

Christel Kamp, Claus O. Wilke, Christoph Adami, and Stefan Bornholdt. Viral evolution under the pressure of an adaptive immune system: Optimal mutation rates for viral escape. *Complexity*, 8(2):28–33, 2002.

M. Kimura. On the evolutionary adjustment of spontaneous mutation rates. *Genetical Research*, 9:23–34, 1967.

M Kimura and T Ota. On some principles governing molecular evolution. *Proc Natl Acad Sci USA*, 71(7):2848–2852, 1974.

Mark Kirschner and John Gerhart. Evolvability. *Proceedings of the National Academy of Sciences*, 95(15):8420–8427, 1998.

Egbert Giles Leigh. Nautral Selection and Mutability. *The American Naturalist*, 104(937):301–305, 1970.

U. Liberman and M.W. Feldman. Modifiers of mutation rate: a general reduction principle. *Theoretical Population Biology*, 30(1):125–142, 1986.

David H. Mathews, Jeffrey Sabina, Michael Zuker, and Douglas H. Turner. Expanded sequence dependence of thermodynamic parameters improves prediction of rna secondary structure. *Journal of Molecular Biology*, 288(5):911–940, 1999.

David H. Mathews, Matthew D. Disney, Jessica L. Childs, Susan J. Schroeder, Michael Zuker, and Douglas H. Turner. Incorporating chemical modification constraints into a dynamic programming algorithm for prediction of RNA secondary structure. *Proc Natl Acad Sci USA*, 101(19):7287–7292, 2004.

Lauren Ancel Meyers and J. J. Bull. Fighting change with change: adaptive variation in an uncertain world. *Trends in Ecology and Evolution*, 17(12):551–557, 2002.

H. Allen Orr. The Rate of Adaptation in Asexuals. *Genetics*, 155(2):961–968, 2000.

Elizabeth A. Ostrowski, Daniel E. Rozen, and Richard E. Lenski. Pleiotropic effects of beneficial mutations in *Escherichia coli*. *Evolution Int J Org Evolution*, 59(11): 2343–2352, 2005.

Paul D. Sniegowski, Philip J. Gerrish, Toby Johnson, and Aaron Shaver. The evolution of mutation rates: separating causes from consequences. *Bioessays*, 22 (12):1057–1066, 2000.

F Taddei, M Radman, J Maynard-Smith, B Toupance, P H Gouyon, and B Godelle. Role of mutator alleles in adaptive evolution. *Nature*, 387(6634):700–702, 1997.

Mark M. Tanaka, Carl T. Bergstrom, and Bruce R. Levin. The evolution of mutator genes in bacterial populations: the roles of environmental change and timing. *Genetics*, 164(3):843–854, 2003.

O Tenaillon, B Toupance, H Le Nagard, F Taddei, and B Godelle. Mutators, population size, adaptive landscape and the adaptation of asexual populations of bacteria. *Genetics*, 152(2):485–493, 1999.

J M J Travis and E R Travis. Mutator dynamics in fluctuating environments. *Proc Biol Sci*, 269(1491):591–597, 2002.

Jason B. Wolf, Edmund D. Brodie III, and Michael J. Wade. *Epistasis and the Evolutionary Process*. Oxford University Press, 2000.

Bibliography

Lauren Ancel and Walter Fontana. Plasticity, Modularity and Evolvability in RNA. *Journal of Experimental Zoology*, 288(3):242–283, 2000.

Jon P. Anderson, Richard Daifuku, and Lawrence A. Loeb. Viral error catastrophe by mutagenic nucleosides. *Annual Review of Microbiology*, 58(1):183–205, 2004.

William R. Atchley, Kurt R. Wollenberg, Walter M. Fitch, Werner Terhalle, and Andreas W. Dress. Correlations Among Amino Acid Sites in bHLH Protein Domains: An Information Theoretic Analysis. *Mol Biol Evol*, 17(1):164–178, 2000.

Stephan Bernhart, Hakim Tafer, Ulrike Muckstein, Christoph Flamm, Peter Stadler, and Ivo Hofacker. Partition function and base pairing probabilities of rna heterodimers. *Algorithms for Molecular Biology*, 1(1):3, 2006.

Erich Bornberg-Bauer and Hue Sun Chan. Modeling evolutionary landscapes: Mutational stability, topology, and superfunnels in sequence space. *PNAS*, 96(19): 10689–10694, 1999.

J. J. Bull, Lauren Ancel Meyers, and Michael Lachmann. Quasispecies Made Simple. *PLoS Computational Biology*, 1(6):0450–0460, 2005.

Christina L. Burch and Lin Chao. Evolution by Small Steps and Rugged Landscapes in the RNA Virus phi6. *Genetics*, 151(3):921–927, 1999.

H. J. Bussemaker, D. Thirumalai, and J. K. Bhattacharjee. Thermodynamic Stability of Folded Proteins against Mutations. *Phys. Rev. Lett.*, 79(18):3530–3533, Nov 1997.

Hue Sun Chan and Erich. Bornberg-Bauer. Perspectives on protein evolution from simple exact models. *Applied Bioinformatics*, 1(3):121–144, 2002.

Francisco M. Codõner, José-Antonio Darós, Ricard V. Solé, and Santiago F. Elena. The Fittest versus the Flattest: Experimental Confirmation of the Quasispecies Effect with Subviral Pathogens. *PLoS Pathogens*, 2(12):1187–1193, Dec 2006.

Matthew C. Cowperthwaite, J. J. Bull, and Lauren Ancel Meyers. Distributions of Beneficial Fitness Effects in RNA. *Genetics*, 170(4):1449–1457, 2005.

Matthew C. Cowperthwaite, J. J. Bull, and Lauren Ancel Meyers. From bad to good: Fitness reversals and the ascent of deleterious mutations. *PLoS Computational Biology*, 2(10):1292–1300, Oct 2006.

James F. Crow and Motoo Kimura. *An Introduction to Population Genetics Theory*. Burgess Publishing Company, 1970.

J. Arjan G. M. de Visser, Joachim Hermisson, Gunter P. Wagner, Lauren Ancel Meyers, Homayoun Bagheri-Chaichian, Jeffrey L. Blanchard, Lin Chao, James M. Cheverud, Santiago F. Elena, Walter Fontana, Greg Gibson, Thomas F. Hansen, David Krakauer, Richard C. Lewontin, Charles Ofria, Sean H. Rice, George von Dassow, Andreas Wagner, and Michael C. Whitlock. Perspective: Evolution and Detection of Genetic Robustness. *Evolution*, 57(9):1959–1972, 2003.

Frederic Delsuc, Henner Brinkmann, and Herve Philippe. Phylogenomics and the Reconstruction of the Tree of Life. *Nature Reviews Genetics*, 6(5):361–375, 2005.

Esteban Domingo. Quasispecies Theory in Virology. *Journal of Virology*, 76(1): 463–465, January 2002.

Esteban Domingo. Quasispecies and the development of new antiviral strategies. *Prog Drug Res*, 60:133–158, 2003.

Jennifer A. Doudna. Structural genomics of RNA. *Nature Structural Biology*, 7(11): 954–6, 2000.

M Eigen. Selforganization of matter and the evolution of biological macromolecules. *Naturwissenschaften*, 58(10):465–523, 1971.

Manfred Eigen. On the nature of virus quasispecies. *Trends in Microbiology*, 4(6): 216–218, 1996.

Manfred Eigen and Peter Schuster. *The Hypercycle: A Principle of Natural Self-Organization*. Springer-Verlag, 1979.

Niles Eldredge, John N. Thompson, Paul M. Brakefield, Sergey Gavrilets, David Jablonski, Jeremy B. C. Jackson, Richard E. Lenski, Bruce S. Lieberman, Mark A. McPeek, and III Miller, William. The dynamics of evolutionary stasis. *Paleobiology*, 31(2):133–145, 2005.

AD Ellington. RNA selection. Aptamers achieve the desired recognition. *Current Biology*, 4(5):427–429, 1994.

C Escarmis, M Davila, and E Domingo. Multiple molecular pathways for fitness recovery of an rna virus debilitated by operation of muller's ratchet. *J Mol Biol*, 285(2):495–505, 1999.

Suzanne Estes, Patrick C. Phillips, Dee R. Denver, W. Kelley Thomas, and Michael Lynch. Mutation Accumulation in Populations of Varying Size: The Distribution of Mutational Effects for Fitness Correlates in Caenorhabditis elegans. *Genetics*, 166(3):1269–1279, 2004.

Ronald Aylmer Fisher. *The Genetical Theory of Natural Selection*. Oxford University Press, Oxford, 1930.

Walter Fontana and Peter Schuster. A computer model of evolutionary optimization. *Biophysical Chemistry*, 26(2-3):123–147, 1987.

Walter Fontana and Peter Schuster. Shaping Space: the Possible and the Attainable in RNA Genotype-Phenotype Mapping. *Journal of Theoretical Biology*, 194(4): 491–515, 1998a.

Walter Fontana and Peter Schuster. Continuity in evolution: on the nature of transitions. *Science*, 280(5368):1451–1455, 1998b.

Walter Fontana, Danielle A.M. Konings, Peter F. Stadler, and Peter Schuster. Statistics of RNA secondary structures. *Biopolymers*, 33(9):1389–1404, 1993a.

Walter Fontana, Peter F. Stadler, Erich Bornberg-Bauer, Thomas Griesmacher, Ivo L. Hofacker, Manfred Tacker, Pedro Tarazona, Edward D. Weinberger, and

Peter Schuster. RNA Folding and Combinatory Landscapes. *Physical Review E*, 47:2083–2099, 1993b.

Sergey Gavrilets. *Fitness Landscapes and the Origin of Species*, volume 41 of *Monographs in Population Biology*. Princeton University Press, 2004.

Greg Gibson and Gunter P. Wagner. Canalization in evolutionary genetics: a stabilizing theory? *Bioessays*, 22(4):372–380, March 2000.

John H. Gillespie. Molecular Evolution Over the Mutational Landscape. *Evolution*, 38(5):1116–1129, 1984.

John H. Gillespie. *Population Genetics: A Concise Guide*. Johns Hopkins University Press, Baltimore, 2004.

John H. Gillespie. A simple stochastic gene substitution model. *Theoretical Population Biology*, 23(2):202–215, 1983.

W. Gruner, U. Giegerich, D. Strothmann, C. Reidys, J. Weber, I. Hofacker, P. Stadler, and P. Schuster. Analysis of RNA sequence structure maps by exhaustive enumeration. I. Neutral Networks. *Monatshefte fur Chemie*, 127:355–374, 1996a.

W. Gruner, U. Giegerich, D. Strothmann, C. Reidys, J. Weber, I. Hofacker, P. Stadler, and P. Schuster. Analysis of RNA sequence structure maps by exhaustive enumeration. II. Structure of neutral networks and shape space covering. *Monatshefte fur Chemie*, 127:375–389, 1996b.

Emil Julius Gumbel. *Statistics of Extremes*. Columbia University Press, New York, 1958.

Robin R Gutell, Jung C Lee, and Jamie J Cannone. The accuracy of ribosomal rna comparative structure models;. *Current Opinion in Structural Biology*, 12(3): 301–310, 2002.

Ivo L. Hofacker, Walter Fontana, Peter F. Stadler, L. Sebastian Bonhoeffer, Manfred Tacker, and Peter Schuster. Fast Folding and Comparison of RNA Secondary Structures. *Monatshefte fur Chemie*, 125:167–188, 1994.

Edward C. Holmes and Andres Moya. Is the Quasispecies Concept Relevant to RNA Viruses? *J. Virol.*, 76(1):460–462, 2002.

Martijn A. Huynen, Peter F. Stadler, and Walter Fontana. Smoothness within ruggedness: the role of neutrality in adaptation. *Proceedings of the National Academy of Sciences*, 93(1):397–401, 1996.

Marianne Imhof and Christian Schlotterer. Fitness effects of advantageous mutations in evolving *Escherichia coli* populations. *PNAS*, 98(3):1113–1117, 2001.

Toby Johnson and Nick H. Barton. The Effect of Deleterious Alleles on Adaptation in Asexual Populations. *Genetics*, 162(1):395–411, 2002.

Gerald F. Joyce. RNA STRUCTURE: Ribozyme Evolution at the Crossroads. *Science*, 289(5478):401–402, 2000.

Yuseob Kim and Wolfgang Stephan. Joint Effects of Genetic Hitchhiking and Background Selection on Neutral Variation. *Genetics*, 155(3):1415–1427, 2000.

Motoo Kimura. Evolutionary Rate at the Molecular Level. *Nature*, 217(5129): 624–626, February 1968.

Mark Kirschner and John Gerhart. Evolvability. *Proceedings of the National Academy of Sciences*, 95(15):8420–8427, July 1998.

Alexey S. Kondrashov, Shamil Sunyaev, and Fyodor A. Kondrashov. Dobzhansky-Muller incompatibilities in protein evolution. *PNAS*, 99(23):14878–14883, 2002.

Rob J. Kulathinal, Brian R. Bettencourt, and Daniel L. Hartl. Compensated Deleterious Mutations in Insect Genomes. *Science*, 306(5701):1553–1554, 2004.

M.R. Leadbetter, Georg Lindgren, and Holger Rootzen. *Extremes and Related Properties of Random Sequences and Processes.* Springer-Verlag, 1983.

Hao Li, Robert Helling, Chao Tang, and Ned Wingreen. Emergence of preferred structures in a simple model of protein folding. *Science*, 273(5275):666–669, August 1996.

Mark Lunzer, Stephen P. Miller, Roderick Felsheim, and Antony M. Dean. The Biochemical Architecture of an Ancient Adaptive Landscape. *Science*, 310(5747): 499–501, 2005.

David H. Mathews. Revolutions in RNA Secondary Structure Prediction. *Journal of Molecular Biology*, 359(3):526–532, 2006.

David H Mathews and Douglas H Turner. Prediction of RNA secondary structure by free energy minimization. *Current Opinion in Structural Biology*, 16(3):270–278, 2006.

David H. Mathews, Jeffrey Sabina, Michael Zuker, and Douglas H. Turner. Expanded sequence dependence of thermodynamic parameters improves prediction of rna secondary structure. *Journal of Molecular Biology*, 288(5):911–940, 1999.

David H. Mathews, Matthew D. Disney, Jessica L. Childs, Susan J. Schroeder, Michael Zuker, and Douglas H. Turner. Incorporating chemical modification constraints into a dynamic programming algorithm for prediction of RNA secondary structure. *PNAS*, 101(19):7287–7292, 2004.

John S. Mattick and Igor V. Makunin. Non-coding RNA. *Human Molecular Genetics*, 15(R1):R17–R29, 2006.

JS McCaskill. The equilibrium partition function and base pair binding probabilities for RNA secondary structure. *Biopolymers*, 29(6-7):1105–1109, 1990.

Lauren Ancel Meyers and J. J. Bull. Fighting change with change: adaptive variation in an uncertain world. *Trends in Ecology and Evolution*, 17(12):551 – 557, December 2002.

Lauren Ancel Meyers, Jennifer F. Lee, Matthew Cowperthwaite, and Andrew D. Ellington. The Robustness of Naturally and Artificially Selected Nucleic Acid Secondary Structures. *Journal of Molecular Evolution*, 58(6):618–625, 2004.

Andres Moya, Santiago F. Elena, Alma Bracho, Rosario Miralles, and Eladio Barrio. The evolution of RNA viruses: A population genetics view. *PNAS*, 97(13):6967–6973, 2000.

R. Niwa and F.J. Slack. The evolution of animal microRNA function. *Curr. Opin. Genet. Dev.*, in press., 2007.

R Nussinov and AB Jacboson. Fast algorithm for predicting the secondary structure of single-stranded RNA. *Proceedings of the National Academy of Sciences*, 77 (111):6309–6313, 1980.

H. Allen Orr. The Population Genetics of Adaptation: The Adaptation of DNA Sequences. *Evolution*, 56(7):1317–1330, 2002.

H. Allen Orr. The Population Genetics of Adaptation on Correlated Fitness Landscapes: The Block Model. *Evolution*, 60(6):1113–1124, 2006.

H. Allen Orr. The Distribution of Fitness Effects Among Beneficial Mutations. *Genetics*, 163(4):1519–1526, 2003.

H. Allen Orr. The Genetic Theory of Adaptation: A Brief History. *Nature Reviews Genetics*, 6(2):119–127, 2005.

H.A. Orr. The Population Genetics of Adaptation: The Distribution of Factors Fixed during Adaptive Evolution. *Evolution*, 52(4):935–949, 1998.

John Parsch, John M. Braverman, and Wolfgang Stephan. Comparative Sequence Analysis and Patterns of Covariation in RNA Secondary Structures. *Genetics*, 154(2):909–921, 2000.

J. R. Peck. A Ruby in the Rubbish: Beneficial Mutations, Deleterious Mutations and the Evolution of Sex. *Genetics*, 137(2):597–606, 1994.

Andrew D Peters and Sarah P Otto. Liberating genetic variance through sex., 2003.

Art Poon and Lin Chao. The Rate of Compensatory Mutation in the DNA Bacteriophage ϕX174. *Genetics*, 170(3):989–999, 2005.

Art Poon, Bradley H. Davis, and Lin Chao. The Coupon Collector and the Suppressor Mutation: Estimating the Number of Compensatory Mutations by Maximum Likelihood. *Genetics*, 170(3):1323–1332, 2005.

Christine Queitsch, Todd A. Sangster, and Susan Lindquist. Hsp90 as a capacitor of phenotypic variation. *Nature*, 417(6889):618–624, June 2002.

Darin R. Rokyta, Paul Joyce, Brian B. Caudle, and Holly A. Wichman. An empirical test of the mutational landscape model of adaptation using a single-stranded DNA virus. *Nature Genetics*, 37(4):441–444, 2005.

Daniel E. Rozen, J. Arjan G. M. de Visser, and Philip J. Gerrish. Fitness Effects of Fixed Beneficial Mutations in Microbial Populations. *Current Biology*, 12(12): 1040–1045, 2002.

S. L. Rutherford and S. Lindquist. Hsp90 as a capacitor for morphological evolution. *Nature*, 396(6709):336–342, November 1998.

Rafael Sanjuan, Andres Moya, and Santiago F. Elena. The distribution of fitness effects caused by single-nucleotide substitutions in an RNA virus. *PNAS*, 101(22): 8396–8401, 2004.

Rafael Sanjuan, Javier Forment, and Santiago F. Elena. In Silico Predicted Robustness of Viroids RNA Secondary Structures. I. The Effect of Single Mutations. *Mol Biol Evol*, 23(7):1427–1436, 2006a.

Rafael Sanjuan, Javier Forment, and Santiago F. Elena. In Silico Predicted Robustness of Viroid RNA Secondary Structures. II. Interaction between Mutation Pairs. *Mol Biol Evol*, 23(11):2123–2130, 2006b.

Erik A. Schultes and David P. Bartel. One Sequence, Two Ribozymes: Implications for the Emergence of New Ribozyme Folds. *Science*, 289:448–452, July 2000.

Peter Schuster and Walter Fontana. Chance and necessity in evolution: lessons from RNA. *Physica D*, 133(1–4):427–452, 1999.

Peter Schuster, Walter Fontana, Peter F. Stadler, and Ivo L. Hofacker. From sequences to shapes and back: a case study in RNA secondary structures. *Proceedings of the Royal Society of London B*, 255(1344):279–284, 1994.

John Maynard Smith. Natural selection and the concept of a protein space. *Nature*, 225(5232):563–564, 1970.

Barbel M. R. Stadler, Peter Stadler, Gunter P. Wagner, and Walter Fontana. The topology of the possible: Formal spaces underlying patterns of evolutionary change. *Journal of Theoretical Biology*, 213(2):241 – 74, 2001.

Heather L. True, Ilana Berlin, and Susan L. Lindquist. Epigenetic regulation of translation reveals hidden genetic variation to produce complex traits. *Nature*, 431(7005):184–187, September 2004.

E van Nimwegen, JP Crutchfield, and M Huynen. Neutral evolution of mutational robustness. *Proceedings of the National Academy of Sciences*, 17(76):9716–9720, 1999.

Michele Vendruscolo, Amos Maritan, and Jayanth R. Banavar. Stability threshold as a selection principle for protein design. *Phys. Rev. Lett.*, 78(20):3967–3970, May 1997.

C. H. Waddington. Canalization of Development and Genetic Assimilation of Acquired Characters. *Nature*, 183(4676):1654–1655, 1959.

C.H. Waddington. Genetic Assimilation of an Acquired Character. *Evolution*, 7(2): 118–126, June 1950.

A. Wagner and Peter F. Stadler. Viral RNA and evolved mutational robustness. *Journal of Experimental Zoology*, 285(2):119–127, August 1999.

Andreas Wagner. Robustness, evolvability, and neutrality. *FEBS Letters*, 579(8): 1772–1778, 2005.

Gunter P. Wagner, Ginger Booth, and Homayoun Bagheri-Chaichian. A population genetic theory of canalization. *Evolution*, 51(2):329–347, 1997.

M. Waterman. Secondary structure of single-stranded nucleic acids. In *Studies on foundations and combinatorics, Advances in mathematics supplementary studies*, volume 1, pages 167–212. Academic Press N.Y., 1978.

Daniel M Weinreich and Lin Chao. Rapid evolutionary escape by large populations from local fitness peaks is likely in nature. *Evolution Int J Org Evolution*, 59 (0014-3820):1175–82, 2005.

Daniel M. Weinreich, Nigel F. Delaney, Mark A. DePristo, and Daniel L. Hartl. Darwinian Evolution Can Follow Only Very Few Mutational Paths to Fitter Proteins. *Science*, 312(5770):111–114, 2006.

Ishay Weissman. Estimation of Parameters and Larger Quantiles Based on the k Largest Observations. *Journal of the American Statistical Society*, 73(364):812–815, 1978.

Michael C Whitlock, Patrick C Phillips, Francisco B.-G. Moore, and Stephen J Tonsor. Multiple Fitness Peaks and Epistasis. *Annual Review of Ecology and Systematics*, 26:601–629, 1995.

Claus Wilke. Quasispecies theory in the context of population genetics. *BMC Evolutionary Biology*, 5(1):44, August 2005.

Claus Wilke, Richard Lenski, and Christoph Adami. Compensatory mutations cause excess of antagonistic epistasis in rna secondary structure folding. *BMC Evolutionary Biology*, 3(1):3, 2003.

Claus O. Wilke and Christoph Adami. Interaction between directional epistasis and average mutational effects. *Proceedings of the Royal Society of London: Series B*, 268(1475):1469–1474, 2001.

Claus O. Wilke, Jia Lan Wang, Charles Ofria, Richard E. Lenski, and Christoph Adami. Evolution of digital organisms at high mutation rates leads to survival of the flattest. *Nature*, 412(6844):331–3, July 2001.

Wade C. Winkler and Ronald R. Breaker. Regulation of bacterial gene expression by riboswitches. *Annual Review of Microbiology*, 59(1):487–517, 2005.

S. Wright. The roles of mutation, inbreeding, crossbreeding and selection in evolution. *Proceedings of the VI International Congress of Genetrics*, 1:356–366, 1932.

Stephan Wuchty, Walter Fontana, Ivo L. Hofacker, and Peter Schuster. Complete suboptimal folding of RNA and the stability of secondary structures. *Biopolymers*, 49(2):145–165, 1999.

Emile Zuckerkandl and Linus Pauling. Molecular disease, evolution, and genetic heterogeneity. In M. Kasha and B. Pullman, editors, *Horizons in Biochemistry*, pages 189—225. Academic Press N.Y., 1962.

M Zuker and P Stiegler. Optimal computer folding of large RNA sequences using thermodynamics and auxiliary information. *Nucl. Acids. Res.*, 9(1):133–148, 1981.

Michael Zuker. On Finding All Suboptimal Foldings of an RNA Molecule. *Science*, 244(4900):48–52, 1989.

Vita

Matthew Cranston Cowperthwaite was born in Bethesda, Maryland on April 27, 1973, the son of Patricia Adele Cowperthwaite and George Edward Cowperthwaite. He graduated from Frederick High School in Frederick, Maryland in 1991. He studied plant biology at the University of Maryland in College Park, Maryland, receiving a Bachelor of Science *magna cum laude* in 1996. For the next 4 years, Matthew worked as a molecular biologist in the laboratory of Hugo K. Dooner at Rutgers University in Pascataway, New Jersey. In September 2002, he entered the Graduate School of The University of Texas.

Permanent Address: 4200 Wildwood Road
Austin, Texas 78722

This dissertation was typeset with LaTeX 2_ε[1] by the author.

[1] LaTeX 2_ε is an extension of LaTeX. LaTeX is a collection of macros for TeX. TeX is a trademark of the American Mathematical Society. The macros used in formatting this dissertation were written by Dinesh Das, Department of Computer Sciences, The University of Texas at Austin, and extended by Bert Kay, James A. Bednar, and Ayman El-Khashab.